UiT
THE ARCTIC
UNIVERSITY
OF NORWAY

FACULTY OF SCIENCE AND TECHNOLOGY

Department of Geology

Origin and accumulation mechanism of shallow gas accumulations in the SW Barents Sea

—

Kristian Kjerkreit

EOM-3901 Master's Thesis in Energy, Climate and Environment

June 2014

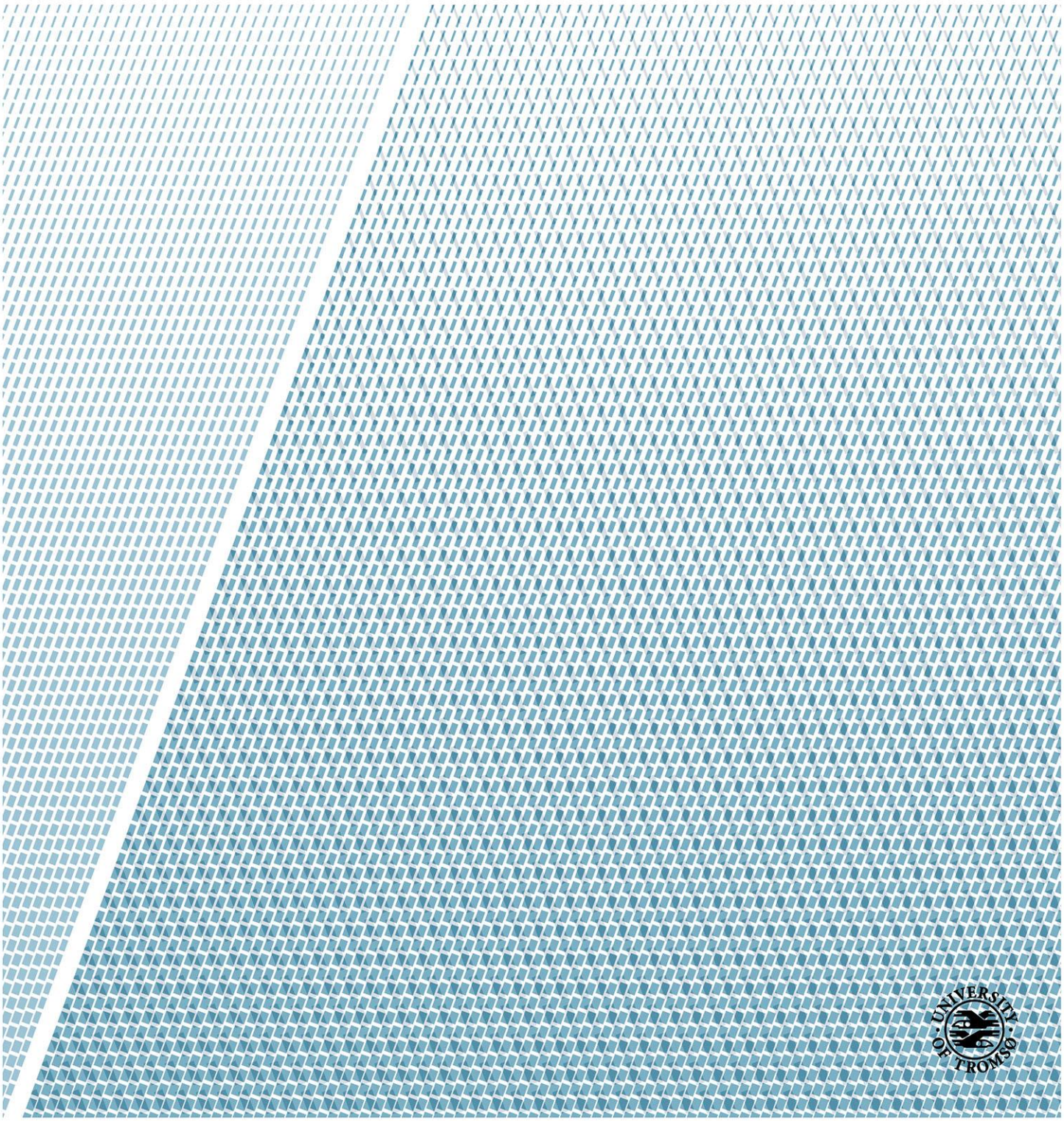

Abstract

Events associated with shallow gas accumulations are reported all over the Norwegian continental shelf. These accumulations are potentially dangerous geo-hazards related to drilling activity, but they can also be of economic interest if the accumulated volumes are large. Petroleum in the Barents Sea has been influenced by the late periods of uplift and erosion creating a complex province. The exact distribution and formation mechanism of shallow gas accumulations have yet to better understood.

This thesis focus on mapping the distribution of shallow gas accumulations located within the Tromsø Basin and adjacent areas in the SW Barents Sea. Data used consists mainly of publicly available 2D seismic data within the study area. 3D seismic data (surveys EL0001 and LN09M01) focus on specified amplitude anomalies associated with shallow gas accumulations, possibly linked with the formation of diagenesis-related BSR. Mapped seismic evidence of shallow gas is associated with bright spots, zones of acoustic masking and chaotic reflection pattern, chimneys and leakage along faults. The main stratigraphic units of this thesis are defined above Torsk fm., below Torsk fm. top and below Kolmule fm. and the upper Kolmule fm.

Overall, the results give a general overview of the location of potential shallow gas accumulations. The general shallow gas origin is most likely of thermogenic generation from sources located at depths below the Kolmule fm. The source is most likely a mixture of source rocks, including the major Hekkingen fm. Major migration pathways within the study area bypass zones of deeper faulting, mainly the Ringvassøy-Loppa Fault Complex to the shallower levels. Migration pathways are also identified towards structural highs along the Tromsø basin border (Loppa High, Veslemøy High and Senja Ridge) and towards salt diapirs within central parts of the basin. Accumulation and migration occur mainly related to the interpreted intra Torsk fm. and below the sealing upper regional unconformity (URU). Accumulation mechanisms are related to structural and stratigraphic trapping and the development of traps associated with diapirs and BSR (both gas-hydrate and diagenesis-related BSR).

Acknowledgements

Først og fremst takk til min veileder førsteamanuensis Stefan Bünz som har gjort denne oppgaven mulig. Det har vært en spennende og lærerik prosess å skrive denne masteroppgaven.

Takk til kontoret innerst i gangen i brakke sør og spesielt Espen Valberg. Vi har holdt sammen fra dag en. Alltid greit å ha noen i hjørnet som man kan rådføre seg med. Det ble mange flotte fussballmatcher, helt til spille ble ødelagt en uke før innleveringsfristen. Kanskje like greit?

Vil også takke mine medstudenter på Energi, Klima og Miljø (kull '09). Det har vært mange fine stunder sammen her i Tromsø. Uansett om du er ferdig nå eller har noen år igjen, lykke til videre.

Fem år som student ved Universitetet i Tromsø går nå mot slutten. Det har vært en krevende, men spennende periode. Tromsø har vært et fantastisk studiested, sommer som vinter. Skiturene har vært viktig for å koble av mellom de store slagene. Takk for alle turene. Takk til alle som var med.

Takk til min familie som alltid har vært der for meg, uansett hva det skulle være.

Til slutt vil jeg takke min kjære Astri. Du gjorde valg av studiested enkelt og har vært med meg igjennom hele studietiden. Nå går vi en spennende tid i møte, og jeg gleder meg virkelig til fortsettelsen!

Kristian Kjerkreit
Tromsø, Juni 2014

"Det e bærre lækkert!"

Potetbonde Olaf Sand

Table of Contents

1 Introduction

Shallow gas accumulations have been reported many places in the Tromsø Basin and adjacent areas in the SW Barents Sea. These gas accumulations might represent significant drilling hazards or potential economic hydrocarbon resources. However, their exact distribution and formation mechanism have yet to be better understood.

1.1 Objective

The primary objective of the thesis is to identify and map shallow gas accumulations in the Tromsø Basin and adjacent areas in the SW Barents Sea (fig. 1.1). This will lead to a better understanding of their distribution, stratigraphic controls and migration and accumulation mechanism in this region.

1.2 Motivation

Offshore exploration in the Norwegian sector of the Barents Sea started in the early 1980's. Seismic surveys, both 2D and 3D, cover large parts of the area. Today more than 100 wells are drilled in the area, including all exploration and production wells, with the number of wells increasing (E24.no, 2013). In 2010, Norway and Russia came to an agreement on the disputed area and the borderline in the Barents Sea, after 40 years of negotiation. This opens up for petroleum activity in new and frontier areas of the Barents Sea. As a petroleum province, the Barents Sea is of great interest as it has a large potential. Several seal and trapping mechanisms exists in various hydrocarbon play models (GeoExPro, 2005b), but still the Barents Sea is considered as an immature hydrocarbon province (NPD, 2013). The Barents Sea is located far from existing infrastructure and is known for its harsh conditions, but new technology has contributed to the opening of this frontier area for hydrocarbon exploration and production. It is therefore believed that the Barents Sea will be a major gas and oil supplier in the future (GeoExPro, 2005b).

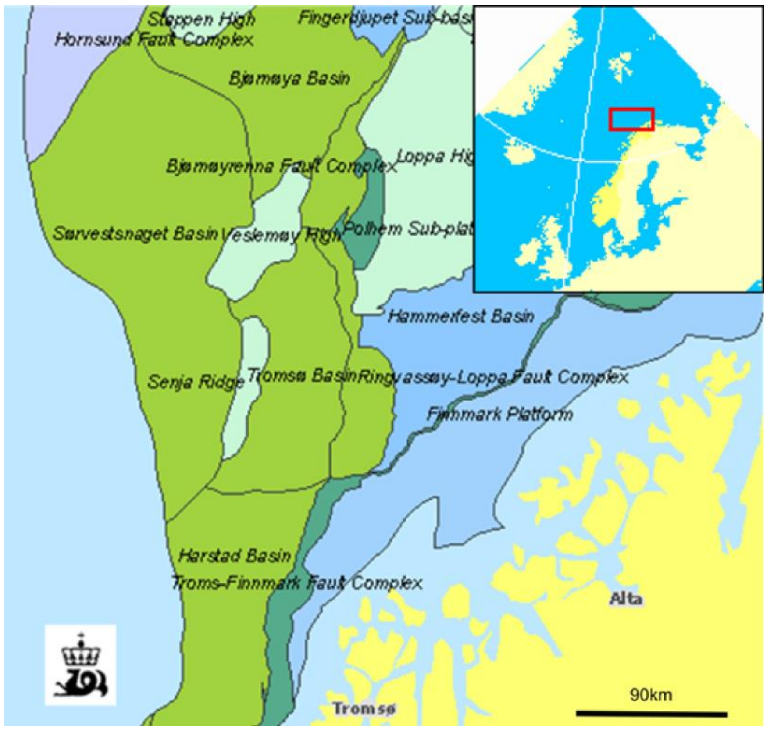

Figure 1.1 - Map of the study area in the SW Barents Sea; the Tromsø Basin and adjacent areas (NPD, 2014).

Understanding of the petroleum generation, migration and accumulation is of interest, as the Barents Sea is considered a complex hydrocarbon province. The Barents Sea has experienced several periods of uplift and erosion due to the cycles of late glaciation of the area. This has led to several factors affecting the hydrocarbons with both positive and negative outcomes such as tilting of reservoir, redistribution of fluids and cooling of source rock. The mapping of shallow gas accumulations can contribute to a better understanding of the geological history in the area.

The study area for this thesis covers the Tromsø Basin and adjacent areas shown in figure 1.1. The Tromsø Basin is a deep geologic basin located in the SW Barents Sea. The exact distribution of fluid flow and shallow gas accumulations in this area has not yet been determined. Determination of the shallow gas distribution in the SW Barents Sea can be of interest for those doing research in the area or on the specific topic and for those working in the area with energy and environment-related work, as shallow gas-charged sediments are known to be a potential environment and geo-hazards.

This thesis discusses different seismic amplitude anomalies associated with potential shallow gas accumulations and fluid-flow features together with possible interpretation pitfalls. There are other studies in the area illustrates the distribution of subsurface fluid-flow systems (Rajan, Bünz, Mienert, & Smith, 2013; Vadakkepuliyambatta, Bünz, Mienert, & Chand, 2013), which is compared and related to the results of this thesis.

1.3 Shallow Gas

Shallow gas is a well-known phenomenon, being accumulations of gas located in the upper lithosphere, close to the surface. As hydrocarbons have low densities, they tend to migrate towards the surface due to both pressure and density differences in the subsurface. If hydrocarbons are trapped below impermeable layers, migration stops and there is a potential buildup of hydrocarbons closer to the surface than from where the hydrocarbons originated.

Shallow gas events are according to the Petroleum Safety Authority Norway (PSA) defined as any gas zone penetrated before the BOP[1] has been installed. Any gas zones penetrated after the BOP is installed are not considered as a shallow gas event. In more detail, shallow gas is defined as a gas-bearing zone that lies at depths just below the surface or the mud line where the mud line is the boundary between earth and water (Wiretrip, 2014). Studies show that a large number of drilled wells in the Norwegian sector have experienced events related to shallow gas accumulations (PSA, 2007).

These definitions are considered more technical definitions related to the petroleum industry. This thesis does not focus on petroleum events and activity, but rather on the natural occurrence of shallow gas accumulations.

It turns out that there is no specific definition to classify a hydrocarbon accumulation as a shallow gas. Several studies have indicated that shallow gas is considered to be gas accumulations located within the upper 1000m of the subsurface (Davis, 1992; Solheim & Larsson, 1987). This thesis uses a wider term for shallow gas set to be approximately within the upper 2000m, and sediments located above the Early Cretaceous with the upper Kolmule fm. as a lower boundary condition. More details

[1] BOP – Blowout preventer. Safety mechanism used during drilling operations.

about subsurface focus area and methods used to define and identify shallow gas accumulations in chapters 2 and 3.

It is important to understand and locate the shallow gas accumulations for three main reasons (Andreassen, Nilssen, & Ødegaard, 2007; Kanestrøm, Skålnes, Riste, Eide, & Strandenes, 1990; Schroot & Schüttenhelm, 2003);

1. The presence of shallow gas may indicate deeper and larger accumulations, together with the fact that there is a working petroleum system in the area.
2. Geo-hazards and potential dangers related to shallow gas accumulations in the subsurface for petroleum exploration and development.
3. Potentially of commercial interest in the future.

Shallow gas is rarely of economic interest today as they are generally small and a probable pressure support is needed to recover the hydrocarbons. They have the potential to become of commercial interest in the future with the development of new and better technology. Shallow gas accumulations with assumed hydrostatic pressure will have up to 10 times less in-place volumes compared to similar size gas accumulations at several thousand meters depth due to the compression of gas caused by the overlaying pressure (GeoExPro, 2005a).

Shallow gas can lead to hazardous events during drilling operations such as blow-outs in over pressurized zones, but also reduction in sediment shear strength that can trigger slide events (Davis, 1992; Solheim & Larsson, 1987). Identifying and knowing the location and extent of shallow gas accumulations in an area reduces the risks associated with drilling and petroleum production. Personnel and environmental safety are important criteria for companies working in the Barents Sea as it is covered by acts and regulations for the Norwegian continental shelf regulated by the Ministry of Petroleum and Energy (MPE) together with the Norwegian Petroleum Directorate (NPD). Better understanding of shallow gas accumulations and migration pathways in the area of petroleum activity is therefore of great interest as it reduces the overall risks of hazardous shallow gas events from happening (Kanestrøm et al., 1990).

1.3.1 Generation

Most natural gas is generated over time by either biogenic or thermogenic processes (Davis, 1992; Floodgate & Judd, 1992). Biogenic gas is generation at shallow depths by biological processes at relatively low temperatures. This activity exists down to depths of approximately 60°C. Temperatures between 60°C-120°C is known as the location of “the golden zone”, being the optimum zone for oil entrapment (Buller, Bjørkum, Nadeau, & Walderhaug, 2005). Higher temperatures (>120°C) generate thermogenic gas. This is a deep generation of gas related to high temperatures. Figure 1.2 summarizes the petroleum charge and its relationship with burial depth, temperature and types of petroleum generated. Migration or uplift are necessary processes for thermogenic-generated gas to be classified as shallow. The third way of natural gas generation is through an abiogenic process, which is related to extremely deep, high temperature chemical reactions (Floodgate & Judd, 1992). Abiogenic generation is defined as generation of hydrocarbons from non-organic content, while both thermogenic and biogenic generation is dependent of organic material to generate hydrocarbons (Davis, 1992; Floodgate & Judd, 1992). Gas can be released into free phase from destabilized gas hydrates, but this is not classified as a source of gas generation.

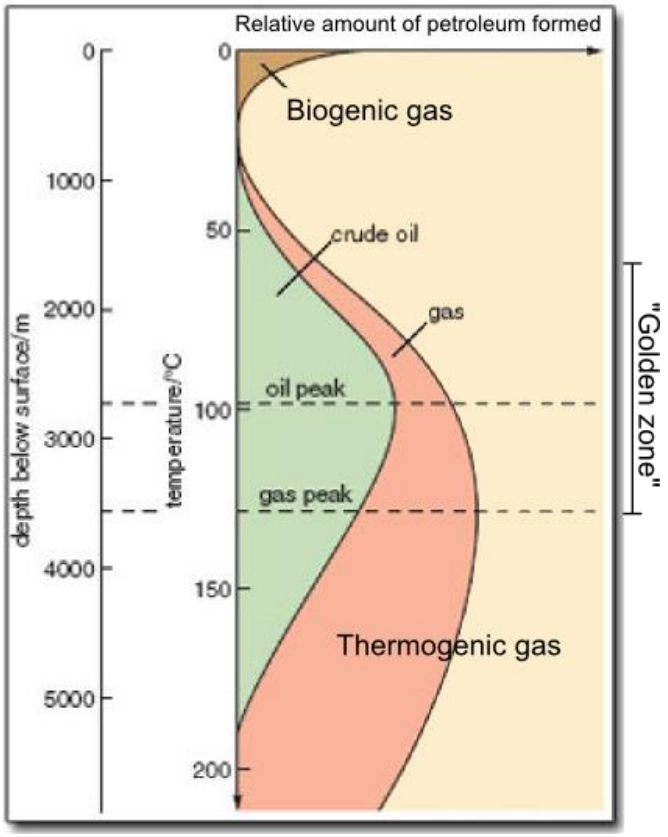

Figure 1.2 – Petroleum charge and the relationship between burial depth, temperature and amount and type of petroleum generated. Modified after Open.edu (2014).

1.3.2 Migration

Migration is the process of transporting hydrocarbon from its source rock to the reservoir. Migration is divided into two main stages; primary and secondary migration (Bjørlykke, 2010; Floodgate & Judd, 1992). Primary migration occurs simultaneously with the generation of hydrocarbons in the source rock to the adjacent reservoir rock, while secondary migration is the flow of gas and fluids within porous and permeable carrier beds to an area of accumulation. Secondary migration must be understood in terms of two-phase or even three-phase flow (Bjørlykke, 2010). Remigration, leakage and seepage are processes defined as tertiary migration (Hindle, 1997). Figure 1.3 shows a summarized sketch of the different migration processes. The driving forces behind migration are controlled by; buoyancy, groundwater flow and pressure and density differences (Hindle, 1997; Momper, 1978).

Migration is subdivided into lateral and vertical migration. Vertical subsurface gas and fluid migration or seepage, has an upward-driven migration pathway occurring across stratified sediments. Vertical migration is less effective in petroleum accumulation as it can only trap petroleum located directly beneath the zone of accumulation. Lateral subsurface gas and fluid migration is migration along the stratigraphy and it can occur more than hundreds of kilometers between the source rock, traps, accumulations and the surface. Lateral migration can drain large volumes of source rock (Thrasher, Fleet, Hay, Hovland, & Düppenbecker, 1996).

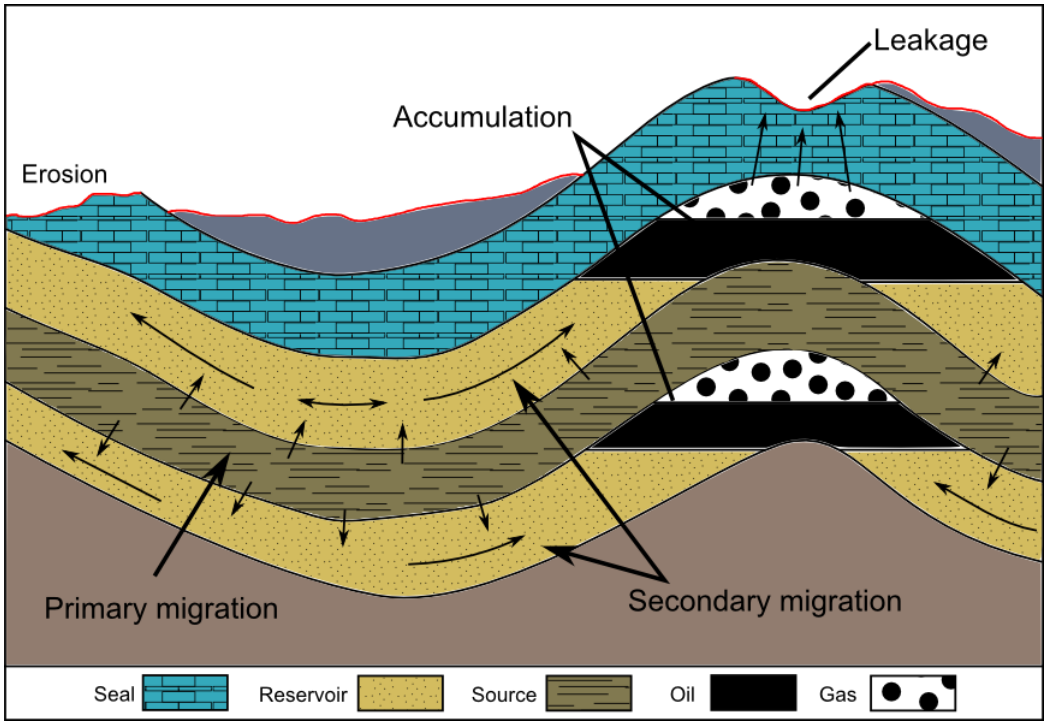

Figure 1.3 – Definitions of petroleum migration (primary and secondary) and accumulation. Modified after Tissot and Welte (1984).

1.3.3 Accumulation

When migration is stopped, there is normally a buildup of hydrocarbons creating an accumulation. Due to density variations of the different phases of hydrocarbons and fluids, accumulations of more than one phase (oil, gas and water) in a reservoir will be divided in layers (fig. 1.3) with gas accumulating on top of the oil leg. For hydrocarbon accumulation to occur, traps require an effective impermeable top seal that will contain the hydrocarbons preventing the reservoir to leak with time. Generally, shales have good sealing properties, while sandstones have good reservoir properties. The hydrocarbons can be trapped mainly within structural or stratigraphic traps (Biddle & Wielchowsky, 1994). Figure 1.4 shows different hydrocarbon trapping mechanisms. Structural traps are related to the geometry that was formed by post-depositional tectonic modifications; anticlinal, fault and deformation traps. Stratigraphic traps are related to the accumulation of hydrocarbons due to lithology changes; variations in facies, breakup in depositional sequence and massive traps (Rafaelsen, 2012). Other types of hydrocarbon traps that exist are; combination of trap types and hydrodynamic trapping mechanisms (Hindle, 1997).

Shallow gas accumulation, migration and generation is summarized in a conceptual model shown in figure 1.5. The figure illustrates different migration pathways (lateral and vertical) along stratigraphy and faults and the occurrence of different accumulation mechanisms (structural and stratigraphic) that are identified in the subsurface.

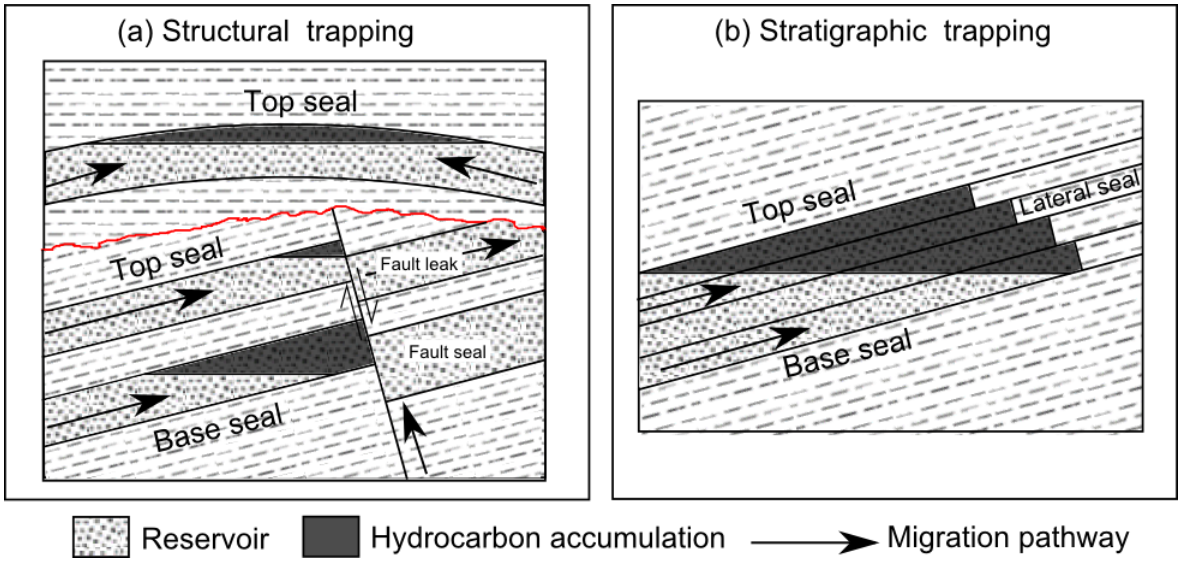

Figure 1.4 - Key elements in (a) structural and (b) stratigraphic hydrocarbon traps. Modified after Biddle and Wielchowsky (1994)

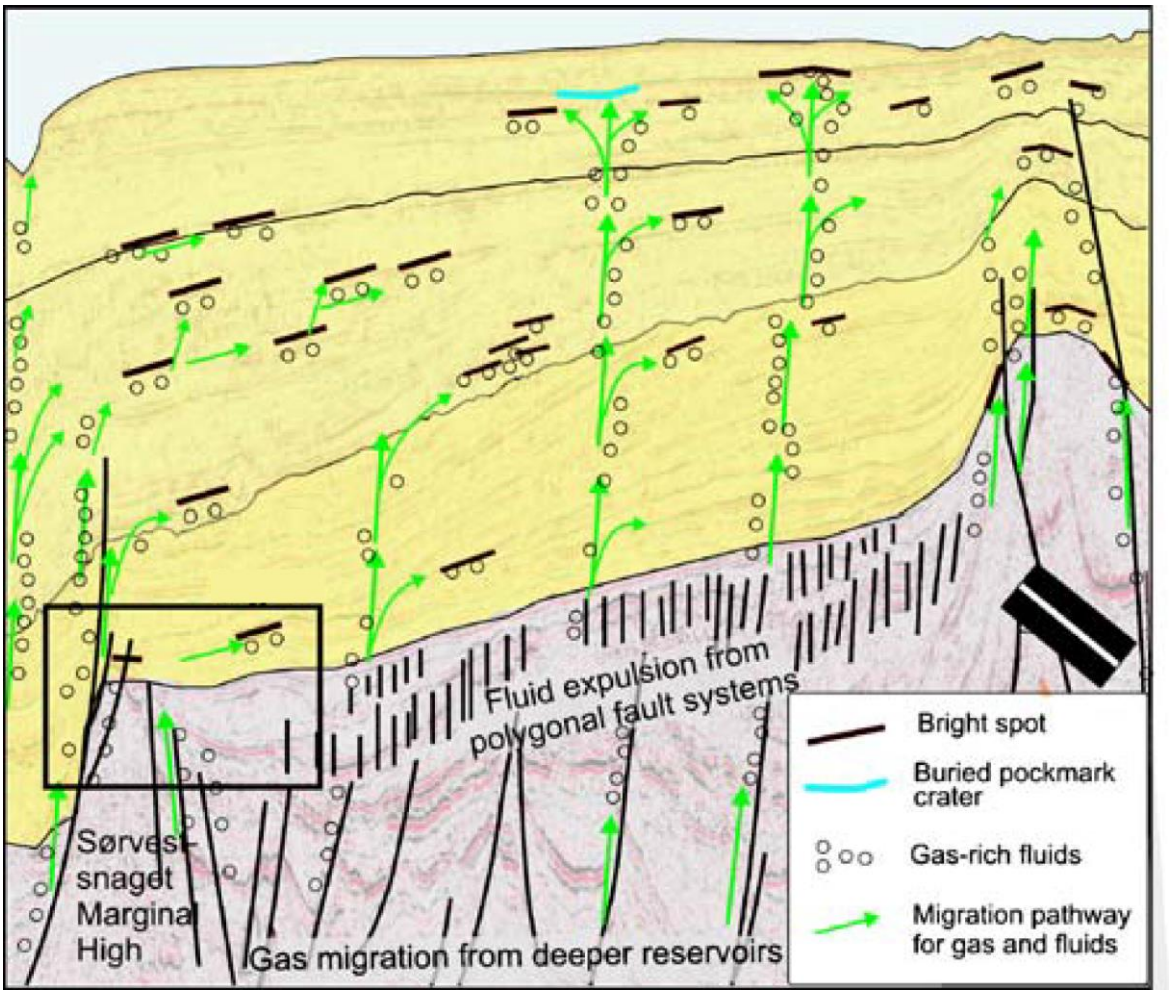

Figure 1.5 – Conceptual model summarizing migration pathways along faults and stratigraphy, with associated bright spots. Black box shows an example of both lateral and vertical migration (Andreassen et al., 2007).

1.4 Seismic Indications of Hydrocarbons

A seismic reflection is a result of acoustic impedance contrasts in the subsurface. The impedance contrast is the product of the subsurface density (ρ) and compressional (P-wave) velocity (v_p) (Veeken, 2007). The seismic reflection can be a result of lithology contrasts, faults, pore fluid properties and seismic artefacts (Veeken, 2007).

Only a small percentage of gas needs to be present in the sediment to drastically reduce the P-wave velocity (fig. 1.6(a)), affecting the AI with a negative reflection coefficient at the top of the gas bearing sediment, and positive reflection coefficient at its base (fig. 1.6(b)) (Andreassen et al., 2007; Kanestrøm et al., 1990).

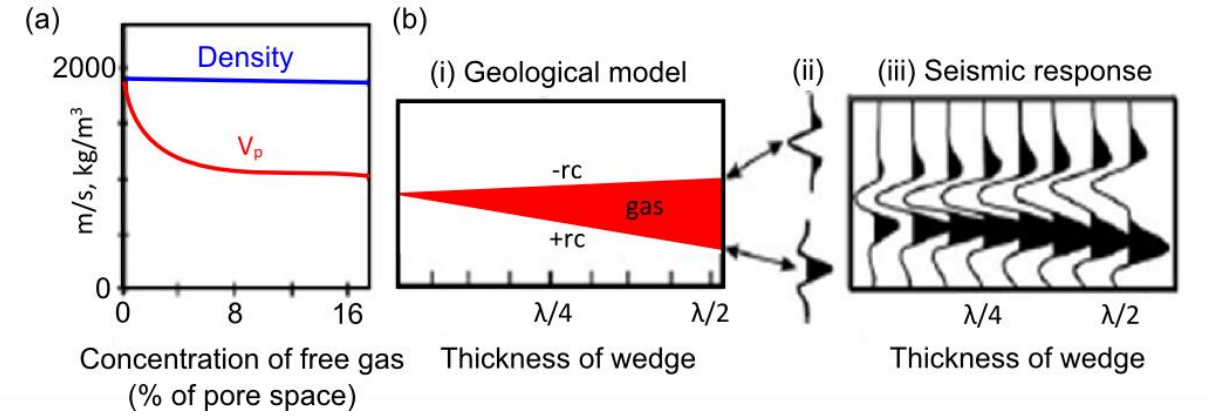

Figure 1.6 – (a) Compressional wave velocity and bulk density as a function of gas saturation in sediments. (b) i) Geological model of a thinning wedge of gas. Low velocity of gas zone causes a negative reflection coefficient (RC) at the top of the wedge and a positive RC at the base of the wedge. ii) Seismic response at top and base of wedge assuming zero-phase seismic using SEG polarity standard. iii) Seismic response of gas wedge as function of its thickness. (Andreassen et al., 2007)

Shallow gas is a subgroup of hydrocarbon indications seen on seismic data. The process of identifying shallow gas is the same as the process of identifying hydrocarbons in a seismic section. There are several well-known seismic indications of hydrocarbons, some of them are known as direct hydrocarbon indicators (DHI). The most common seismic amplitude anomalies identified and associated with hydrocarbons are; bright spot, dim spot, flat spot, acoustic masking, pull-down, phase-reversal, and chimneys/pipes. These are well-known features that are also defined as seismic evidence of shallow gas by Judd and Hovland (1992). Examples of different indications of hydrocarbons and fluid flow on seismic data are seen in figure 1.6, and briefly described below (Andreassen et al., 2007; Cukur, Krastel, Tomonaga, Çağatay, & Meydan, 2013; Garcia-Gil, Vilas, & Garcia-Garcia, 2002; Kanestrøm et al., 1990).

1.4.1 Seismic Response

Acoustic turbidity/chaotic reflections relates to chaotic reflection pattern caused by scattering of the acoustic signal compared to adjacent areas.

Acoustic blanking/masking is the faint or absence of reflections due to absorption of acoustic energy in the overlaying gas-charged sediments.

Bright spots are local increase in reflection amplitude, related to high-amplitude anomalies. Negative-polarity or phase-reversed reflections can represent top of low density or low velocity events in seismic data, often a sign of hydrocarbons or gas-charged sediments. It could also be related to other geological features such as coal, lignite or gravel layers. More details about seismic anomaly pitfalls in chapter 1.6.

Enhanced reflections (ER) are related to the increase in reflection amplitude, normally in a lateral extent close to gas chimney and fluid-flow systems. ER are accumulations associated with trapping by either impermeable layers or very porous sediments.

Gas chimneys/pipes are related to fluid leakage within the subsurface, usually identified as vertical structures with disturbed or destroyed seismic reflections due to the upward migration of fluids. These fluids can be mud, water, oil or gas.

Pull-down is an effect created by the reduction in velocity, resulting in seismic reflections received later than the surrounding reflections. This effect causes a velocity-sag pulling the reflections down.

Dim-spot is a local decrease in amplitude along a reflection, often an effect caused by gas situated above shales or other sediments with low velocity or density.

Bottom-simulating reflectors (BSR) are shallow, high amplitude reflections often parallel to the seafloor. The BSR can be a result of the free gas accumulating at the base of the pressure and temperature dependent gas hydrate stability zone (GHSZ) (fig. 1.8). BSR can also be related to the results caused by diagenetic transformation of siliceous sediments from Opal A to Opal C/T (microcrystalline quartz) (Berndt, Bünz, Clayton, Mienert, & Saunders, 2004; Davies & Cartwright, 2002). The BSR is described in more details in section 1.5, and figure 1.9, showing a seismic response of the gas-hydrate related BSR.

Figure 1.7 illustrates examples of different seismic fluid flow and hydrocarbon indicators, note the phase-reversal of the seismic reflections, indicated with the wiggle trace from the seabed reflector and the identified bright spots (Andreassen et al., 2007). Table 1.1 summarizes the amplitude terms related to hydrocarbon leakage on seismic data, while table 1.2 summarizes the terms describing anomalous patterns on seismic data (Løseth, Gading, & Wensaas, 2009).

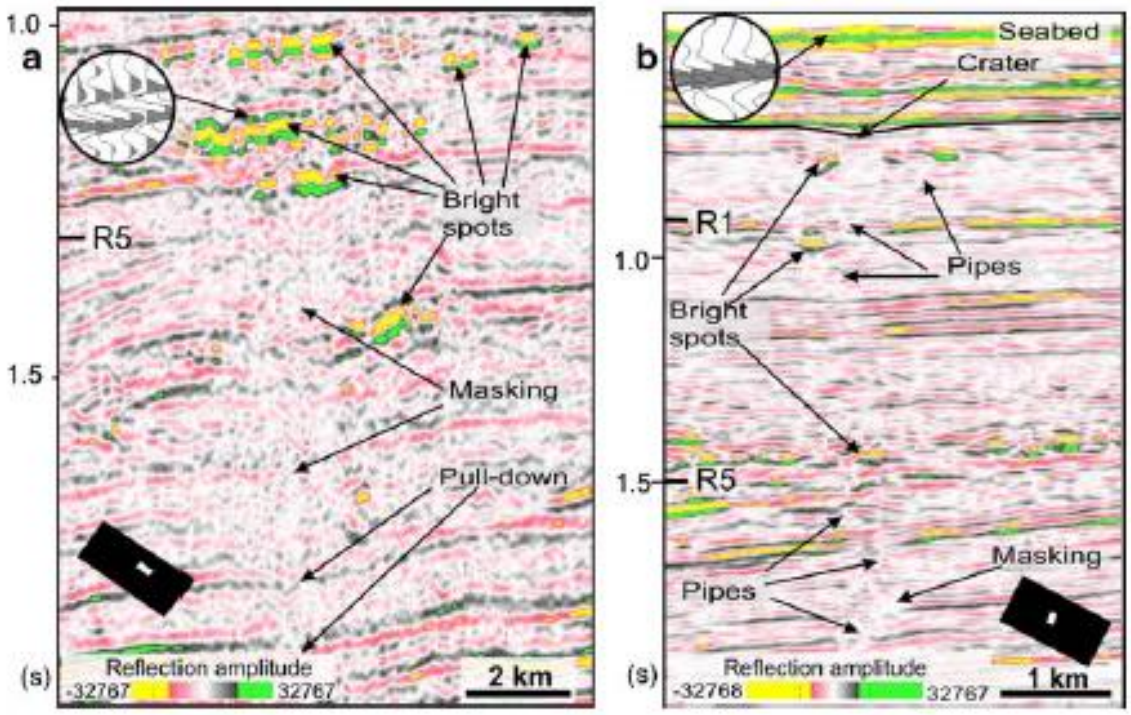

Figure 1.7 – Different seismic indications of fluid flow and hydrocarbons. (a) Seismic profile showing acoustic masking, bright spots and pull-down effects. Wiggle trace display a phase-reversed bright spot. (b) Seismic profile showing acoustic pipes, crater, masking and bright spots in association with a pipe system. Wiggle trace display the seabed reflection. (Andreassen et al., 2007)

Table 1.1 - Summary of amplitude terms related to hydrocarbon leakage on seismic data (Løseth et al., 2009).

Term	Definition
Brights, bright spot or high amplitude anomaly	Local increase in positive or negative amplitude along a reflection for any reason.
Dim spot (or dim zone)	Local decrease in positive or negative amplitude along a reflection or in a zone for any reason.
V-shaped bright	High amplitude V-shaped reflection in vertical section that is discordant to reflections from depositional surfaces. Seldom more that 2–3 km wide.
Flat spot	Relatively flat seismic reflection with an angle to the stratigraphic reflections.
Phase reversal	Phase shift of 180° along a continuous reflection, so that a peak becomes a trough and vice versa.
AVO	Amplitude variation with offset.
Reduced continuity	Local reduction of continuity of a seismic event.
Increased continuity	Local increase of continuity of a seismic event.
Reduced frequency	Local decrease of frequency.
Bottom simulating reflectors (BSR)	High amplitude reflection that often is parallel to seabed.

Table 1.2- Summary of terms describing anomalous patterns on seismic data (Løseth et al., 2009).

Term	Definition
Vertical wipe-out zone	The area on a seismic section where the reflections from the stratigraphic layers are deteriorated so the primary reflections either are absent or very weak.
Vertical dim zone	The area on a seismic section where the reflections from the stratigraphic layers are visible but have lower continuity and amplitude than in adjacent areas.
Vertical high amplitude or bright zone	The area on a seismic section where several high amplitude reflection anomalies occur that naturally can be grouped together.
Discontinuity zone	The area on a seismic section where the reflections from the stratigraphic layers are more discontinuous than in adjacent areas.
Chaotic reflection zone	The area on a seismic section where the reflection pattern is chaotic compared to adjacent areas.
Local depression features	Negative real down-bending or sag of a seismic reflection. The underlying reflections can be truncated, be parallel to the described structure or they can have any type of reflection pattern (e.g., chaotic).
Mounds	Positive structure of any shape rising above the normal top of a reflection. The reflection pattern below the mound can be of any type.
Push down	Apparent down-bending produced by a local, shallower low-velocity region.
Pull up	Apparent uplift produced by a local, shallower high-velocity region.

1.5 Bottom-Simulating Reflectors (BSR)

Bottom-simulating reflectors (BSR) are reflections found at shallow depths close to the seafloor reflection. It can be caused by either; (1) the contrast in the overlying gas hydrates and the underlying free gas and gas-saturated sediments, known as a gas-hydrate related BSR, or by (2) diagenesis of siliceous sediments with the Opal A to Opal C/T and quartz transformation, known as a diagenesis-related BRS (Berndt et al., 2004). The BSR is related to hydrocarbon accumulations in a potential free-gas zone located beneath the seismic reflection.

1.5.1 Gas-Hydrate Related BSR

Gas-hydrate related BSR indicate the base of the gas hydrate stability zone (GHSZ) and is a transition zone to where gas hydrates no longer exist due to subsurface pressure and temperature changes (Bünz, Mienert, & Berndt, 2003; MacKay, Jarrard, Westbrook, & Hyndman, 1994). This reflector generally parallels the seafloor reflector. Gas hydrates need low temperatures and high pressure to be present in a hydrate phase. At the base of GHSZ, the hydrates will no longer exist in a hydrate phase. Below the GHSZ, the gas hydrates will change phase into dissolved or free gas, creating a zone of free gas accumulations accumulating below the GHSZ. Enhanced reflections and bright spots on seismic data indicate this level. Figure 1.8 illustrates the temperature and pressure conditions required to form gas hydrates within the GHSZ. The BSR may be caused by the high velocity of the gas hydrate above the BSR, or by the low velocity of free gas below the BSR (MacKay et al., 1994). Both scenarios are characterized by a negative reflection coefficient (Andreassen, 2009). The Barents Sea margin is located within the pressure-temperature zone for gas hydrates, so gas hydrates are expected to exist in the area (Andreassen et al., 2007). Amplitude anomalies associated with gas-hydrate related BSR is generally associated to the occurrence of free gas and the reduction in velocity and not the gas hydrates (Bünz & Mienert, 2004; Haacke, Westbrook, & Hyndman, 2007; Sain, Minshull, Singh, & Hobbs, 2000). An example of a seismic response of BSR is illustrated in figure 1.9 showing the phase-reversal of the BSR as a product of the reduced P-wave velocity in the gas-charged sediments. These accumulations of free gas are classified as shallow gas accumulations.

1.5.2 Diagenesis-Related BSR

Diagenesis is the process which transforms unconsolidated sediments into sedimentary rocks (Buller et al., 2005). Diagenesis is controlled by subsurface pressure and temperature conditions. The diagenesis-related BSR is a less studied phenomenon than the gas-hydrated related BRS. This reflector is a result of diagenesis of siliceous-rich sediments and the transformation of Opal A to Opal C/T and quartz. The diagenesis-related BSR does not have to parallel the current seafloor reflection, as it can be a result of diagenesis related to paleoenvironments. The diagenesis-related BSR can exist in a group of high-amplitude reflections rather than a single incident (Berndt et al., 2004). The acoustic impedance contrast from the siliceous sediments and the different stages of diagenesis of Opal A, Opal C/T and quartz has a positive impedance contrast and as of this the diagenesis-related BSR is known to have the same positive polarity as the seafloor reflection (Berndt et al., 2004). The Opal A to Opal C/T transition is a less hazardous BSR that could be fossilized and associated with in situ temperatures outside the range normally expected for their stability field (Davies & Cartwright, 2002). The Opal A to Opal C/T give rise to one BSR, while the Opal C/T to quartz give rise to a deeper BSR dependent on the subsurface conditions (Berndt et al., 2004).

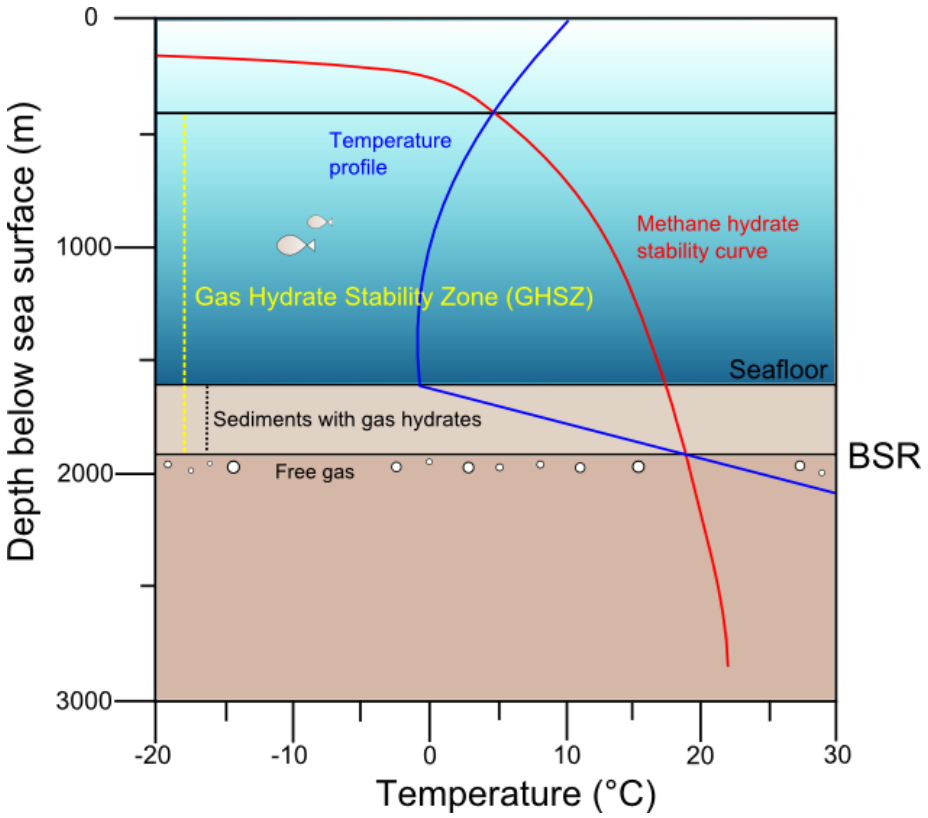

Figure 1.8 - Gas hydrate stability zone (GHSZ) shown in a depth vs temperature and pressure diagram with a given geothermal gradient for polar regimes. Modified after Chand and Minshull (2003).

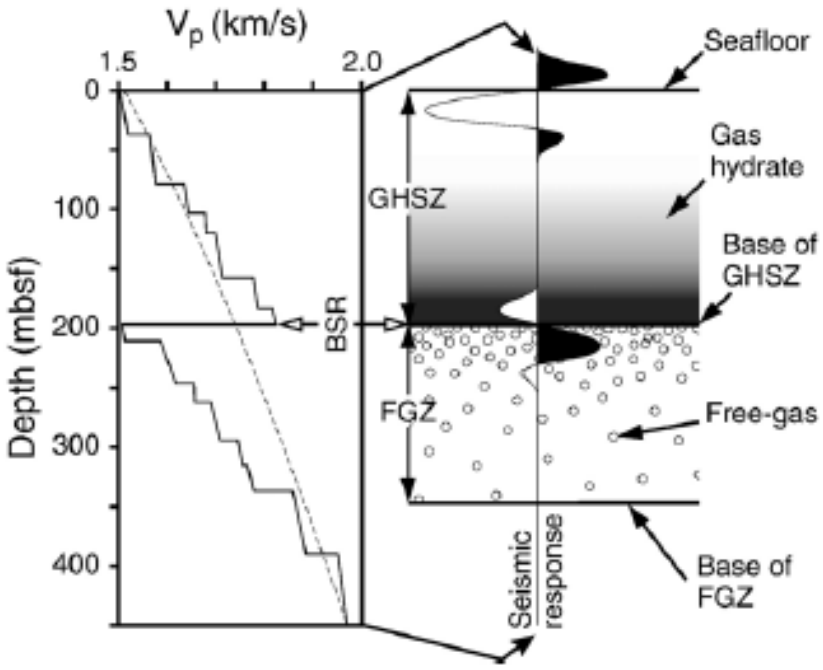

Figure 1.9 – Illustration of a sedimentary section containing gas hydrates above a zone of free gas (FGZ). The P-wave velocity (V_p) increases with depth. The BSR is normally a product of the drastic reduction in velocity caused by the gas charged sediments below the gas hydrates and GHSZ. The seismic response shows the BSR as a phase-reversed anomaly (Haacke et al., 2007).

1.6 Amplitude Anomaly Pitfalls

Not all seismic bright spots or amplitude anomalies are caused by the properties of hydrocarbons. There are several geological situations that may produce the same effects on seismic data as hydrocarbons and gas-charged in sediments. Some situations that can create similar seismic anomalies with high amplitudes are:

- carbonates
- igneous intrusions
- thinning beds at tuning thickness
- coal beds

Carbonates and igneous intrusions are generally associated with a positive reflection coefficient. Amplitude anomalies caused by reflections at tuning thickness could have high amplitudes and be of negative or positive polarity dependent on its specific properties. Coal beds could have the same seismic effect, having low velocity and density, and could therefore easily be misinterpreted. The more gas effects observed and identified together, the more likely it is to be a response to the gas itself (Andreassen et al., 2007).

1.7 Seismic Resolution

The seismic resolution is the ability to distinguish single features. It states the minimum distance between two features so that the two different features can be defined rather than being one (Sheriff, 1977). Resolution within seismic interpretation is differentiated in horizontal and vertical resolution (Veeken, 2007). The resolution of the seismic data is dependent on the frequency (f), velocity (v) and wavelength (λ) of the seismic signal. The vertical resolution limit is normally a quarter of the dominant seismic signal wavelength, while the horizontal resolution is related to the width of the Fresnel zone (Andreassen, 2009).

2 Study Area

This thesis focuses on shallow gas accumulations and migration within the SW Barents Sea with the main study focused on the Tromsø Basin and adjacent areas (fig. 1.1).

2.1 Barents Sea

The Barents Sea was named after the Dutch navigator and explorer Willem Barentsz (1550-1597) in honor of his frontier and early expeditions to the far north. In 1596, Barentsz set out on a quest to be the first to navigate successfully from Europe to Asia through the Northeast Passage. Along the journey he discovered Bjørnøya and an island they named Spitsbergen, the main island of Svalbard (Wikipedia, 2014).

The Barents Sea is a shallow part of the Arctic Ocean (fig. 2.1). It is an epicontinental and marginal sea located north of Norway and Russian (Solheim & Elverhøi, 1993) bounded by relatively young passive continental margins in the north and west (Faleide, Gudlaugsson, & Jacquart, 1984). The International Hydrographic Organization (IHO, 1953) defines the Barents Sea summarized as;

In the west, the shelf-edge to the Norwegian Sea act as an oceanographic boundary. The islands of Svalbard lies in the northwest, and the islands Franz Josef Land and Novaya Zemlya are located in the northeast and east. The Norwegian mainland and the Kola Peninsula border the south.

Figure 2.1 shows the location of the Arctic Oceans and the Barents Sea. The extent of the Barents Sea stretches from approximately 72°N to 80°N covering an area of approximately 1.2 million km^2. Average water depth is 230m with a maximum water depth of 450m (GeoExPro, 2005b). The southern and western parts of the Barents Sea are known to be more or less ice-free all year round (NPD, 1996).

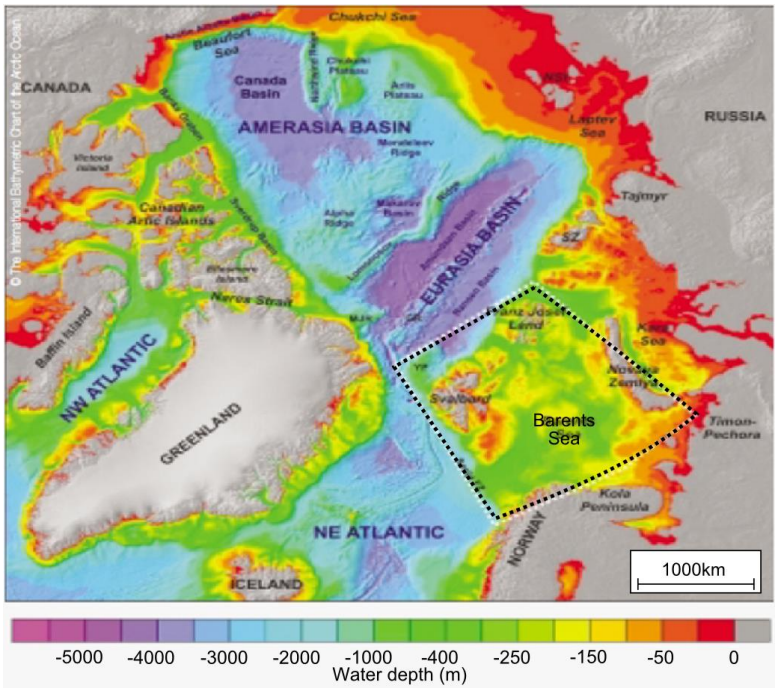

Figure 2.1 - Map of the Arctic Oceans, with location of the Barents Sea. The map shows the seafloor bathymetry (GeoExPro, 2005b).

The western part of the Barents Sea is known to have a more complex tectonic history than the eastern part. This is a result of the development of the Barents Sea as a response to the Cenozoic opening of the Norwegian-Greenland Sea and the Eurasian basin (Faleide, Vågnes, & Gudlaugsson, 1993; Fiedler & Faleide, 1996). This thesis has a focus on the Tromsø Basin (TB) and adjacent areas in the SW Barents Sea, which include parts of the Hammerfest Basin (HB), Harstad Basin, Veslemøy High (VH), Senja Ridge (SR), Loppa High (LH), Polheim Sub Platform (PSP), Bjørnøya Basin (BB), Sørvestnaget Basin (SB), Bjørnøyrenna Fault Complex (BFC) and Ringvassøy-Loppa Fault Complex (RLFC). Locations of the different geological features are shown in figure 2.2 illustrating the main structural elements of the Greater Barents Sea.

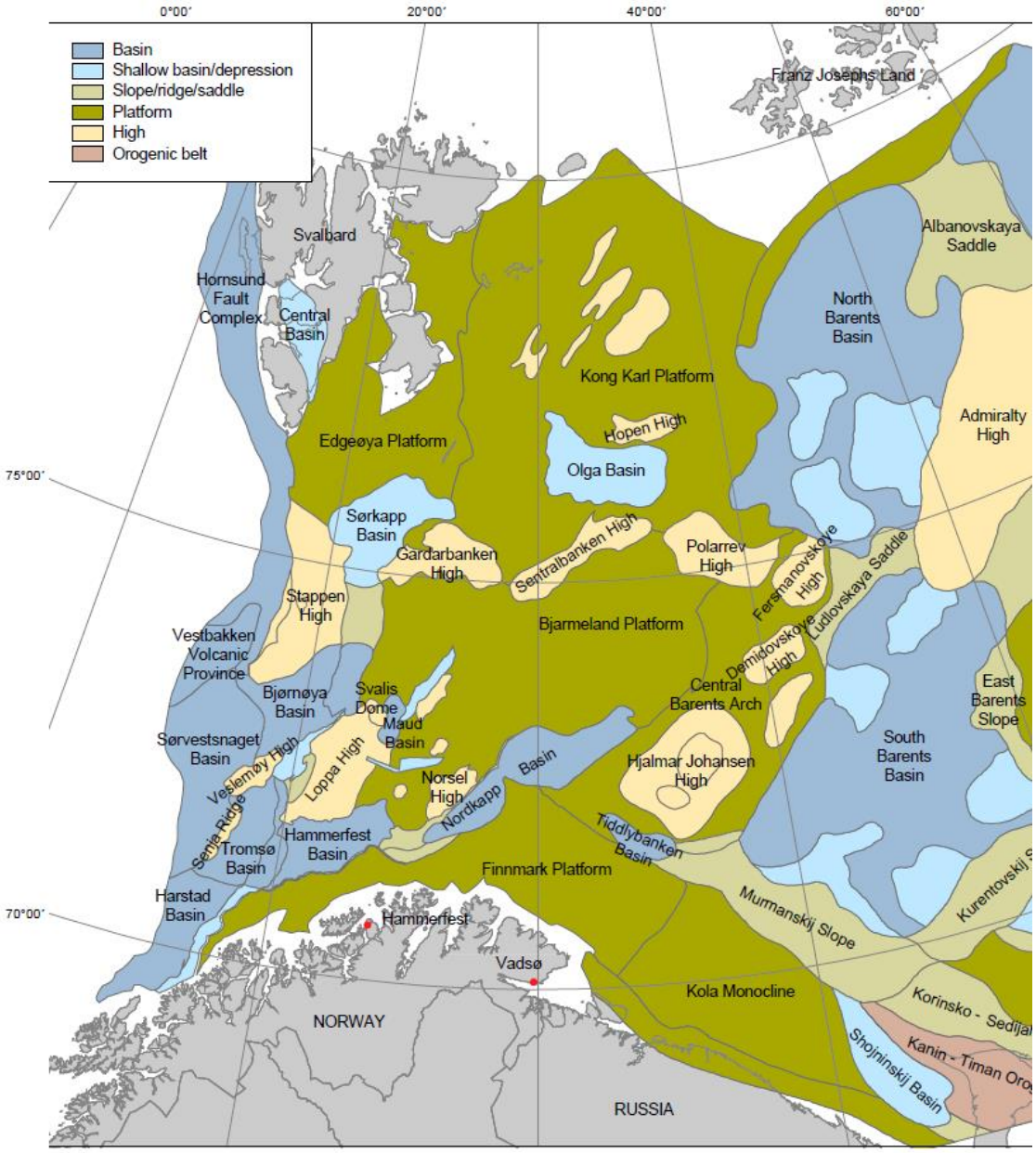

Figure 2.2 – Structural elements of the Barents Sea (Henriksen et al., 2011b). The Tromsø Basin and adjacent areas is located to the SW Barents Sea.

2.1.1 Geological Provinces

The SW Barents Sea is subdivided into three main geological provinces separated by tectonic activity, related to major fault zones or subsurface heights. These provinces are described in detail by Faleide et al. (1993). Summarized the different geological provinces are the following;

- Southwestern basin province
- Eastern platform province
- Western continental margin

The continental margin in the western Barents Sea evolved in response to the Cenozoic opening of the Norwegian-Greenland Sea mainly through rifting and sheared margin. After the breakup there was an episode of rifting and fault activity and the passive margin developed in response to subsidence and sediment loading during the widening and deepening of the Norwegian-Greenland Sea (Faleide et al., 1993). Sedimentation rates were low until Late Pliocene when the Northern-Hemisphere Glaciation led to a rapid progradation and increased sedimentation which formed huge depocenters near the shelf edge in front of bathymetric troughs in the western Barents Sea (Faleide, 2008).

The general trend of the geological structures and features located within the SW Barents Sea is of a NE-SW orientation. The general trend for all of the Barents Sea is said to be in the same NE-SW direction (Brekke, Sjulstad, Magnus, & Williams, 2001; Gudlaugsson, Faleide, Johansen, & Breivik, 1998). This is a result of the extensional direction between Greenland and the northern Europe being manly N-S to NE-SW oriented during the development of the Barents Sea (Brekke et al., 2001).

2.1.1.1 Southwestern Basin Province

The southwestern basin province consists of deep Cretaceous and early Tertiary basins such as the study area for this thesis, the Tromsø Basin, but also the adjacent Harstad, Bjørnøya and the Sørvestnaget Basins.

2.1.1.2 Eastern Platform Province

The eastern part of the Barents Sea, further east than 20°E, consist of basins and highs not having experienced the same subsidence as other parts of the SW Barents Sea. Finnmark Platform, Hammerfest Basin, and Loppa High are structural features within this geological province (Faleide et al., 1993).

2.1.1.3 Western Continental Margin

The western continental margin consists of Mesozoic basins and highs including the oceanic Lofoten Basin and the Vestbakken Volcanic province.

2.1.2 Nomenclature and Stratigraphy

The Barents Sea nomenclature is defined and summarized by the NPD (1996) in figure 2.3. The western Barents Sea has in general a more or less continuous sedimentary succession ranging from the Upper Paleozoic to the Cenozoic (Glørstad-Clark, Faleide, Lundschien, & Nystuen, 2010). Kviting, Knurr, Stø and the Tubåen formations are in general of clastic sandstones, while the other formations are mainly of shale material (Gabrielsen, Faerseth, & Jensen, 1990). Only the formations within the area of interest, formations above the Kolmule fm. are briefly described. These formations are the Kolmule, Kveite, Kviting and Torsk formations.

2.1.2.1 Kolmule Formation

The Kolmule formation belong within the Nordvestbanken group and is a formation that consists in general of dark gray to green claystone and shale. It can be silty in parts with minor thin siltstone interbeds and limestone and dolomite stringers, with traces of glauconite and pyrite known to occur. The Kolmule formation is deposited in an open marine environment with its lower parts correlating to prodeltaic to open shelf deposits of the Carolinefjellet formation on the Svalbard Platform (NPD, 2014). The base of the unit has a regionally significant transgressive pulse while the top of the unit is mainly eroded by the Cretaceous uplift of the northern shelf margins (Dalland, Worsley, & Ofstad, 1988).

2.1.2.2 Kveite Formation

The Kveite formation belong within the Nygrunnen group and is a formation that consists mainly of greenish-gray to gray shale and claystone with thin interbeds of limestone and siltstone. The formation appears to be characteristically developed in the Tromsø Basin and across the Ringvassøy-Loppa Fault Complex into the Hammerfest Basin, thinning eastwards passing into the sands and carbonates of the Kviting formation. Its depositional environment consists of deep open shelf environment with a normal circulation (Dalland et al., 1988).

2.1.2.3 Kviting Formation

The Kviting formation belong within the Nygrunnen group and is a formation that consists of calcareous sandstone interbedded with sandy glauconitic mudstones from a deep to shallow shelf environment with a normal circulation. Its extent is apparently restricted to the central and eastern parts of the Hammerfest Basin (Dalland et al., 1988). The Kviting and Kveite formations are deposited at the same stratigraphic levels.

2.1.2.4 Torsk Formation

The Torsk formation belong within the Sotbakken group and is a formation that consists of light to medium grey or greenish-gray generally non-calcareous claystone. Rare siltstone and limestone stringers occur in the unit with tuffaceous horizons often identified within the lower parts. This formation is recognized throughout Tromsøflaket with little lithological variation. The depositional environment in the Torsk formation is of open to deep marine shelf with no significant coarse clastic supply (Dalland et al., 1988).

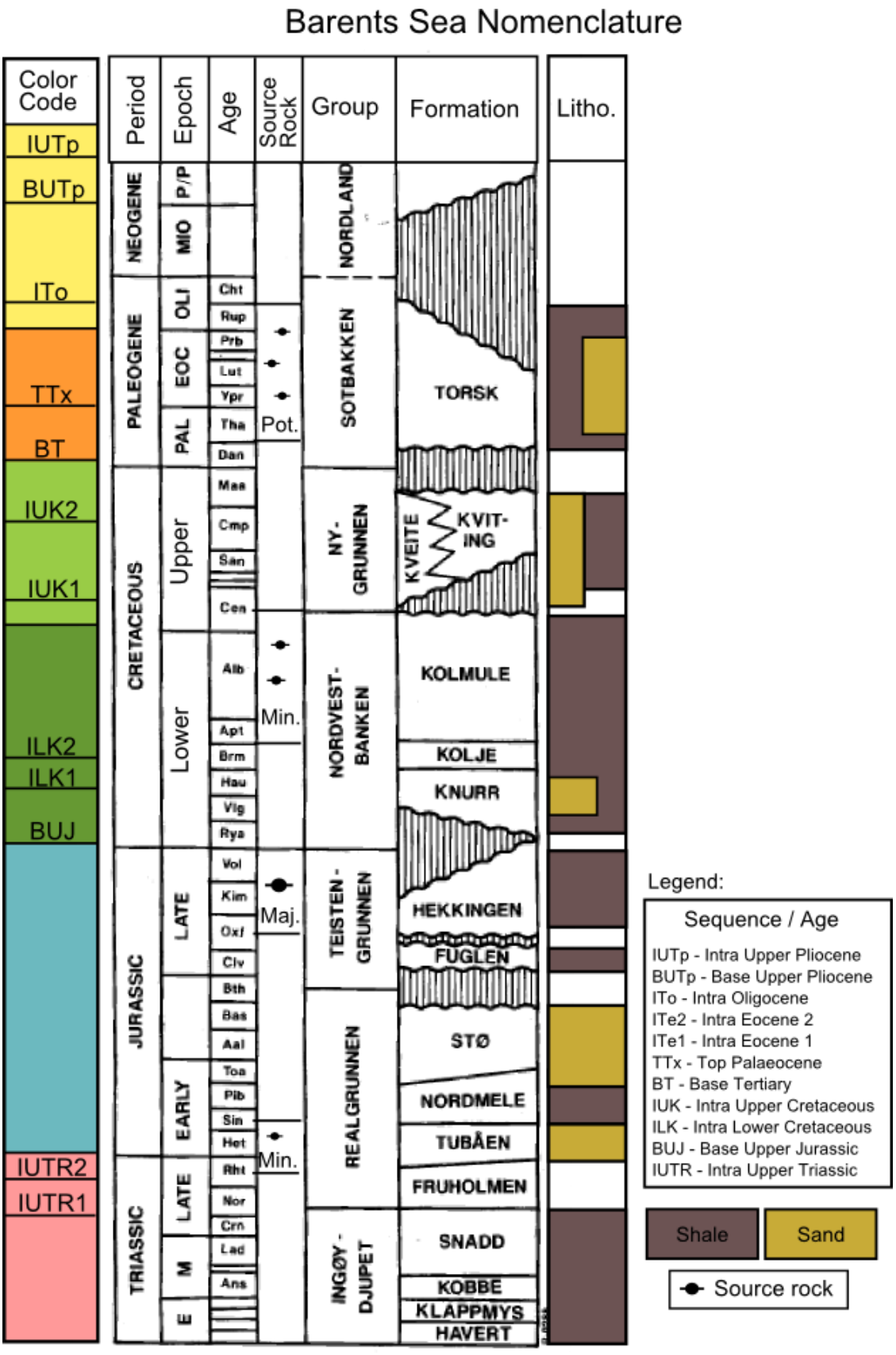

Figure 2.3 – Barents Sea nomenclature defined by the NPD. The figure has information about age, sequence, main reflectors, source rock, lithology and formations. Modified after Gabrielsen et al. (1990) and Vadakkepuliyambatta et al. (2013).

2.1.3 Uplift and Erosion

The Barents Sea region has been exposed to different magnitudes of uplift and erosion. Uplift and erosion are geological processes that are closely related. Estimates of net erosion range from 0m to more than 3000m increasing from the west towards the east (Henriksen et al., 2011a; Reemst, Cloetingh, & Fanavoll, 1994). These estimates are based on vitrinite reflectance, fission track analysis and mass balance calculations (Reemst et al., 1994). The net erosion is defined as the difference between the maximum burial depth and the present day burial depth for a marker horizon, but the processes may however occur in several stages (Henriksen et al., 2011a). The net erosion for the Barents Sea is summarized in figure 2.4 with the study area located west of the Loppa High. Figure 2.5 shows the results of the erosion and is illustrated by a conceptual W-E profile from the Barents Sea across the Tromsø and Hammerfest Basins (Henriksen et al., 2011a). Notice the eastward increase in net erosion.

Over large parts of the study area there is a thin horizontal layer just below the sea floor. This reflector has a lower boundary that truncates older beds forming a major unconformity, the upper regional unconformity known as URU. The top of this layer is interpreted to be sediments of Quaternary age (Faleide et al., 1984). The URU separates the Quaternary glacial sediments from the deeper Tertiary and older pre-glacial sedimentary rocks. It was formed in response to the Pliocene-Pleistocene glacial period (Chand et al., 2008). Most of the unlithified sediments located in the Barents Sea are of glacial deposits during the last glaciation of the area (Faleide et al., 1996). There has been both isostatic and tectonic-related uplift in the SW Barents Sea (Fiedler & Faleide, 1996).

The results of several cycles of uplift and erosion has influenced the hydrocarbon generation, migration and accumulation. In this case, the Barents Sea has suffered negative effects due to the uplift and erosion in terms of petroleum exploration (Henriksen et al., 2011a). Known effects are gas expansion, cooling of source rock, failure of seal, reservoir spillage, reservoir quality deterioration, reactivation of faults and fractures and tilting of structures (Doré & Jensen, 1996). Accumulation of hydrocarbons depends on several mechanisms working together. Uplift and erosion will in general lead to a pressure relief and temperature reduction. If earlier oil-filled structures are uplifted, the pressure relief could lead to a reactivation of faults and fractures in both the sealing and the surrounding rock material. Gas can also be released from the oil, and due to gas/oil density differences, the gas will force oil out of the trap. This could be an explanation of how a structure could be gas-filled and at the same time not filled-to-spill, which is the reported case in the Hammerfest Basin (Doré, 1995). Local pressure gradients and fluid flow of pore water can also contribute to push oil out of reservoirs. These local pressure gradients are known to occur in areas that has experienced great ice cover (NPD, 1996).

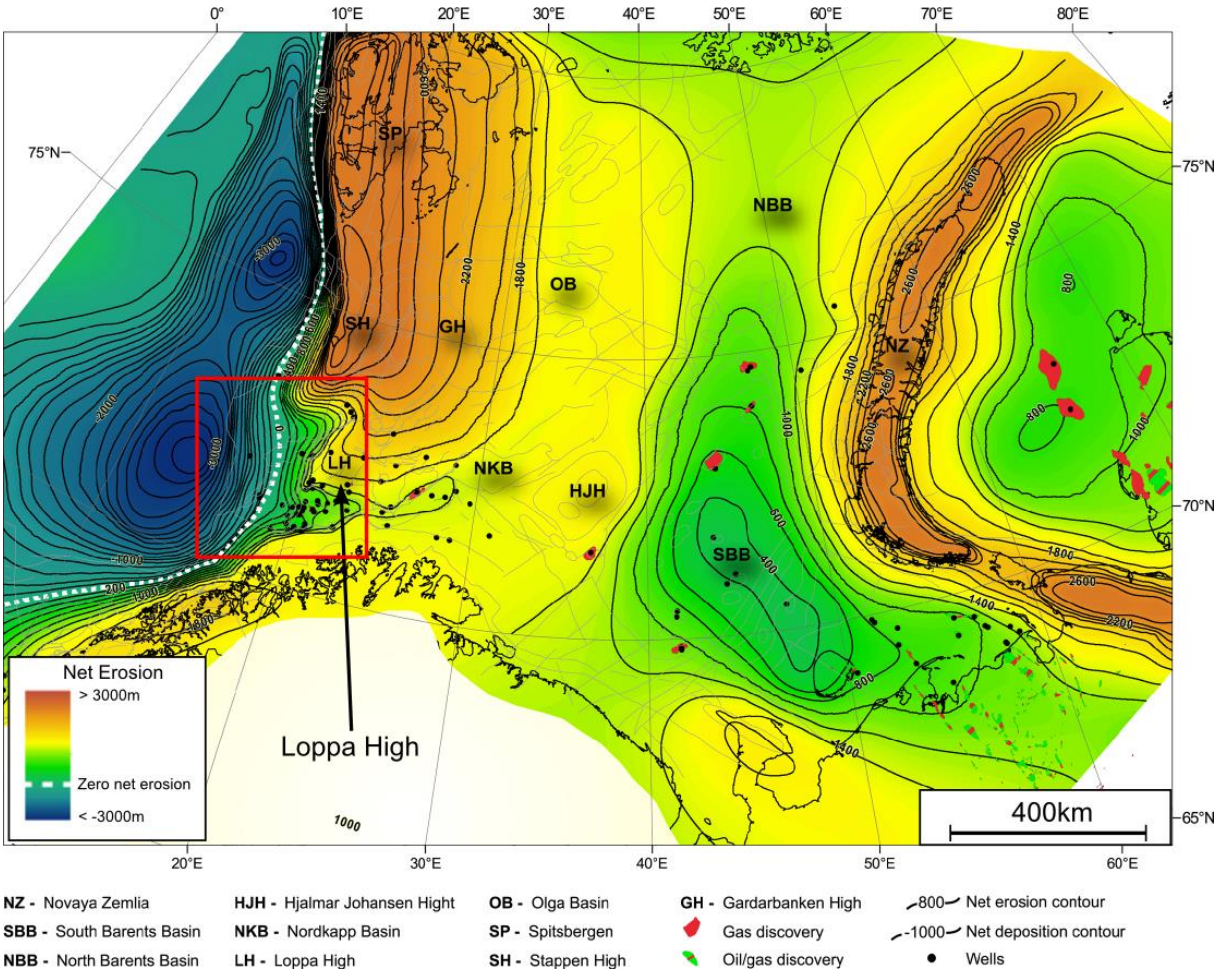

Figure 2.4 – Regional map illustrating the estimated net erosion of the Greater Barents Sea. In the west, there has been no erosion, only subsidence. The net erosion value varies from zero to 3000m (Henriksen et al., 2011a). Study area (red box) is located west of Loppa High crossing the line of zero net erosion.

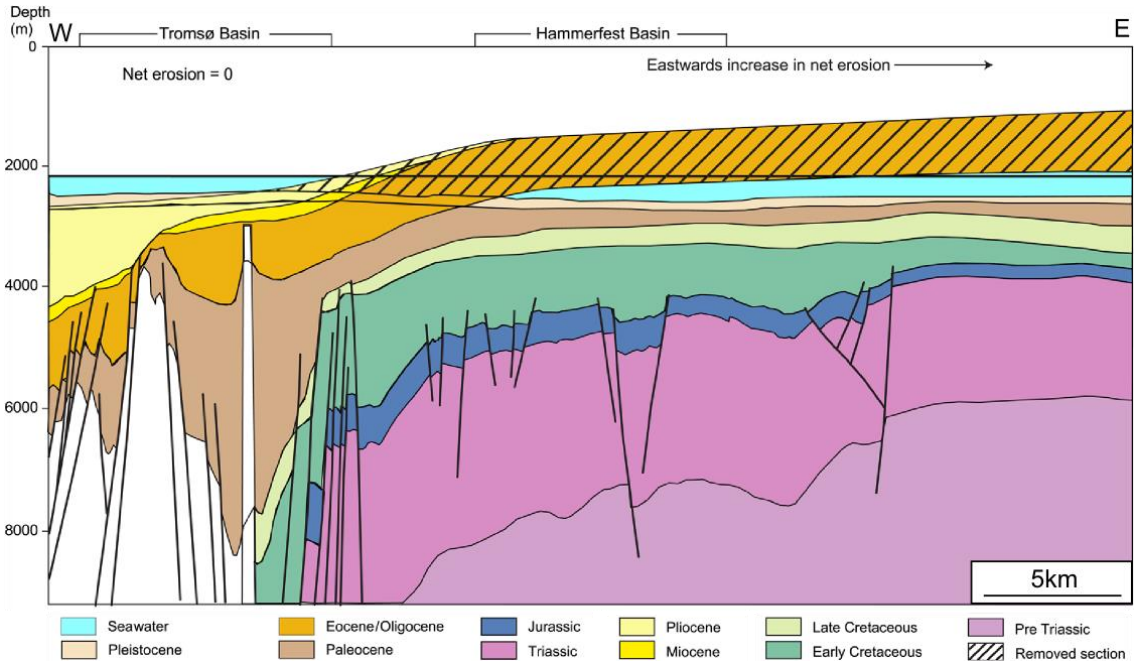

Figure 2.5 – Net erosion of the Barents Sea showing stratigraphy and the difference in erosion from west to east over parts over the study area (Henriksen et al., 2011a).

2.1.4 Source Rock

Numerous source-rock formations are present in the SW Barents Sea (Vadakkepuliyambatta et al., 2013). Potential source rock material is found in the Torsk, Kolmule, Hekkingen, Tubåen and Snadd formations. The Torsk fm. is of probable gas-prone shale and coals, mainly located within the western margin. The Kolmule fm. is a minor source rock, while the Hekkingen fm. is the major source rock with the highest petroleum potential in the Barents Sea (Gabrielsen et al., 1990). The source rock potential is variable due to the large differences in both uplift and erosion of the area. The different source rocks are summarized in the Barents Sea nomenclature (fig. 2.3).

2.1.5 Geological Plays

Geological play models are geographic and stratigraphic defined zones where specific sets of geological factors exist so that hydrocarbons may be provable (NPD, 2014). A working petroleum system with the geological factors present are needed to define a play. This includes; reservoir rock, mature source rock, trap and migration pathways. Several different geological plays are defined in the Barents Sea. Plays that interact with the area of study are presented in figure 2.6. Three different geologic plays defined by the NPD (2014) are located close to and within the study area;

- (a) Lower to Middle Jurassic play
  - Bjl,jm-6 (blue)
- (b) Upper Jurassic to Lower Cretaceous play
  - Bju,kl-3 (green)
- (c) Paleocene and Supra Paleocene play
  - Beo-1 (orange)

Snøhvit and Goliat are existing hydrocarbon fields within the Lower to Middle Jurassic play model. The likelihood of petroleum presence increases with a nearby geological play. Other geological plays defined in the Barents Sea are the Triassic, Middle to Upper Permian, Carboniferous to Permian and the Lower Carboniferous play. These plays cover other parts of the Barents Sea and are therefore not included in this thesis, as its focus is mainly on the Mid-Jurassic and younger sediments within the Tromsø Basin.

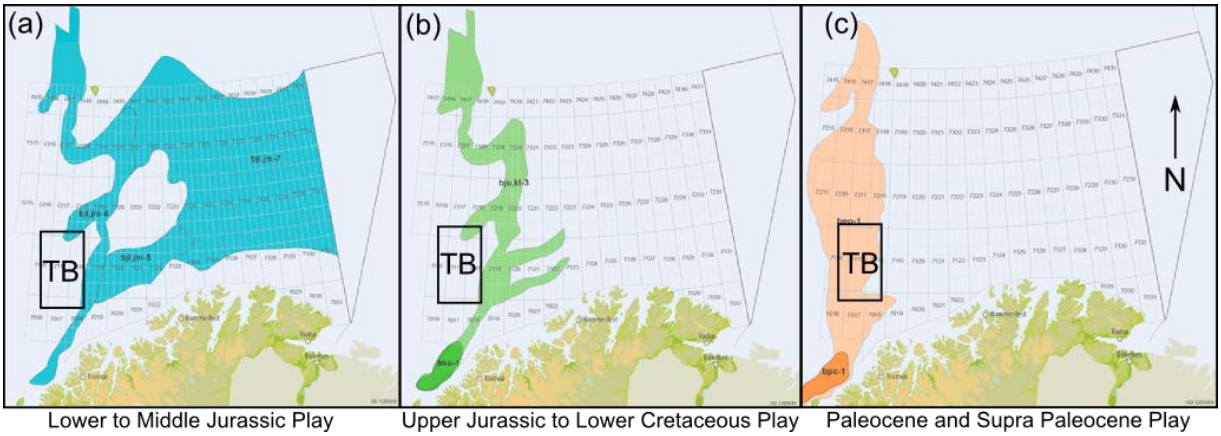

Figure 2.6 – Barents Sea geological plays defined by the NPD. (a) Lower to Middle Jurassic play. (b) Upper Jurassic to Lower Cretaceous play. (c) Paleocene and Supra Paleocene play. These plays are located close to or related to the study area and the Tromsø Basin (black box). The plays are associated with potential occurrence of shallow gas accumulations as there are known working petroleum systems within the study area (NPD, 2014).

2.2 Tromsø Basin

Definition of a basin (Gabrielsen, Faerseth, Hamar, & Rønnevik, 1984);

"Basin: A low area, tectonic in origin, in which sediments have accumulated (e.g. a circular centrocline, a fault-bounded intramontane feature, or a linear crustal down warp). Such features were basins at the time of sedimentation, but are not necessarily so today."

The Tromsø Basin is a north-south oriented, deep Cretaceous sedimentary basin, characterized by the predominance of diapiric structures (Øvrebø & Talleraas, 1977). The depth of the basin basement is calculated to be roughly 10-13 km (Gabrielsen et al., 1990).

2.2.1 Geographical Location

The study area of this project is the Tromsø Basin and adjacent areas in the SW Barents Sea (fig. 1.1 and 2.2). The Tromsø Basin is defined by the Gabrielsen et al. (1990) to be located at the geographical coordinates from 71°N to 72°15'N and from 17°30'E to 19°50'E. The Senja Ridge borders the Tromsø Basin to the east. Along its western flank, The Ringvassøy-Loppa Fault Complex separates the Tromsø Basin from the Hammerfest Basin and the Loppa High. Towards the southeast, the Troms-Finnmark Fault Complex is located. The Harstad Basin borders the south and southwestern parts of the Tromsø Basin and along the northern border, the Veslemøy High separates the Tromsø Basin from the Bjørnøya Basin.

2.2.2 Development and Evolution

The Tromsø Basin mainly evolved in response to Late Jurassic-Early Cretaceous extension (Faleide et al., 1993). Similar to the rest of the Barents Sea, there is a NNE-SSW trending axis within the Tromsø Basin. Several salt diapirs are situated mainly in the south and central parts of the basin. These are mapped by Faleide et al., (1993; 1984), and seen in figure 2.7, which is a showing a more detailed structural map of the SW Barents Sea with three different composite profiles crossing Tromsø Basin in the north, south and central parts of the basin. The main faults located within Tromsø Basin have a NNE direction. A large deep-seated salt massif rising towards the surface is located in the central parts of the basin, with isolated diapirs spread around within the basin borders (Faleide et al., 1984). The main structural elements within the SW Barents Sea are seen in both figures 2.2 and 2.7. Figure 2.2 shows an overview of the structural elements of the Greater Barents Sea (Henriksen et al., 2011b), while figure 2.7 shows a more detailed map of the SW Barents Sea tectonic framework (Faleide et al., 1993).

Evolution of the Tromsø Basin is summarized in figure 2.8, and described in detail by Faleide et al. (1984). The development of the Tromsø Basin and its nearby located highs and basins is illustrated in figure 2.9, showing major deposition, subsidence, uplift and faulting, and at what times these geological events occurred. Major subsidence events occurred in Mesozoic, mainly in Late Cretaceous, while the major faulting events occurred in Late Jurassic and Late Cretaceous (Faleide et al., 1984). The evaporites, later developing into salt diapirs, were deposited in Paleozoic, mainly during Devonian, Carbon and Permian (Bugge et al., 2002).

Erosion in the Tromsø Basin range from 0m-1000m, with the geological basin being a part of the drainage area of the Bjørnøya Fan located in the W Barents Sea (Fiedler & Faleide, 1996). This sedimentary wedge consists mainly of Late Pliocene-Pleistocene glacial deposits (Glørstad-Clark et al., 2010) and can be seen across Tromsø Basin as the westward, upper sedimentary wedge (fig. 2.5).

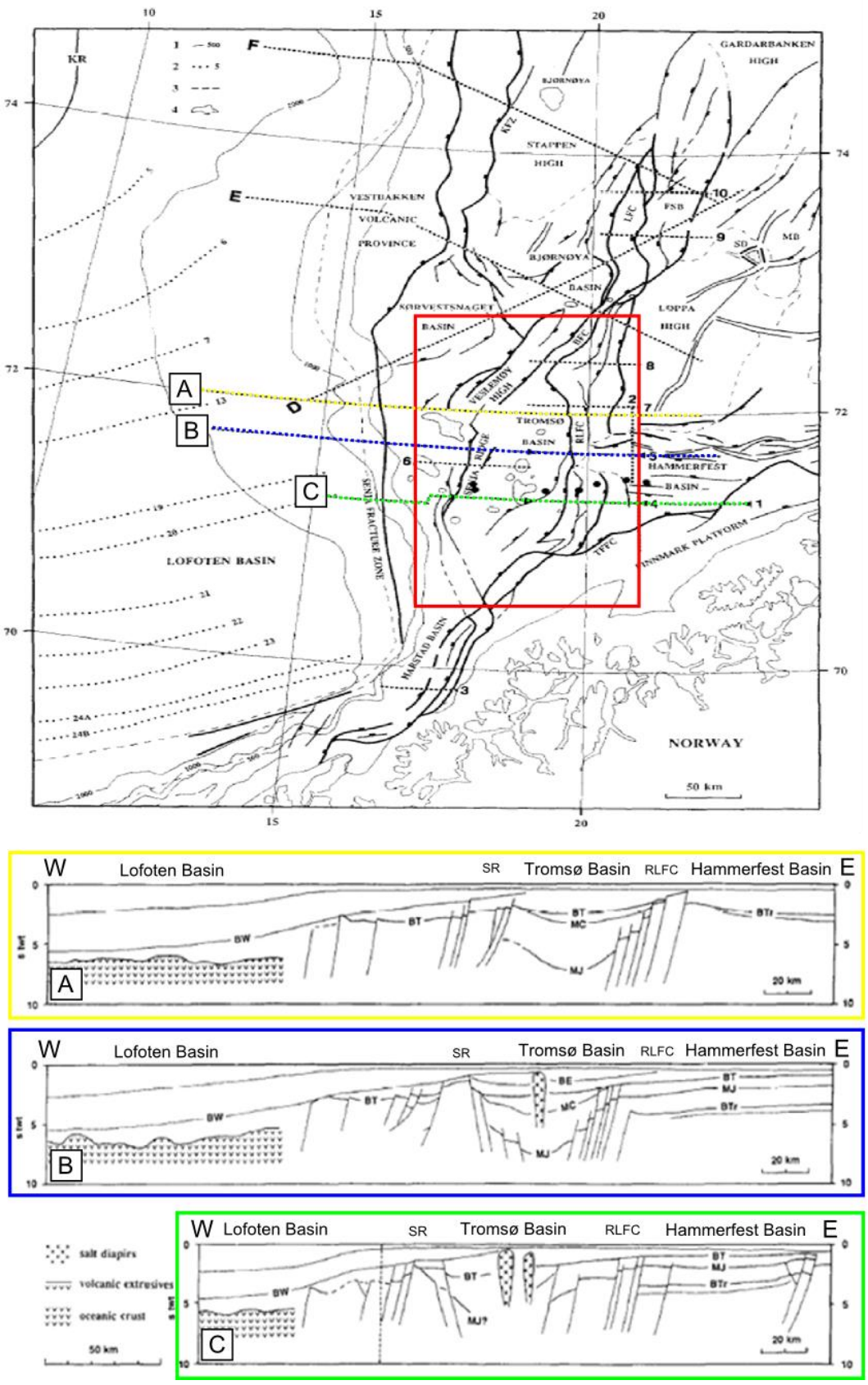

Figure 2.7 - Main structural features in the SW Barents Sea and location of selected seismic lines shown. Seismic line A, B and C cover the Tromsø Basin. Red box indicates the study area. Three different lines (A-C) show the difference in the northern, central and southern parts of TB. Several salt diapirs are located within the basin boundaries, being visible on the map. (Faleide et al., 1993)

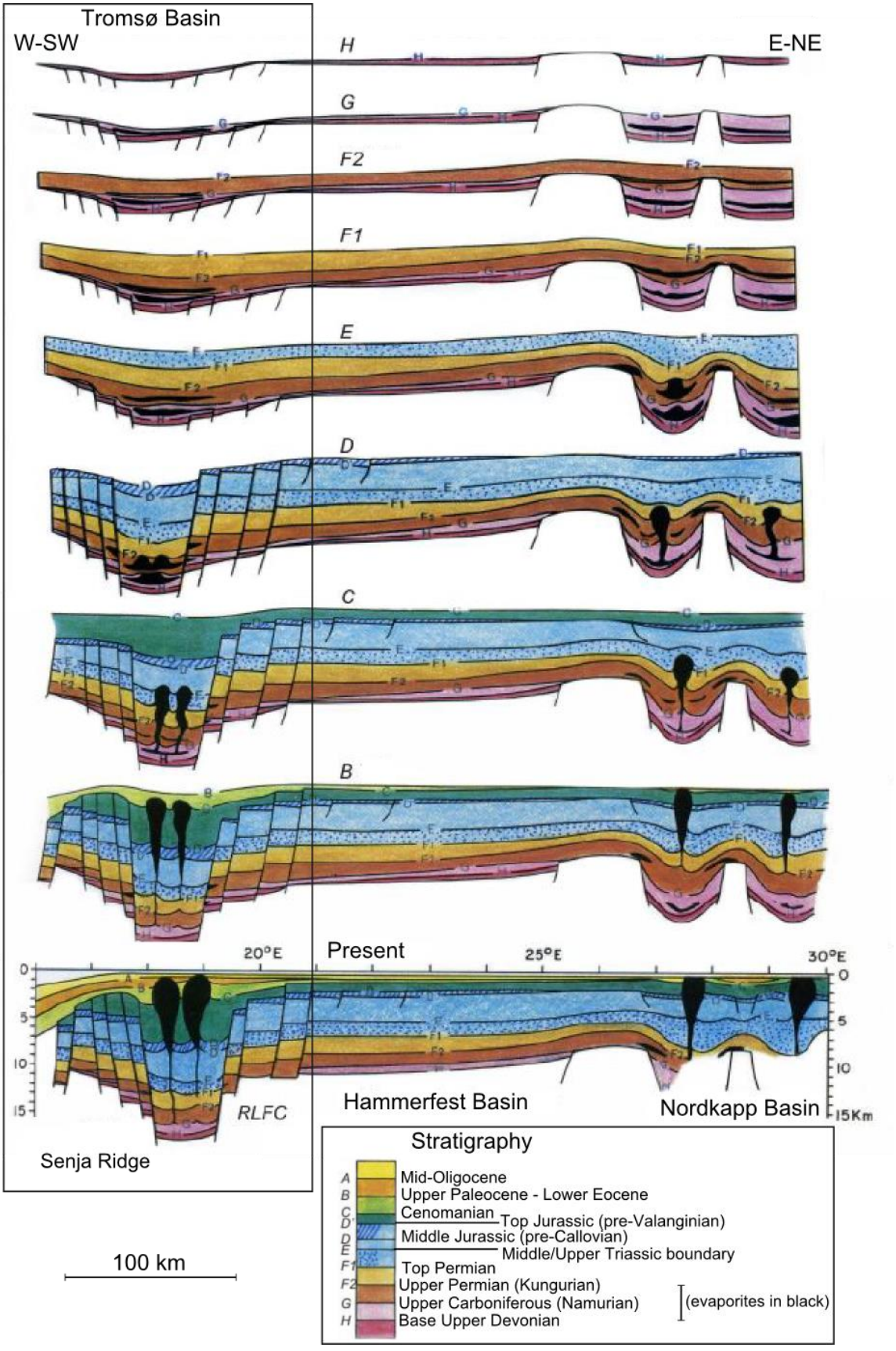

Figure 2.8 – Evolution of the SW Barents Sea and the Tromsø Basin (black box) (Faleide et al., 1984).

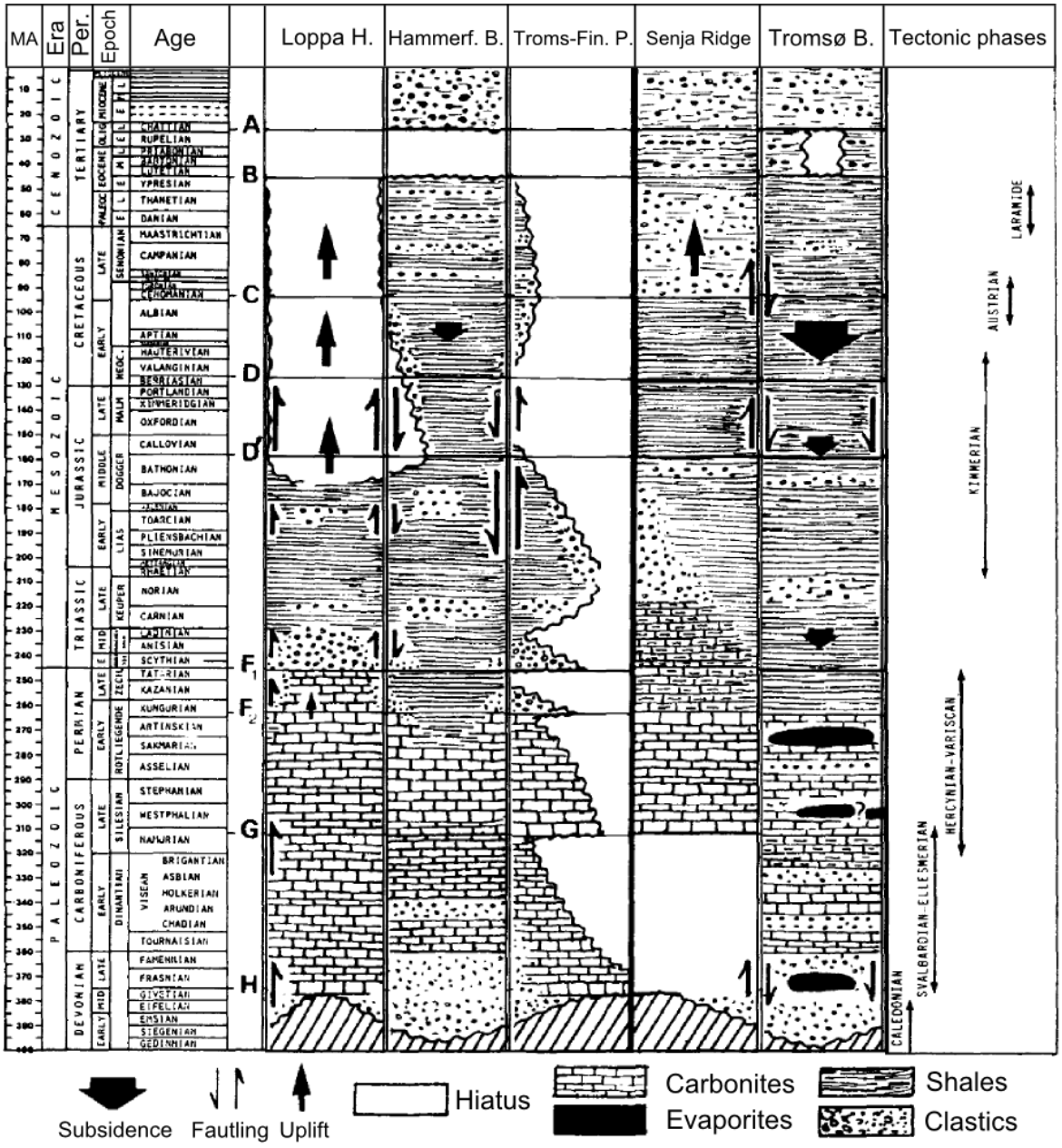

Figure 2.9 – Development of the Tromsø Basin and adjacent areas, showing major geological events, such as uplift, faulting and subsidence, together with main deposition and hiatus (Faleide et al., 1984). Figure is based the same tectono-sedimentary evolution illustrated in figure 2.8 (age A-H).

Figure 2.10 shows a simplified composite W-E profile across the Tromsø Basin based on work by Faleide et al. (1993) and Gabrielsen et al. (1990). The figure uses a seismic line across Tromsø Basin and the same colors as described in the Barents Sea stratigraphy and nomenclature (fig. 2.3), showing the main reflectors available in the dataset. These reflectors are the Torsk, intra Torsk and the Kolmule formations. It illustrates the same geological features described earlier, being a deep sedimentary basin with diapiric structures located in the basin center. The salt layer is thought to be of Permian age, but may also be from Upper Devonian evaporates deposited in a graben located below the basin (Faleide et al., 1984).

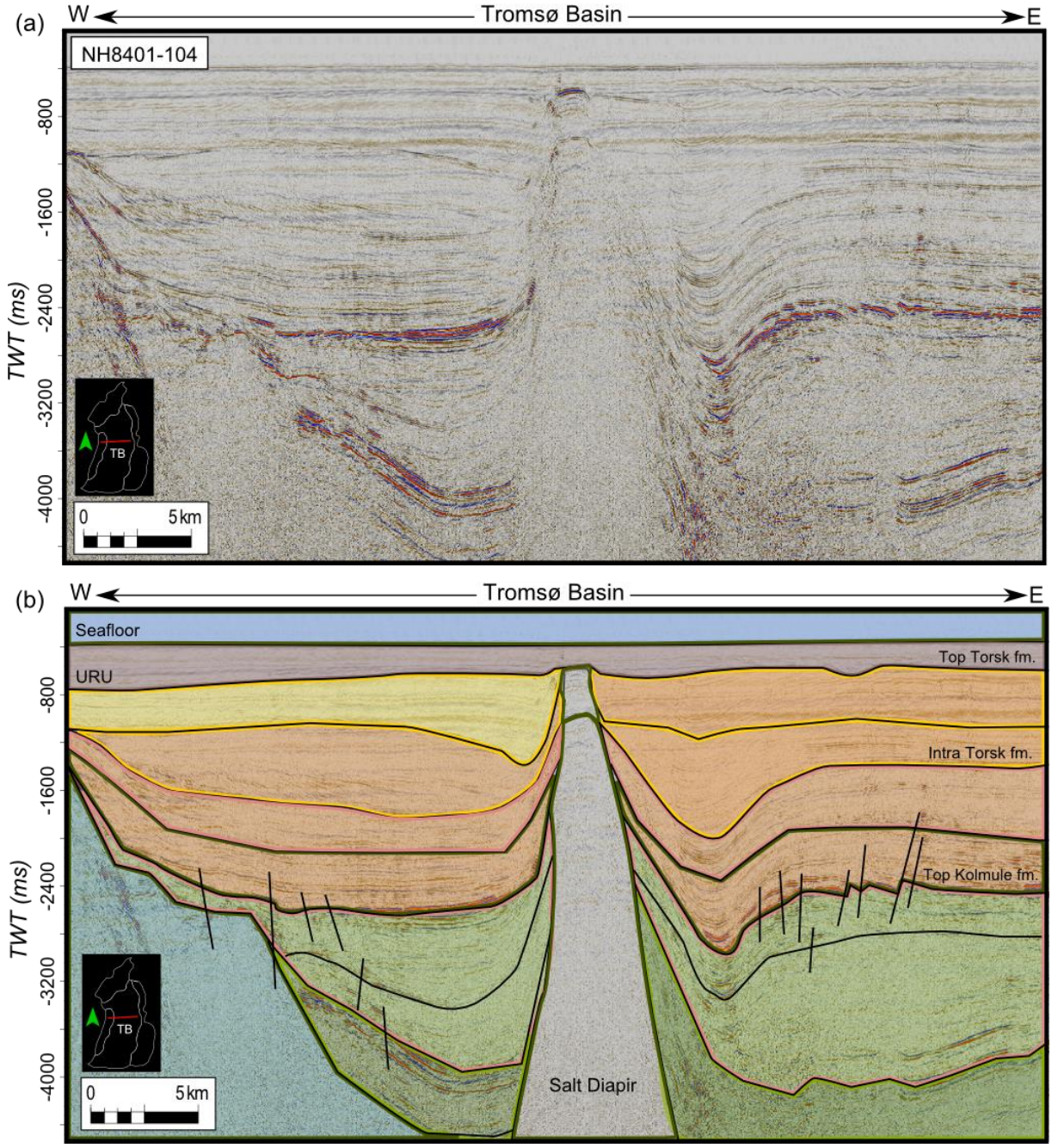

Figure 2.10 – (a) Seismic 2D line NH8401-104 across the Tromsø Basin. (b) Simplified profile, using seismic 2D line (a) and based on work from Faleide et al. (1993) and Gabrielsen et al. (1990). Figure uses same colors as shown in the Barents Sea nomenclature (fig. 2.3) to identify different sequences and ages. Torsk, intra Torsk and Kolmule formations are interpreted in the available data. Notice the bright spot located above the salt diapir.

2.2.3 Well Data

To get an overview of the stratigraphy of the Tromsø Basin and adjacent areas in the SW Barents Sea, gamma ray log data from four different publicly available wells are correlated giving a simplified overview of the study area stratigraphy (fig. 2.11). The four wells are located in the north, south, east and west of the Tromsø Basin. Wellbore 7117/9-2 is located west of Tromsø Basin, close to the Senja Ridge. Wellbore 7219/8-1S is located north of Tromsø Basin, close to the Veslemøy High. Wellbore 7119/7-1 is located east of Tromsø Basin, close to Ringvassøy-Loppa Fault Complex. Wellbore 7019/1-1 is locates south of Tromsø Basin, close to the Troms-Finnmark Fault Complex. The wellbore correlation is based on defined group formation tops.

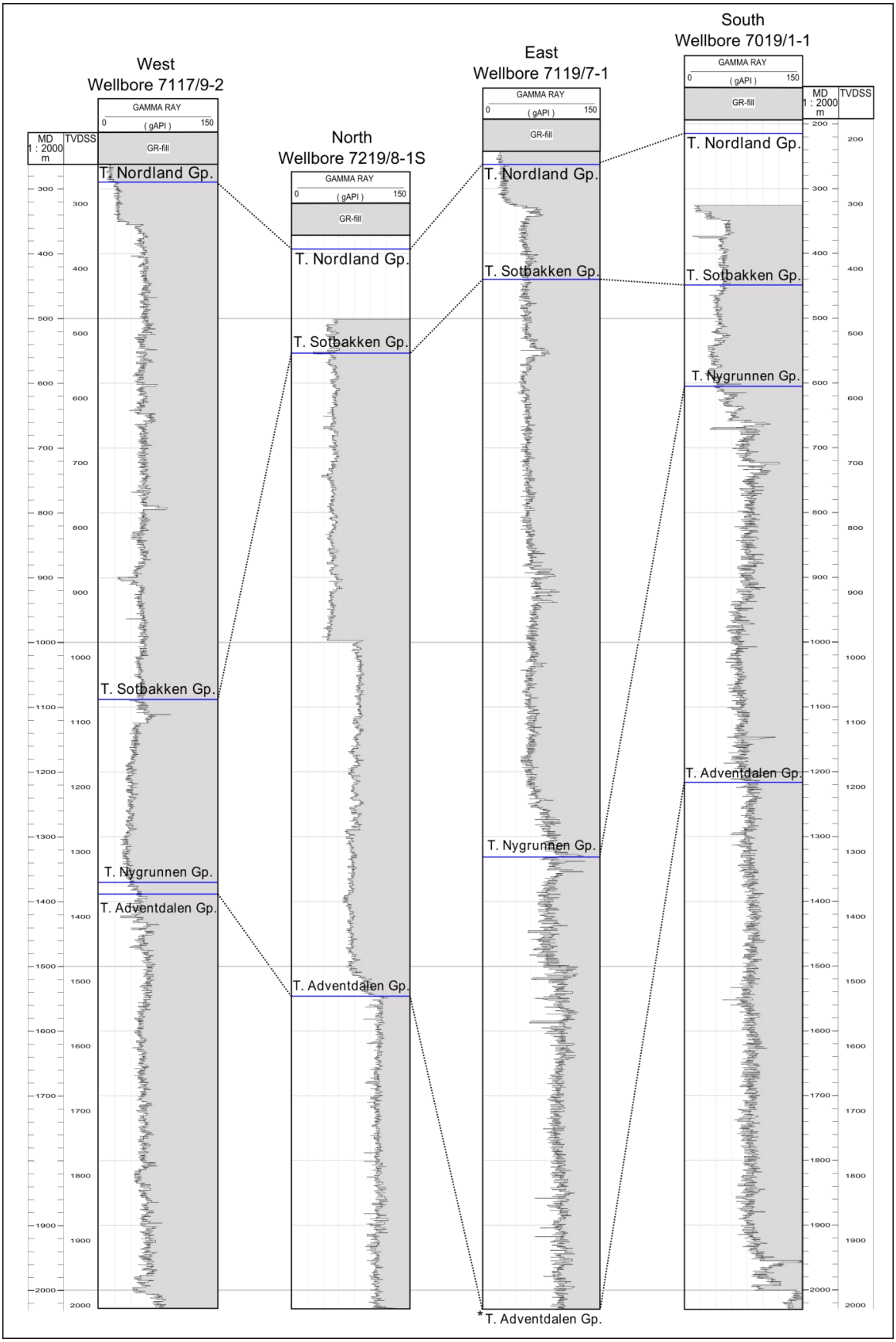

Figure 2.11 – Correlated gamma ray log data from wells located close to or in the Tromsø Basin giving a brief overview of the stratigraphy in the area. *T. Adventdalen Gp. Wellbore 7119/7-1 is located deeper than 2000m and is not seen in figure.

The lithostratigraphic groups used in the wellbore data (fig. 2.11) is based on work by the Committee on the Stratigraphy of Svalbard (Stratigrafisk Komite for Svalbard, SKS). The Barents Sea equivalents are summarized in figure 2.12 based on work by Dallmann (1999). The Kolmule fm. located within the Nordvestbanken Group is part of the equivalent Adventdalen Group. The younger formations, the Torsk, Kveite and Kviting, has no group equivalents and are part of the same groups for the Svalbard and the Barents Sea lithostratigraphy. The Torks fm. belong within the Sotbakken Group, while the Kveite and Kviting fm. belong to the Nygrunnen Group.

<table>
<tr><th colspan="3">Hammerfest Basin / Western Barents Shelf</th></tr>
<tr><th>WORSLEY et al. 1988</th><th colspan="2">SKS, present volume</th></tr>
<tr><td>Nygrunnen Group</td><td colspan="2">Nygrunnen Group</td></tr>
<tr><td>Nordvestbanken Group</td><td colspan="2" rowspan="2">Adventdalen Group</td></tr>
<tr><td>Teistengrunnen Group</td></tr>
<tr><td>Realgrunnen Group</td><td rowspan="2">Kapp Toscana Group</td><td>Realgrunnen Subgroup</td></tr>
<tr><td rowspan="2">Ingøydjupet Group</td><td>Storfjorden Subgroup</td></tr>
<tr><td>Sassendalen Group</td><td>Ingøydjupet Subgroup</td></tr>
</table>

Figure 2.12 – Lithostratigraphic group equivalents for the Western Barents Sea used in the wellbore data (fig. 2.11) (Dallmann, 1999).

3 Methods and Data

The database used in this thesis consists of both 2D and 3D seismic data. A large number of different 2D seismic surveys are used to map the exact distribution of shallow gas accumulations and fluid-flow features in the Tromsø Basin and adjacent areas in the SW Barents Sea. The seismic data is provided by the NPD Petrobank and are all publicly available. The 3D seismic covers only smaller parts of the study area and the data is used to focus on more specific amplitude anomalies with their lateral extent mapped using the wider coverage of the 2D seismic data.

3.1 Definition and Identification of Shallow Gas Accumulations

To identify shallow gas accumulations, the term shallow has to be defined. As mentioned in the introduction, there is no specified definition of what and where a shallow gas accumulation is located. It has suggested that shallow gas accumulations are identified and located within the upper 1000m of the lithosphere (Davis, 1992; Solheim & Larsson, 1987). This thesis uses the term shallow gas as amplitude anomalies identified to be hydrocarbon accumulations located at depths above the Early Cretaceous sediments with the upper parts of the Kolmule fm. being the lower boundary condition for the identification of shallow gas accumulations. This classification bases on what started as a definition of a depth at 2000ms TWT within the seismic data due to the quality of the available seismic data. Assuming a p-wave velocity of approximately 2000m/s, 2000ms TWT will equal 2000m on the seismic data. The general trend for this depth is the location of the Kolmule fm. top. As this study is trying to understand the stratigraphic controls in this region, this is set to be the new boundary condition use for the term shallow gas based on the 2000m depth condition. This boundary varies with location within the SW Barents Sea, but it gives an indication of at what depths the shallow gas accumulations are identified. The depth of the Kolmule fm. across the Tromsø Basin (fig. 2.10) gives an indication of the depths the mapping of shallow gas accumulations is performed in this thesis. The focus has been on seismic amplitude anomalies associated with shallow gas accumulations down the upper Kolmule fm. Other formations of interest in the study are the Torsk fm. and the intra Torsk fm., both located above the Kolmule fm. The identification of shallow gas accumulation on the seismic data is based on seismic indications of hydrocarbons, chapter 1.4.

3.2 Seismic Data

3.2.1 2D Seismic Data

The seismic data consists of several 2D multi-channel seismic profiles covering a large area of the SW Barents Sea. These seismic 2D lines come from many different seismic surveys giving them different properties such as variations in signal quality, and both horizontal and vertical resolution. These surveys date back from the early 80's and up to date. Lines and surveys used in this thesis are selected to cover parts of the Tromsø Basin and adjacent areas. All available 2D seismic data is publicly available. Figure 3.1 illustrates the available 2D seismic data. The map shows the outline of the main geological features in the Barents Sea (similar to fig. 2.2). The different 2D surveys are indicated with different colored lines (fig. 3.1(b)). Table 2.1 lists all the available 2D seismic groups and surveys available for this project.

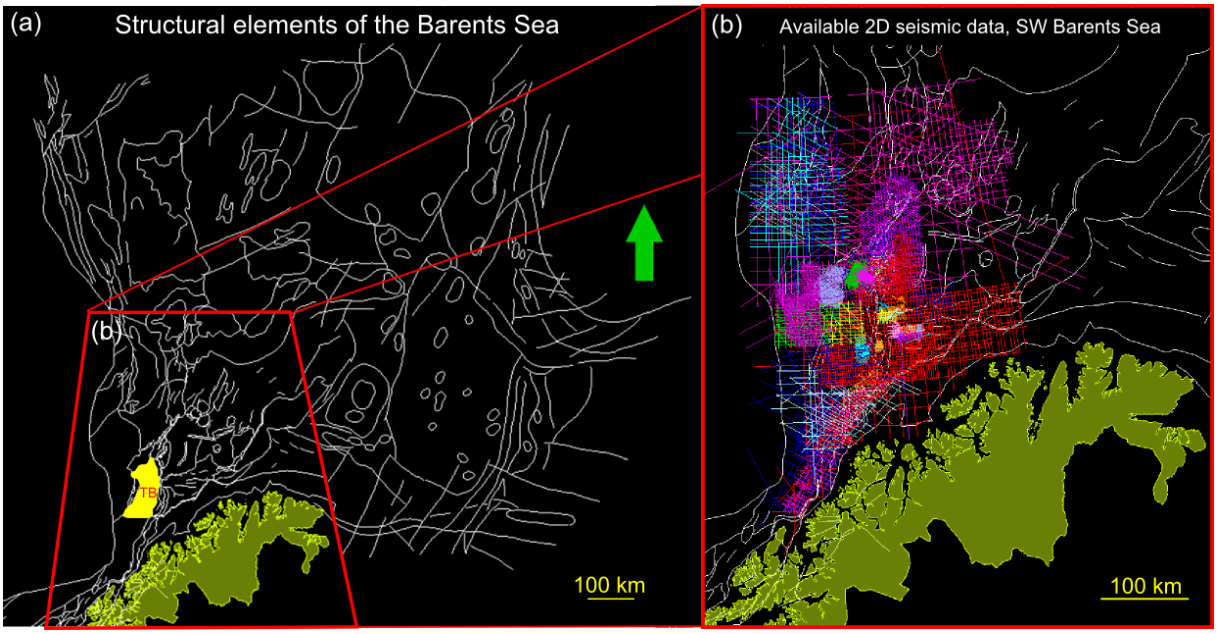

Figure 3.1 – Available 2D seismic data. (a) Location of the SW Barents Sea and structural elements available in the Petrel software. Tromsø Basin is indicated in yellow. (b) Red box is a zoomed image with location in the Barents Sea shown in (a). This shows all publicly available 2D seismic data from the SW Barents Sea. The different 2D seismic surveys are illustrated in different colors.

Table 3.1 – List of available seismic 2D surveys in the SW Barents Sea.

Main group Survey	**Subgroup Survey**
TGS BSW	
TGS TR	**TR82R1, TR83R1, TR84R1, TR73R1, TR74R1, TR75R1, TR77R1**
BARENTS SEA 2D	**EL8401, EL9701, EL0001, F86, GBW88, LHSG89, NH8205, NH8401, NH8402, NH8403, NH8505, NH8506, NH8610, NH8904, NH9702, NH9703, NPD-BJRE84, NPD-BJV287, NPD-BV-BVRE87, NPD-TR84, NPD-TR85, SG8962, SG9106, SG9115, SG9309, SG9401, SH8601, SH9103, ST8624, ST8725, ST8817, ST912-R98, ST9706, T89, TGS90, TGS83**

Existing data available in the 2D seismic consists of previously mapped fluid-flow features and leakage along faults. The results in this thesis uses these data to identify potential shallow gas accumulations, their potential migration pathways and the stratigraphic levels of origin. Figure 3.2 shows an overview of the available mapped data being gas chimneys and leakage along faults. This data is similar to other studies in the SW Barents Sea (Vadakkepuliyambatta et al., 2013). Predefined formation tops are also available in the 2D seismic data. This data is based on work from earlier master theses from the University of Tromsø (UiT). The predefined formation tops with the best coverage and quality consists mainly of the Torsk fm. and the Kolmule fm., with an intra Torsk fm. available (fig. 3.5).

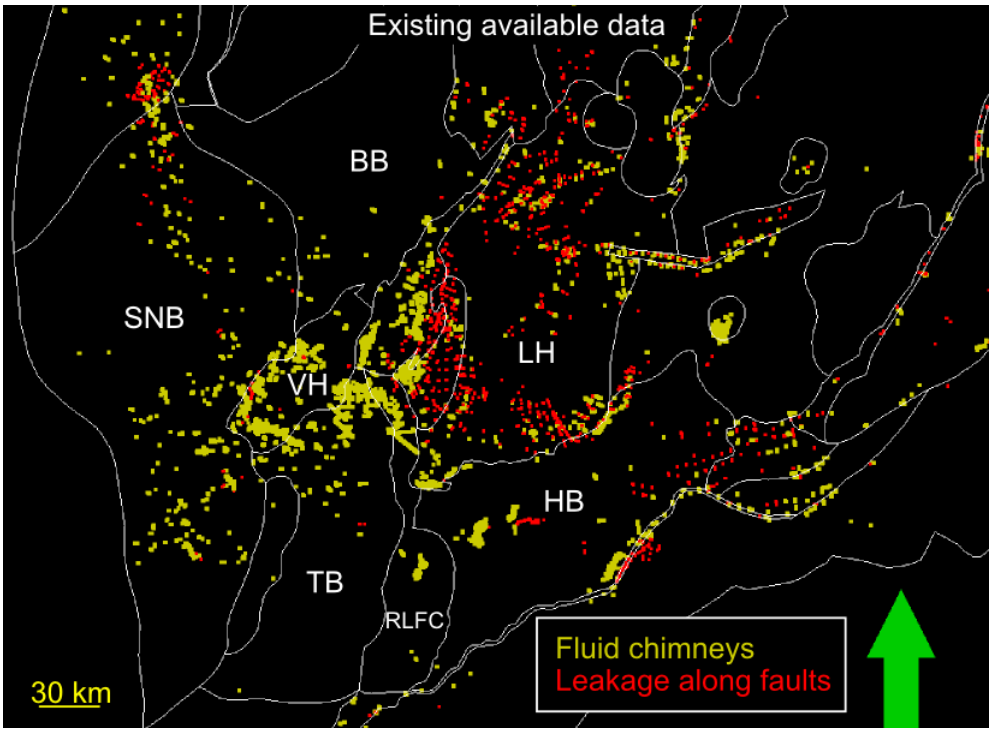

Figure 3.2 – Existing data available for use in this thesis showing mapped fluid chimneys (yellow) and leakage along faults (red) in the Tromsø Basin and adjacent areas in the SW Barents Sea.

3.2.2 3D Seismic Data

Two 3D seismic surveys, EL0001 and LN09M01, are also part of the data used in this thesis. The exact location of the two available 3D seismic surveys is seen in figure 3.3. Elf Petroleum Norge AS acquired the seismic survey in 2000. The survey covers an area of 22km (xline) x 45km (inline), and is located within the Veslemøy High, just NW of the Tromsø Basin, extending into the northern parts of the basin. The seismic survey LN09M01 is a merged dataset that consists of several different seismic surveys. The survey covers an area of 38km (xline) x 42km (inline), and is located in NW of the Hammerfest Basin and on the western flank of the Loppa High. It also covers a small part of the Ringvassøy-Loppa Fault Complex.

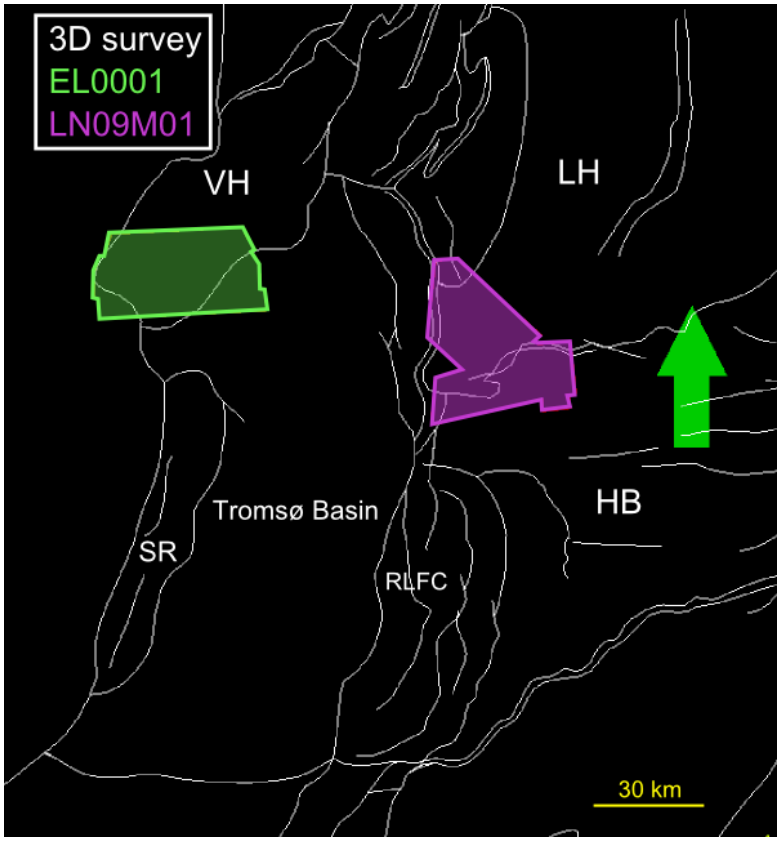

Figure 3.3 – Tromsø Basin with locations of 3D seismic surveys available for this thesis. Seismic survey EL0001 is colored green and located north and NW of Tromsø Basin, above the Veslemøy High. Seismic survey NH09M01 is colored purple and located east of the Tromsø Basin, close to and within the Hammerfest Basin.

3.3 Interpretation and Visualization Tools

All seismic data in this project is interpreted using the Schlumberger owned interpretation and visualization software Petrel 2013 edition. This software provides various seismic attribute analysis and seismic visualization.

3.3.1 Petrel Software

Figures directly from the Petrel software use a green and red arrow oriented towards the north. In the 2D figures, the arrow is green as it is only seen from above, while in 3D figures, the arrow is green on the arrow top side and red on the arrow bottom side. This gives a better understanding of the figure orientation in space. Mainly 2D visualization is used for figure simplification.

The Petrel software uses negative sign in front of depths. An example is -500ms TWT that refers to the two-way travel time (TWT) of the seismic signal. In the text, the depth in time is referred to as positive (500ms TWT).

All figures with seismic data are illustrated and visualized using the Petrel seismic default setting (fig. 3.4) having positive amplitudes indicated as yellow/red and negative amplitudes indicated as blue. Zero amplitudes are illustrated using gray. The figures can have this legend included in their legend, but the numerical values are removed, as they are not of that great interest. Instead, positive and negative amplitudes are indicated (fig. 3.4).

Mapping of shallow gas anomalies uses mainly the horizon interpretation method available in the Petrel software. The horizon interpretation method has two different available methods of choice; the manual interpretation and the guided auto-tracking. The method most frequent used in this thesis is the manual interpretation, as it gives the user better control of the interpretation. As the potential shallow gas accumulations are in general not that continuous and large in extent as a normal seismic horizon, the manual interpretation method was the preferred method. The method chosen at different interpretations is also dependent on the seismic quality of the data. There are large differences in seismic quality as there are large numbers of different seismic surveys used in this thesis. The guided auto-tracking picks points automatically within given parameters and is available for both 2D and 3D data. This method is primarily used on 3D seismic data for tracking of horizons and surfaces.

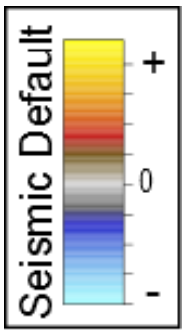

Figure 3.4 – Seismic default settings used on most figures that include seismic sections and data. Positive amplitudes are shown in yellow and red, while negative amplitudes are shown in blue.

3.3.1.1 Seismic Attributes

Seismic attributes used in the Petrel software are; the structural attribute, structural smoothing and the seismic surface attribute RMS amplitude. RMS amplitude mapping is only available for 3D seismic data, while structural smoothing of the seismic data is available for both 2D and 3D seismic data.

Structural smoothing is a smoothing of the input signal guided by the local structure to increase the continuity of the seismic reflector. It uses a Gaussian weighted averaging filter that eliminates noise and increases the signal-to-noise ratio for any structural interpretation. Details might be lost in the process, but overall it makes the seismic data easier to interpret (Schlumberger, 2009).

RMS amplitude calculates the root mean square (RMS) on instantaneous trace samples over a user specified volume or window used to distinguish high-amplitude anomalies. The RMS amplitude may be a direct indicator of hydrocarbon accumulation that is isolated from background features by an amplitude response. It is also an important attribute used for the characterizing of different sedimentary environments (Schlumberger, 2009).

3.3.1.2 Seismic Horizons

Different mapped seismic horizons are available in the 2D dataset used. These horizons are related to earlier work and master theses from UiT. Horizons used in the work of this thesis are mainly the Late Cretaceous and Tertiary formations being the Kolmule fm. top (orange), Torsk fm. (yellow) and an intra Torsk fm. (pink). A seismic example of these formation horizons are shown in figure 3.5. The seafloor reflector is also mapped. Figure 3.5(b) shows the seismic horizon Torsk fm. within the study area illustrating the 2D seismic coverage.

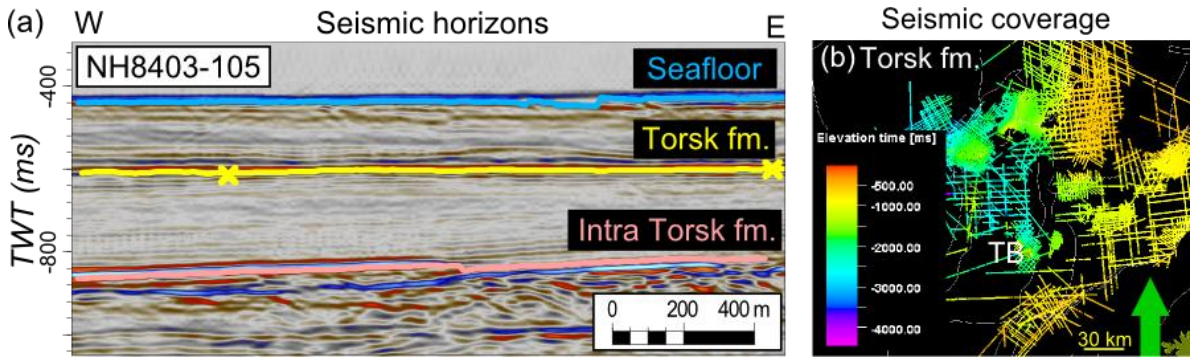

Figure 3.5 – Seismic horizons available in the 2D seismic data. (a) Seismic section with horizons of interest being the upper most horizons; Torsk fm. (yellow), Intra Torsk fm. (pink), and the Kolmule fm. (orange, not shown in this figure). Colored cross indicates crossing seismic lines with the same mapped seismic horizons. (b) 2D map of study area showing mapped Torsk fm. horizon illustrating the seismic coverage of the Torsk fm. as a result from available 2D data.

4 Results

The results are mainly based on observations and interpretations using the Petrel software and the seismic 2D and 3D data available in the SW Barents Sea. The seismic 3D datasets consists of the EL0001 and the merged dataset LN09M01. The seismic 2D data used consists of data from surveys publicly available within the study area and has its focus on the Tromsø Basin (TB) and its adjacent areas such as the Senja Ridge (SR), the Veslemøy High (VH), Loppa High (LH) and the Ringvassøy-Loppa Fault Complex (RLFC). The main objective of this thesis is to identify and map out shallow gas accumulations. The 2D data is used to map the general distribution of shallow gas accumulations, while the 3D dataset is used to look at more specific amplitude anomalies, possibly related to shallow gas accumulations. The amplitude anomalies of interest within the 3D surveys are mapped to see their lateral extents. This is to be able to find out more about potential migration pathways and origin of the shallow gas accumulations in the area, and to see if there is any connection with the deep Cretaceous Tromsø Basin. Due to the large amounts of seismic 2D data covered by this thesis the results will mainly focus on and present only an overview of the work and interpretations performed on the seismic data.

4.1 Quality of Seismic Data

Quality of the seismic 2D data varies a lot depending on the different surveys. The surveys are all using different vertical and horizontal resolution, which is not calculated and taken into account for the different surveys. The seismic data generally have a large seismic peak with smaller troughs on each side as its seafloor reflection to indicate a known positive acoustic impedance contrast. This is known as zero-phase polarity standard after the Society of Exploration Geophysics (Sheriff, 1973) and is similar to what is seen in figures 1.6(b), 1.7, 4.1 and 4.2. Figure 4.1 shows an example of variations in seismic quality from different surveys. NH9703 is a 2D seismic survey from 1997 (fig. 4.1(a)) while NH8401 is a similar 2D seismic survey from 1984 (fig. 4.1(b)). The wiggle trace illustrates the same seafloor reflection (box 1 and 3) being a positive seismic reflector, and a bright spot (box 2 and 4) being a potential shallow gas accumulation, as a phase-reversed negative reflection compared to the seafloor reflection. These seismic lines are shot in the same parallel W-E direction across the Tromsø Basin and they are located very close to each other. Their location is seen in the smaller map, showing the outline of the Tromsø Basin and adjacent structural elements. The quality of the seismic from the newer NH9703 survey is higher compared to the quality of the seismic from the older NH8401 survey. In general for the 2D seismic data in this thesis, only the upper 2000-2500ms TWT of good seismic quality.

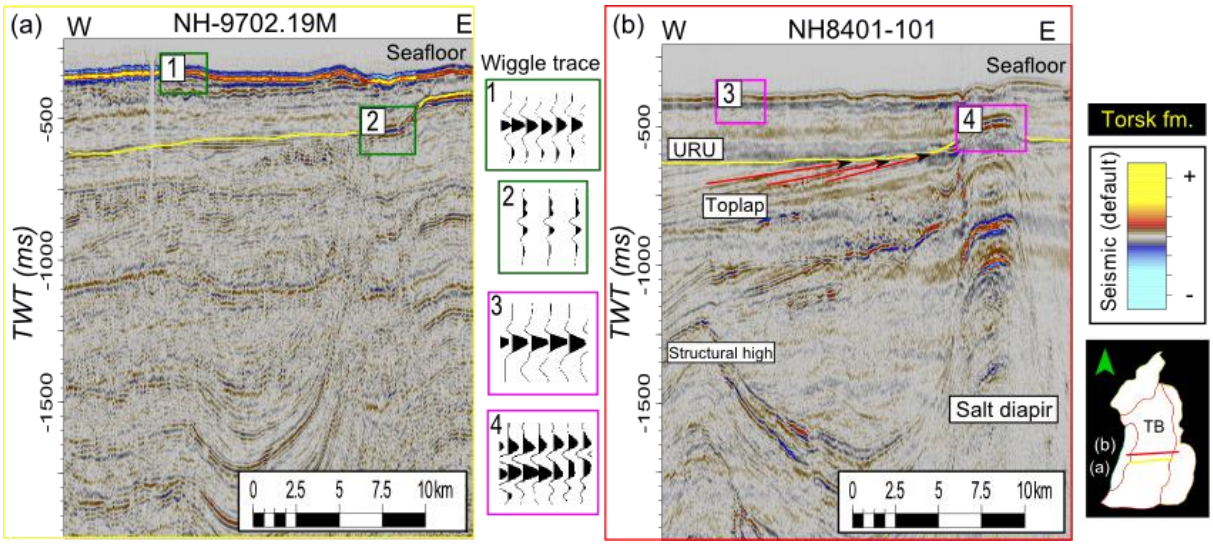

Figure 4.1 - Difference in the 2D seismic quality. (a) Seismic section showing the seafloor and its wiggle trace (1) and a bright spot and its wiggle trace (2). (b) Seismic section located close to (a) showing the same features with the seafloor and its wiggle trace (3) and the bright spot and its wiggle trace (4). Notice the phase-reversal of the bright spot (2 and 4) compared to the seabed reflection (1 and 3). The URU is identified related to seismic toplap.

4.2 Identification of Shallow Gas Accumulations

Indications of shallow gas accumulations are found throughout the majority of the study area. Bright spots located above fluid-flow features are good indicators of hydrocarbon accumulations. The bright spots mapped out are generally high-amplitude anomalies with a phase-reversed signal compared to the seafloor reflection (fig. 4.2). The seafloor reflection is known to have a positive AI contrast and is used as a reference to interpret bright spots of negative polarity. Examples of this are seen in figures 4.1 and 4.2, showing the wiggle trace of both the seafloor reflection and different bright spots being potential shallow gas accumulations. Amplitude anomalies are more easily identified associated with the mapped subsurface fluid-flow systems (fig. 3.2) in the study area. Shallow gas accumulations associated with fluid chimneys varies in both stratigraphic extent and location. Some show

indications of shallow gas accumulating beneath and within the Kolmule or Torsk formations while others show indications of leakage all the way up the seabed. Figure 4.2 illustrates different examples from the seismic 2D data with bright spots related to subsurface fluid-flow systems. Figure 4.2(a) shows isolated vertical fluid chimneys and associated bright spots being phase-reversed amplitude anomalies. The associated wiggle trace is shown in small boxes, showing both the mapped bright spot amplitude anomaly and the seafloor reflection. Figure 4.2(b) illustrates a zone of acoustic masking, being a much larger extent of a fluid-flow system and the associated mapped phase-reversed bright spots. The short, horizontal dark yellow lines are the mapped gas chimneys located in the available dataset, with vertical lines illustrating the lateral extent. The Torsk (yellow) and Kolmule (orange) formation tops are also displayed as horizons across the seismic data. These formations are the pre-existing mapped horizons available in most of the 2D datasets (fig. 3.5). Figure 4.2(a) has potential shallow gas accumulations located within the Torsk fm., while figure 4.2(b) shows both leakage to the seafloor (upper right side) and accumulations just beneath the Torsk fm. top (lower left side) acting as a boundary in this particular case. There are no indications of further leakage above this individual bright spot.

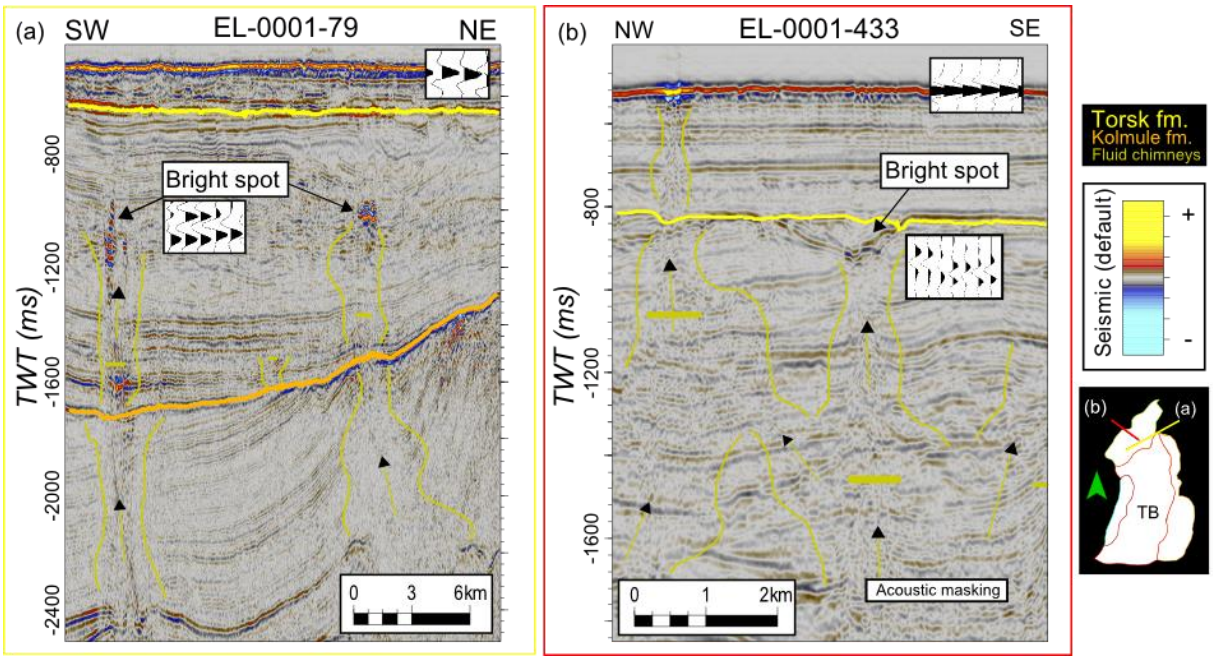

Figure 4.2 - Mapped fluid-flow systems and associated bright spots. (a) Bright spots located above isolated fluid chimneys within the Torsk fm. (b) Bright spot located above a larger fluid-flow system located just beneath the Torsk fm. top. Left side of the figure indicates leakage up to the seabed. Possible migration pathways are marked with dark yellow arrows. Wiggle trace signal shows phase-reversed bright spots compated to the seabed reflector.

The amplitude anomalies identified and mapped are primarily bright spots that are negative and phase-reversed (compared to seafloor reflector) and enhanced reflections located above or close to existing fluid-flow systems interpreted as gas chimneys. Acoustic masking and chaotic reflection patterns are seismic anomalies found in association with the mapped fluid-flow systems (fig. 4.3). Figure 4.3(a) shows an area of chaotic reflections and an example of an enhanced reflection, while figure 4.3(b) shows an area of acoustic masking or wipe-out zone located in a fluid-flow system, beneath a large bright spot. This specific bright spot is a large potential shallow gas accumulation. The base of this feature also show a reversed-phase reflection, most likely related to the base of the gas accumulation. This example is similar to what is illustrated in figure 1.6(b). There are no

indications of seepage to the seafloor or other areas located above these features, being evidence of this to be fluids or gas still trapped in the subsurface. Its origin is difficult to identify as the seismic signal loses its strength further down. The features seem to bypass the Kolmule fm., indicating that this could be potential deep-source generated hydrocarbons (Cartwright, Huuse, & Aplin, 2007). Both zones of potential gas accumulations are located close to and beneath the Torsk fm. top. and the URU.

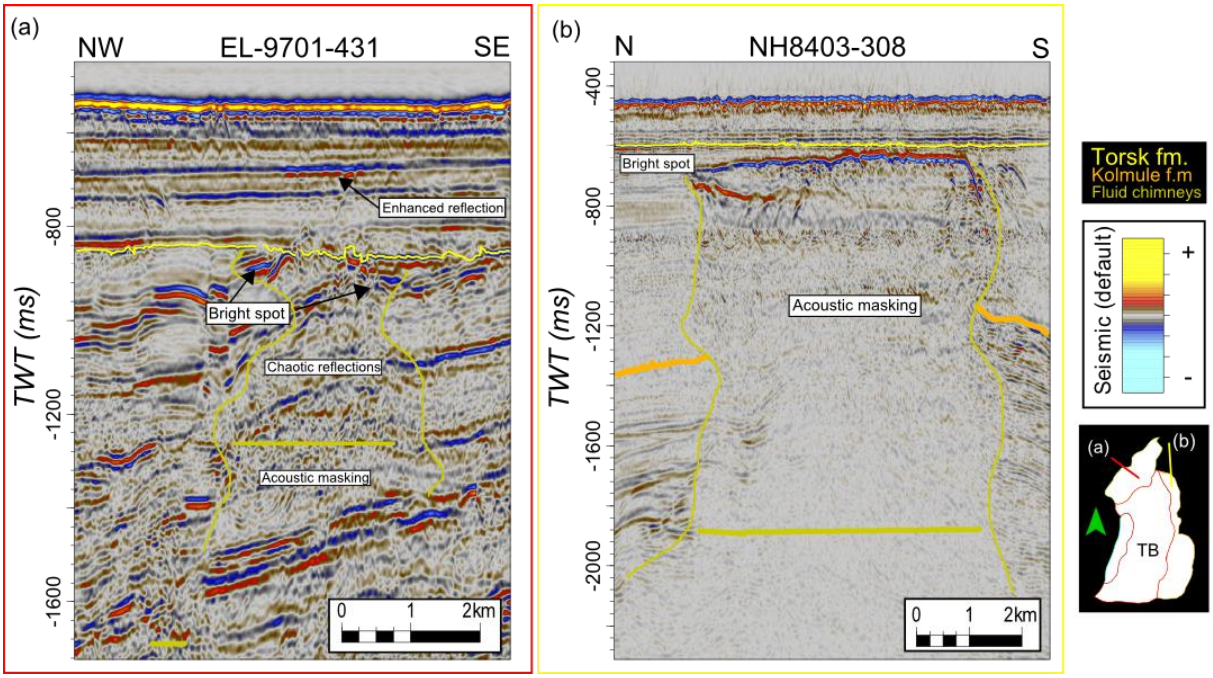

Figure 4.3 - Amplitude anomalies located close to existing mapped fluid flow. (a) Seismic section showing enhanced reflection, bright spot, chaotic reflection pattern and acoustic masking located close, within and above mapped gas chimneys. (b) Seismic section with a larger bright spot being a potential shallow gas accumulation, located above an area of acoustic masking and a deep source fluid-flow system. Both features are located just beneath the Torsk fm. top.

Mapping of shallow gas accumulations in association with fluid-flow systems and leakage along faults is based on the existing mapped data available, which is related to the study by Vadakkepuliyambatta et al., 2013. The existing data available in this thesis is mapped out in Petrel and indicated in the program as mapped areas of gas chimneys and leakage along faults. The results from the Petrel software are seen in figures 4.3 and 4.4. Figure 4.4 gives an indication of the existing data available for this thesis using the Petrel software. Figure 4.4(a) shows one type of mapped fluid flow associated with faulting and is indicated by light green horizontal lines. These lines are interpreted to be leaking faults. Figure 4.4(b) shows the already mentioned existing gas chimneys and zones of fluid flow. The Petrel software displays only the horizontal lines indicating leakage along faults and chimneys together with the different formation top horizons. Indications of faults and gas chimney extent is added only for a better visualization of the figures. Figure 4.4(b) shows stratigraphic boundaries along both the Kolmule and Torsk formation tops, but also smaller indications of boundaries located within the Torsk fm. at different stratigraphic levels. These indications within the Torsk fm. are not as bright amplitude anomalies as those located closer to the Kolmule and Torsk fm. tops, but they still represent potential shallow gas accumulations. Zones above or close to mapped fluid chimneys and leakage along faults are often associated with DHI, as there are several indicators located in the same area increasing the potential for hydrocarbon accumulation. This is seen in figures 4.2-4.4.

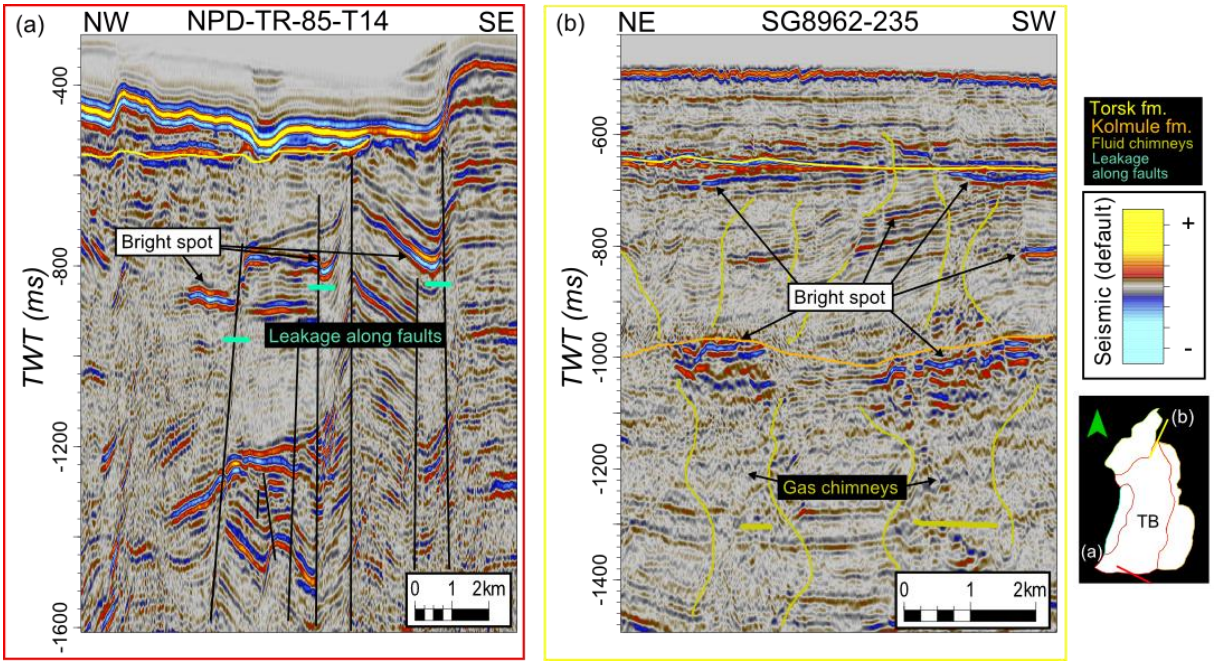

Figure 4.4 – Available defined seismic data. (a) Mapped leakage along faults and (b) fluid-flow systems interpreted to be gas (or fluid) chimneys. Mapped potential shallow gas accumulations are marked as bright spots.

Mapping amplitude anomalies associated with shallow gas accumulations in areas without fluid-flow systems and leakage along faults are often associated with either enhanced reflections or isolated bright spots. The enhanced reflections or bright spots are generally located along sealing structures or stratigraphy. There are two different types of amplitude anomalies shown in figure 4.5. Figure 4.5(a) shows a reflection being a flat enhanced reflection located just below the intra Torsk fm. top. Figure 4.5(b) shows a reflection along a dipping stratigraphy located at a level just beneath the Kolmule fm. top.

Within the Tromsø Basin and adjacent areas there is known to exist several structural highs and salt diapirs (Faleide et al., 1993). Trapping of hydrocarbons is known to occur in either stratigraphic or structural traps. Close to diapiric features there can exist different anticlinal, faulted, unconformity and pinch-out traps (Rafaelsen, 2012). An example of trapping of shallow gas along with potential migration pathways is seen in figure 4.6. Figure 4.6(a) shows a trap associated with different stratigraphic layering in the subsurface while figure 4.6(b) shows an anticlinal trapping related to the intrusion of the diapir structure with potential traps forming at the sides and above the feature. Both features in figure 4.6 are located below the Torsk fm. top at a depth between 1200ms and 1600ms TWT and they are both located in the southwestern part of Tromsø Basin.

Possible shallow gas accumulations associated with BSR are also part of the mapped shallow gas accumulations. These reflections are not very easy to identify as BSR, but there exists amplitude anomalies that can be interpreted as potential BSR in the study area (fig. 4.7). BSR is likely to be related to gas hydrates or diagenesis. It is generally located at deeper water depths and might be easier to spot on dipping reflectors (fig. 4.7(b)). The seafloor bathymetry across Tromsø Basin is more or less a flat surface, with the shelf-edge towards the west. The uncertainty related to the identification of BSR in this area is high. Whether or not they are BSR is not of importance in this thesis as the amplitude anomalies are still associated with shallow gas accumulations and therefore mapped within the area of interest. The BSR is known to be associated with the accumulations and

presence of free gas in sediments beneath the gas hydrate stability zone (GHSZ). Identified BSR (fig. 4.7) are located below 300-500ms TWT below the seafloor reflection. It is more important to distinguish between potential gas-hydrate related BSR and diagenesis-related BSR to understand the accumulation mechanism.

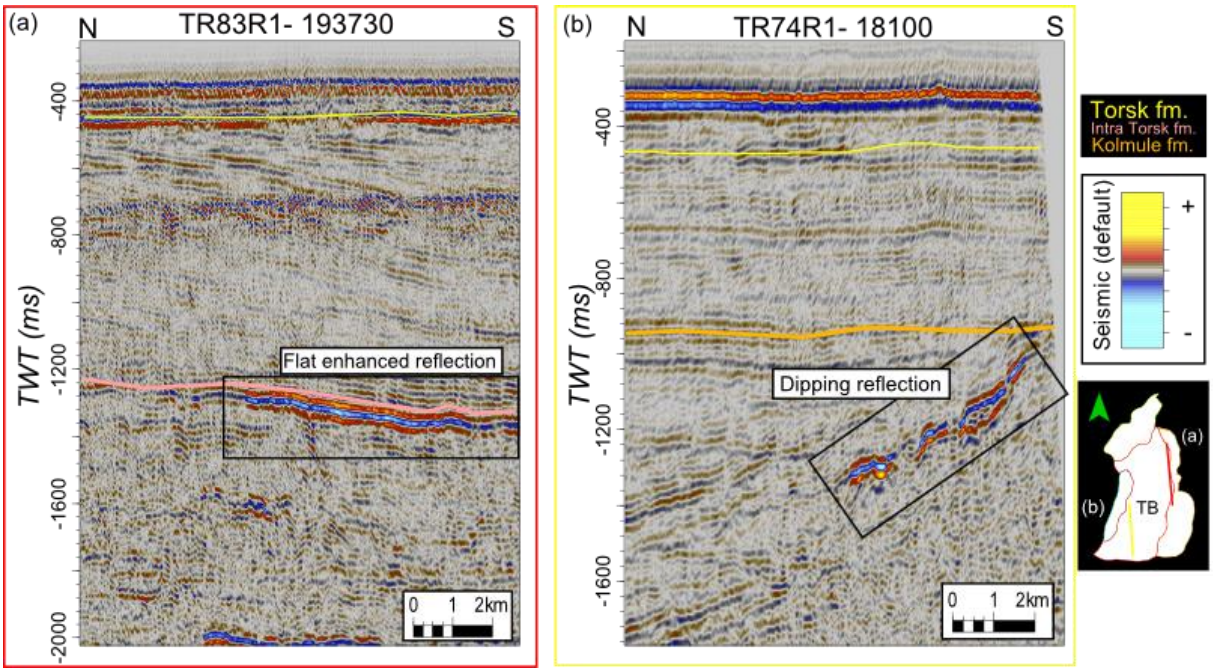

Figure 4.5 - Seismic sections showing examples of (a) mapped flat enhanced reflection, and (b) mapped dipping reflecion, associated with shallow gas anomalies.

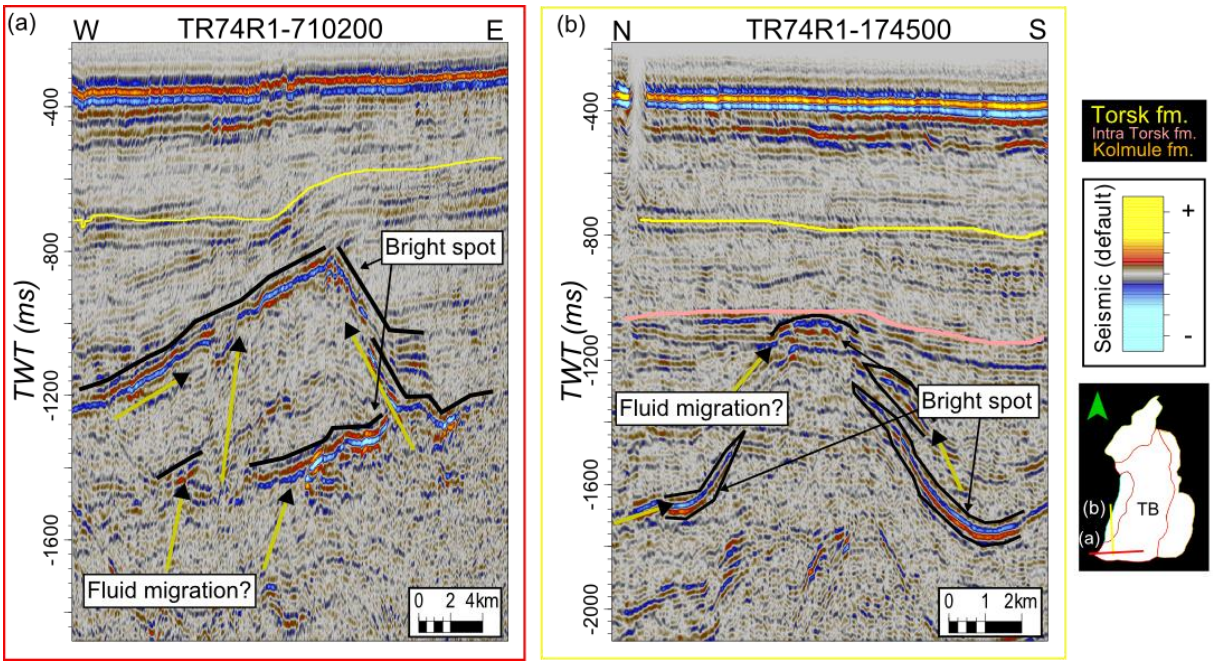

Figure 4.6 - Different structural and stratigraphic trapping of hydrocarbons. (a) Seismic section showing potential stratigrapich trapping and migration. Migration pathways marked with arrows. (b) Seismic section showing traps located close to a structural feature (diapir) with potential traps located both at structure sides and on top.

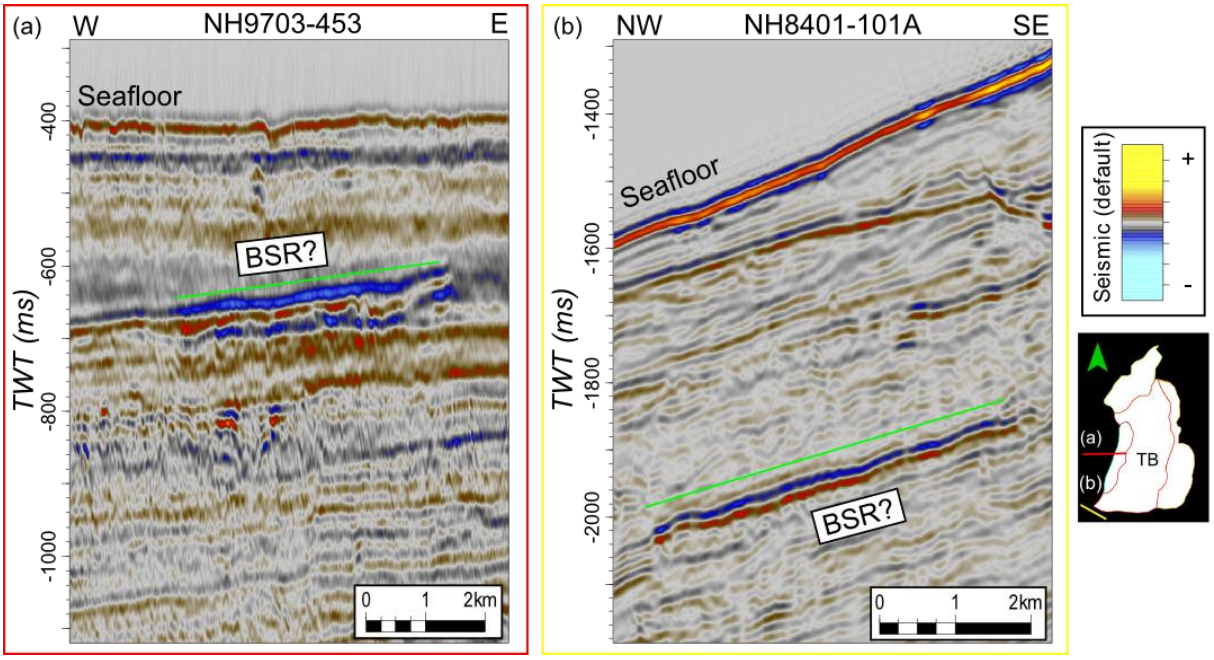

Figure 4.7 - Potential bottom simulating reflector (BSR) located at a certain depth (approx. 300-500ms TWT) beneath the seafloor reflection. (a) Horizontal potential BSR located below a shallow and flat seabed. (b) Potential BSR located beneath a deeper and dipping seafloor.

4.3 Interpretation Pitfalls

Multiples and enhanced reflections are different pitfalls related to the mapping of potential shallow gas accumulations (fig. 4.8). Figure 4.8(a) shows enhanced reflections located above a zone of mapped fluid flow with the Torsk fm. top as a possible stratigraphic boundary. The fluid chimney bypasses the Kolmule fm. top, being a deep source feature. The enhanced reflection and the bright reflection located above the chaotic reflections are mapped as potential shallow gas accumulations due to their signal strength and reversed polarity compared to the seafloor reflection. Areas of chaotic reflection patterns make the identification of shallow gas accumulations a difficult process within these zones. Figure 4.8(b) shows different seismic artefacts being multiples that may be misinterpreted and mapped as bright spots associated with potential shallow gas accumulations. Multiples change polarity each time it is reflected. A potential seabed multiple is also visible and could be misinterpreted as phase-reversed enhanced reflections or bright spots. At both sides of the subsurface structural high, which is the most likely source for the multiples, there is identified and mapped brights spots being potential amplitude anomalies associated with shallow gas accumulations.

Problems associated with mapping using only seismic 2D data is the poor seismic coverage (fig. 3.5(b)). Seismic lines located next to each other can be interpreted giving two different results. An example of this is seen in figure 4.9 showing two seismic lines from the same survey. Figure 4.9(a) shows a seismic anomaly interpreted as an isolated bright spot, while figure 4.9(b) show the same bright spot associated with a mapped fluid-flow feature. On the distribution maps in section 4.4, results of the 2D seismic data can appear as chaotic and fragmented. 3D seismic data does not have this same coverage problems and the distribution of features are based on the actual feature extents.

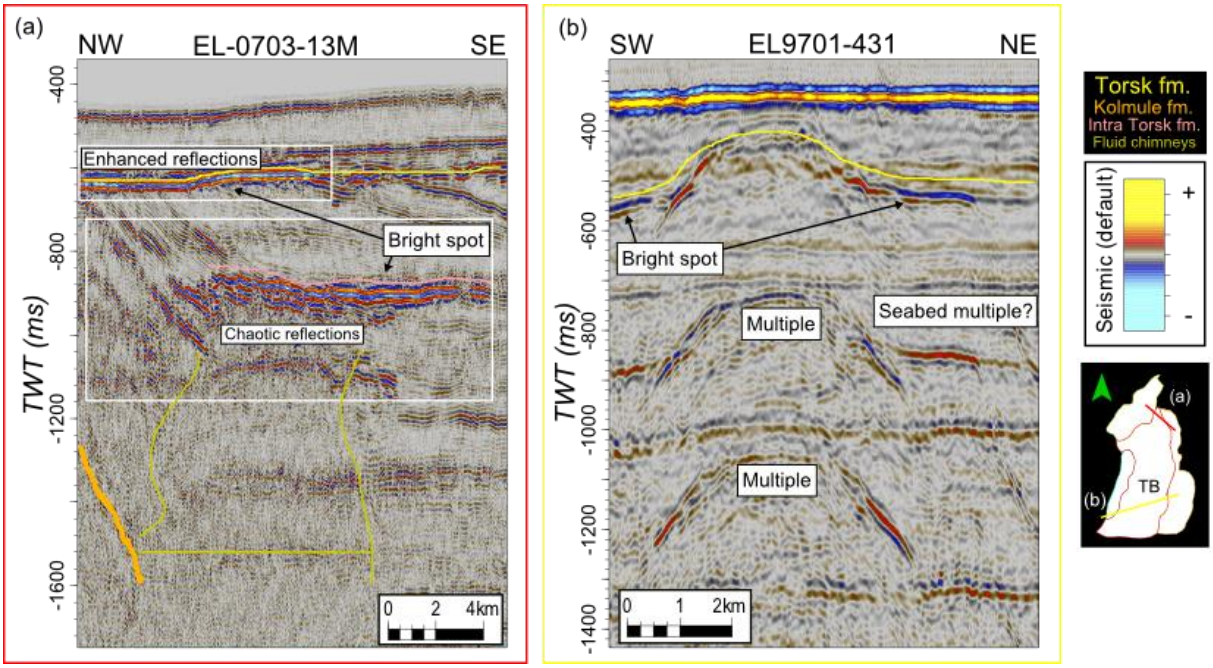

Figure 4.8 - Potential pitfalls related to the mapping of shallow gas accumulations. (a) Seismic section showing strong positive enhanced reflections and an area of chaotic reflection pattern located above a fluid chimney. (b) Seismic section showing a possible seabed multiple and other multiples that could be misinterpreted as bright spots related to potential shallow gas accumulations. Marked bright spots are mapped as shallow gas accumulations

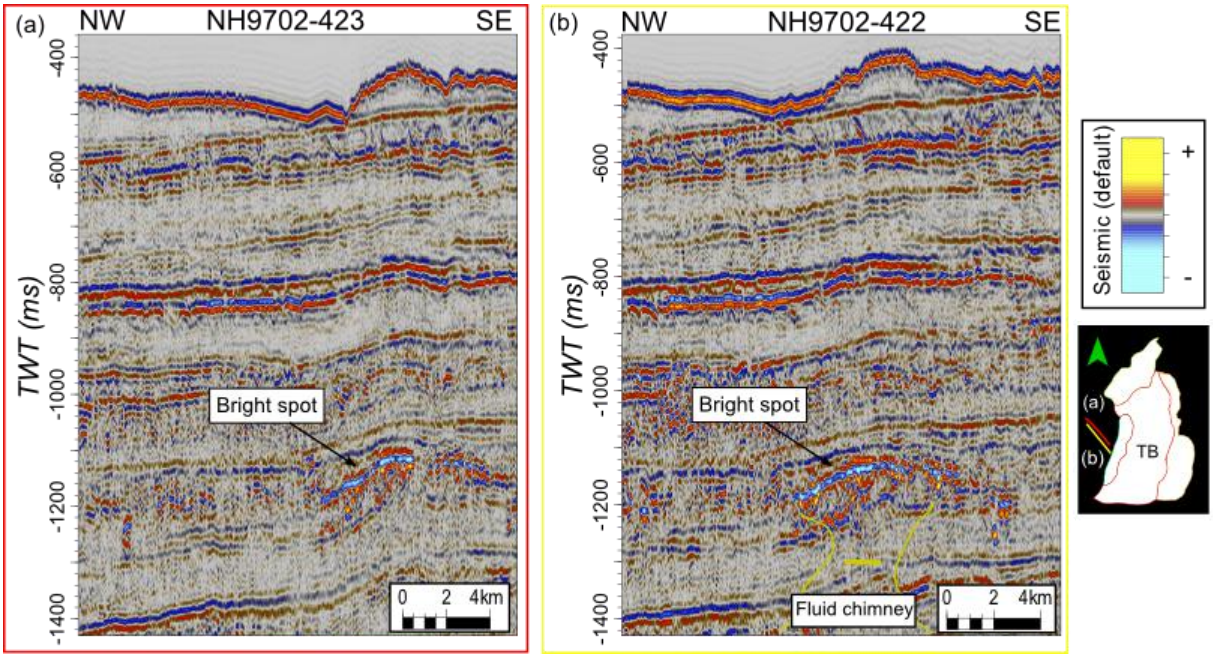

Figure 4.9 - Seismic sections located close to each other showing the same amplitude anomaly but potential different interpretations. (a) Seismic section showing only location of a mapped isolated bright spot. (b) Seismic section showing the same mapped bright spot (a) but in addition an area of mapped fluid chimney beneath the bright spot.

After identifying and mapping out all the areas of interest with different seismic amplitudes anomalies within the study area, a more detailed mapping was initiated to illustrate and display the distribution of the different seismic anomalies and shallow gas accumulations.

4.4 Distribution of Shallow Gas Accumulations

Mapping the distribution of shallow gas accumulations in the Tromsø Basin and adjacent areas of the SW Barents Sea is divided into several types of maps showing different distributions of seismic anomalies associated with potential shallow gas accumulations. Mapping out all seismic amplitude anomalies that are potential shallow gas accumulations only using 2D seismic data does not visually give any decent or beneficial results. The data from the results are therefore divided into potential shallow gas accumulations located in different stratigraphic units. These units are based on anomalies located: above the Torsk fm., within the Torsk, Kveite and Kviting formations and within the upper Kolmule fm. Examples of amplitude anomalies mapped within the different stratigraphic units are seen in figures 4.10-4.12 (a) with the shallow gas distribution maps in (b). The same setup goes for the figures 4.13-4.16.

Figures 4.13-4.16 show other distribution maps that are important parts of the results. These maps show the extent of seismic amplitude anomalies associated with shallow gas accumulations being; deep source features, flat and dipping reflections, salt diapirs and structural highs. The distribution map of structural highs and salt diapirs in the study area (fig. 4.16) is not a product of mapped seismic amplitude anomalies. It maps the distribution of these structural features based on the seismic stratigraphy. This is used to compare the lateral extent of the shallow gas anomalies together with the distribution of the salt diapirs and structural highs within the study area.

4.4.1 Above Torsk fm.

Identification and distribution of shallow gas accumulations located within the Neogene period, above the Torsk fm. is summarized in figure 4.10. The distribution is in general located towards the western parts of the study area, within the Sørvestnaget Basin.

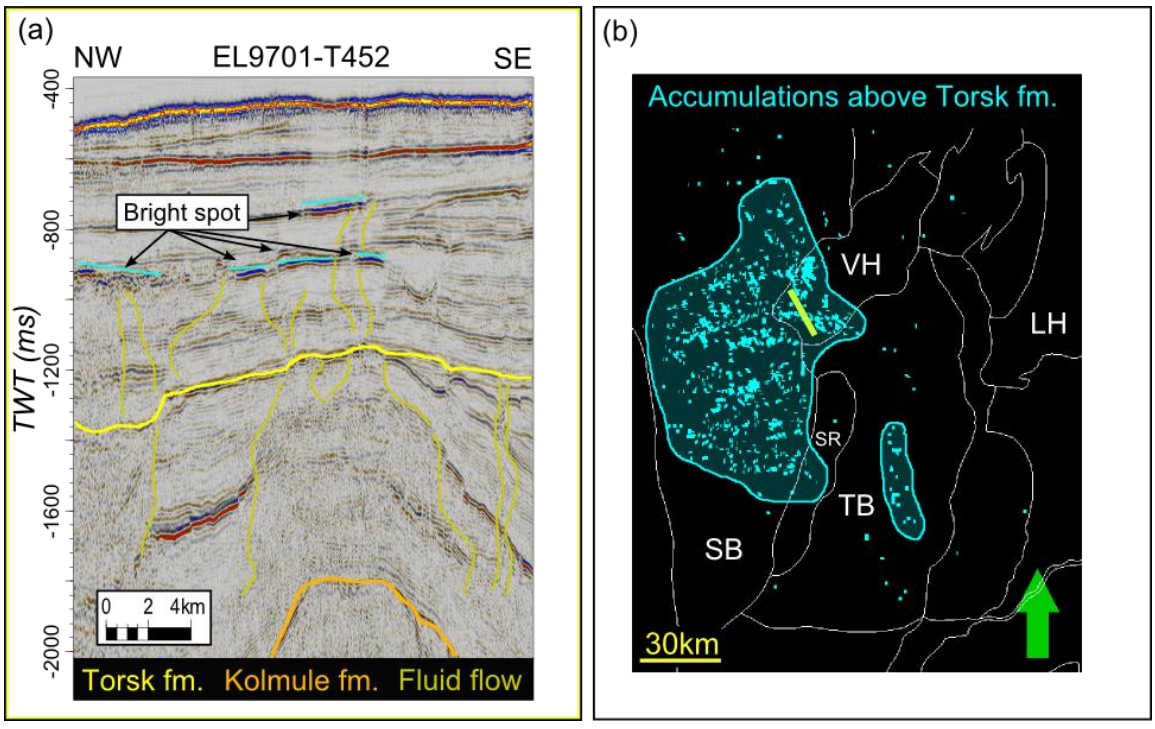

Figure 4.10 – Distribution of shallow gas accumulations located above Torsk fm. (a) Seismic section showing examples of mapped phase-reversed bright spots within this unit. (b) Distribution map of the anomalies associated with potential shallow gas accumulations located above the Torsk fm. in the Tromsø Basin and adjacent areas in the SW Barents Sea. Location of (a) is marked with a yellow line in (b).

4.4.2 Below Torsk fm. top and Above Kolmule fm.

Identification and distribution of shallow gas accumulations located within the Paleocene and the upper Cretaceous period, being below the Torsk fm. top and above the Kolmule fm. is summarized in figure 4.11. The general trend for the mapped shallow gas accumulations within this unit is located in general over the central and northern parts of the study area. These areas include the Veslemøy High and the Ringvassøy-Loppa Fault Complex.

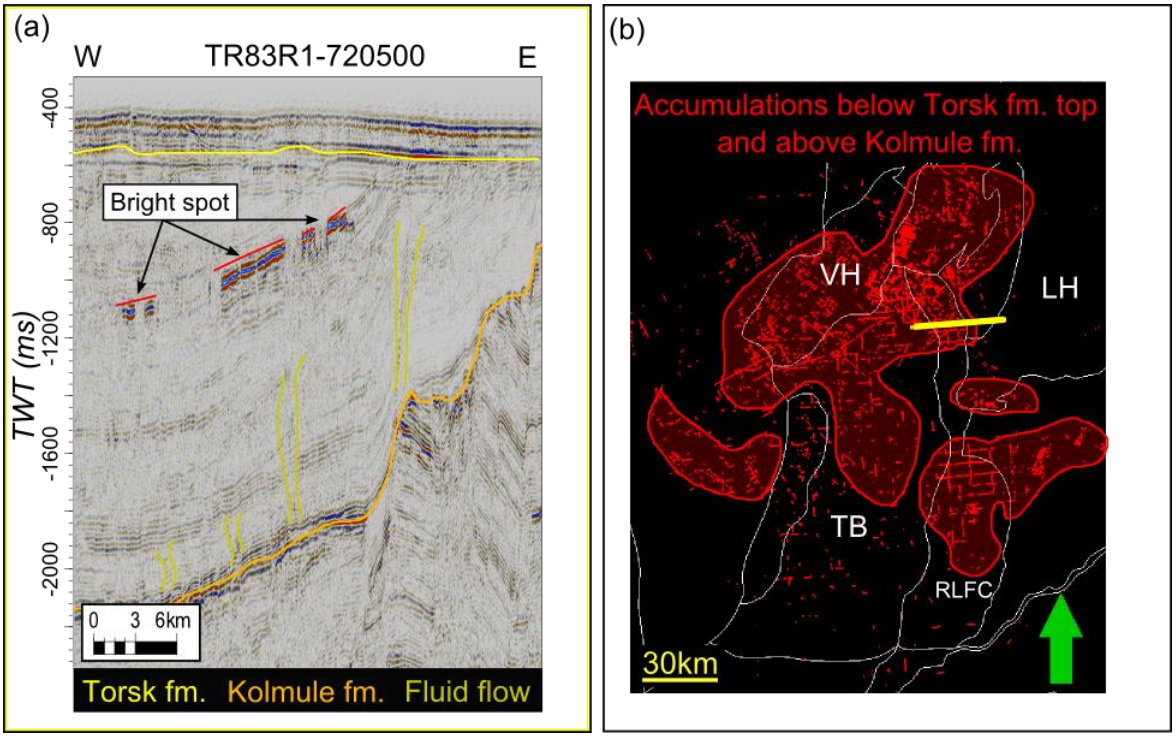

Figure 4.11 - Distribution of shallow gas accumulations located below Torsk fm. top and above the Kolmule fm. (a) Seismic section showing examples of mapped phase-reversed bright spots within this unit. (b) Distribution map of the anomalies associated with potential shallow gas accumulations located in the Tromsø Basin and adjacent areas in the SW Barents Sea, located within the unit below Torsk fm. top and above the Kolmule fm. Location of (a) is marked with a yellow line in (b).

4.4.3 Upper Kolmule fm.

Identification and distribution of shallow gas accumulations located within the lower Cretaceous period, within the upper Kolmule fm. is summarized in figure 4.12. The general trend for the mapped shallow gas accumulations within this unit are located in the eastern and northeastern parts of the study area, towards the Loppa High.

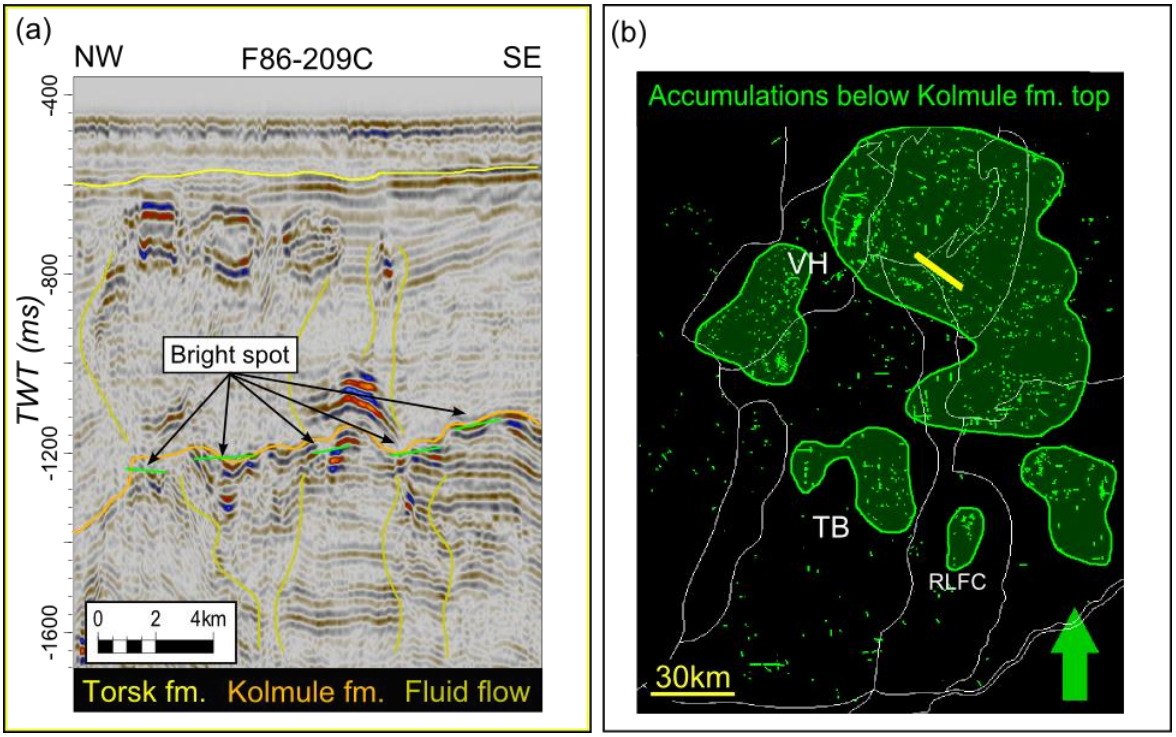

Figure 4.12 - Distribution of shallow gas accumulations located within the upper Kolmule fm. (a) Seismic section showing examples of mapped phase-reversed bright spots within this unit. (b) Distribution map of the anomalies associated with shallow gas accumulations in the Tromsø Basin and adjacent areas in the SW Barents Sea located within the upper Kolmule fm. Location of (a) is marked with a yellow line in (b).

4.4.4 Deep Source Features

For comparison reasons deep source features are also mapped. These are features in connection with mapped fluid chimneys and leakage along faults showing strong indications of amplitude anomalies originating or migrating from a deep source. The term deep refers to coming from below the Kolmule fm. top. Figure 4.13 shows an example and the distribution of features mapped being of this kind. Figure 4.13(a) shows a seismic section with a deep source reflection bypassing the Kolmule fm. top and terminating within the Torsk fm. This anomaly is also mapped in as an anomaly located within the stratigraphic unit below Torsk fm. top and above the Kolmule fm. (fig, 4.11). Figure 4.13(b) illustrates the distribution of these deep source features located within the study area. The highest density of these features are located in the northern parts of the study area, above the Ringvassøy-Loppa Fault Complex.

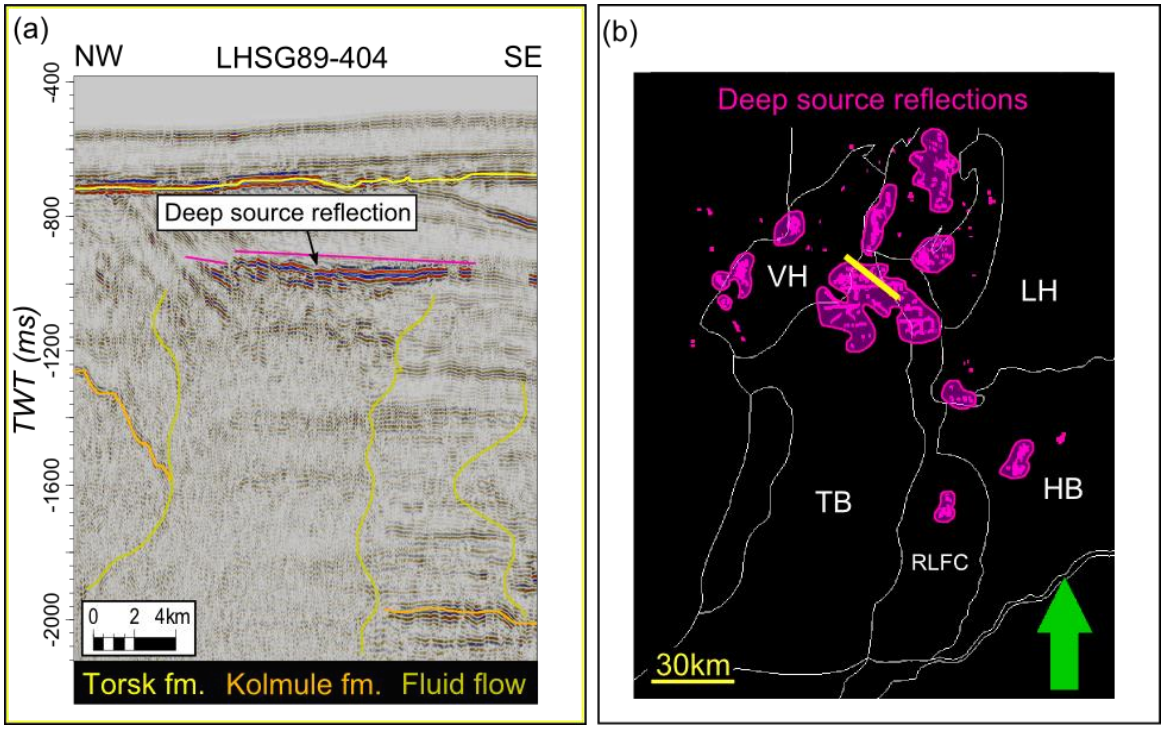

Figure 4.13 - Distribution of shallow gas accumulations associated with fluid flow from a deep source bypassing the Kolmule fm. (a) Seismic section showing an example of a phase-reversed bright spots mapped with the associated fluid chimney from a potential deep source. (b) Distribution map of anomalies in association with shallow gas accumulations within the Tromsø Basin and adjacent areas in the SW Barents Sea. Location of (a) is marked with a yellow line in (b).

4.4.5 Flat and Dipping Reflections

Distribution of seismic amplitude anomalies that are related to dipping or flat reflections are seen in figures 4.14 and 4.15. Seismic sections in figures 4.14(a) and 4.15(a) show examples of amplitude anomalies mapped out as these features. By distinguishing between these two types of features, it can be possible to see if there is any correlation in areas of flat and parallel bedding or in areas of dipping and angled strata by combining the different distribution maps. The Tromsø Basin is known to contain several diapiric structures and is bordered by structural highs, the Senja Ridge, the Veslemøy High and the Loppa High. The highest density of the dipping reflection features is mainly located along structural borders (Veslemøy High, Senja Ridge and Loppa High), above faulted zones (Ringvassøy-Loppa Fault Complex) and central parts of the Tromsø Basin (fig. 4.14(b)). The highest density of flat reflection features are mainly located above structural highs (Veslemøy High) and spread over the northern parts of the Tromsø Basin (fig. 4.15(b)).

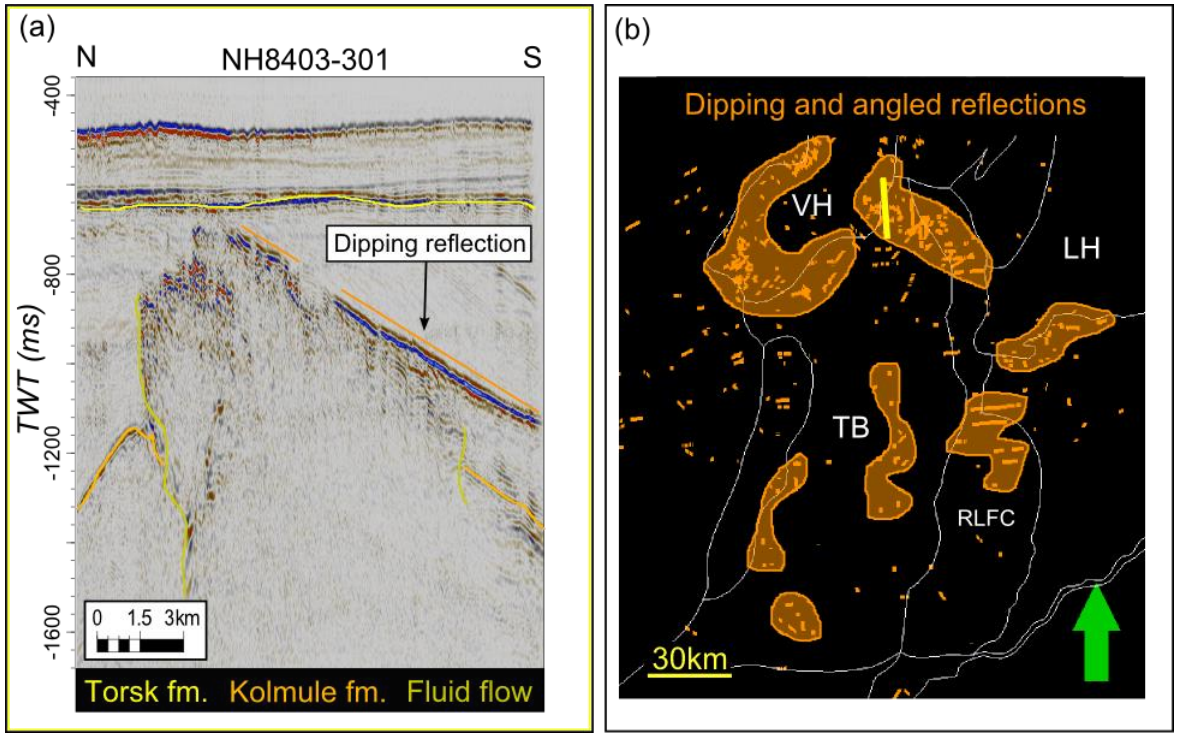

Figure 4.14 - Distribution of shallow gas accumulations associated with dipping and angled reflections associated with shallow gas accumulations. (a) Seismic section showing an example of a mapped dipping reflection with the associated fluid chimney from a potential deep source. (b) Distribution map of dipping anomalies within the Tromsø Basin and adjacent areas in the SW Barents Sea. Location of (a) is marked with a yellow line in (b).

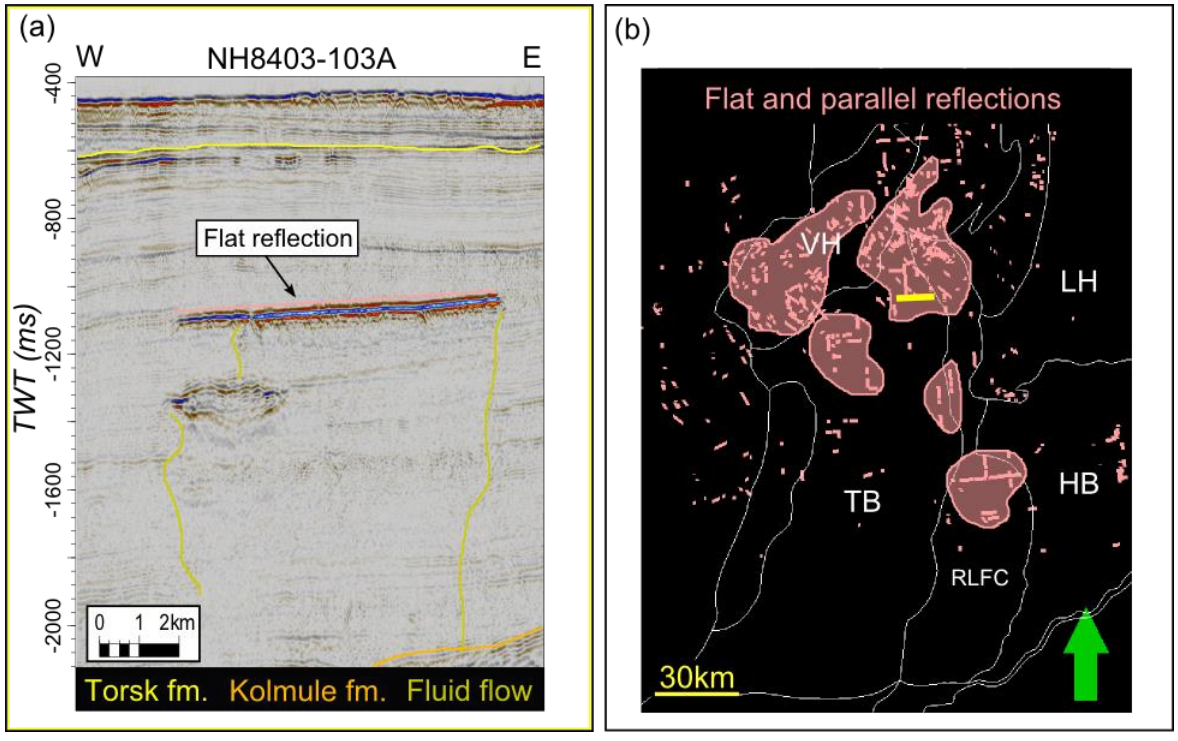

Figure 4.15 Distribution of shallow gas accumulations associated with flat and parallel reflections associated with shallow gas accumulations. (a) Seismic section showing an example of a mapped flat reflection with the associated fluid chimney. (b) Distribution map of flat and parallel anomalies within the Tromsø Basin and adjacent areas in the SW Barents Sea. Location of (a) is marked with a yellow line in (b).

4.4.6 Salt Diapirs and Structural Highs

Mapping the distribution of structural highs and salt diapirs within the study area is summarized in figure 4.16. Figure 4.16(a) shows an example of a seismic 2D line with the mapped subsurface structural highs and salt diapirs, while figure 4.16(b) shows the distribution map of these subsurface structural highs and salt diapirs. Diapir structures are mapped in other studies (Faleide et al., 1993) and are therefore known to exists in this region, but they are not predefined within the available seismic data for this thesis. Mapping of these structures are applied only to the structures that are piercing or noticeably uplifting the subsurface stratigraphy located above the upper Kolmule fm. top. Mapped features are mainly located in central Tromsø Basin and along the borders to the Senja Ridge and the Veslemøy High.

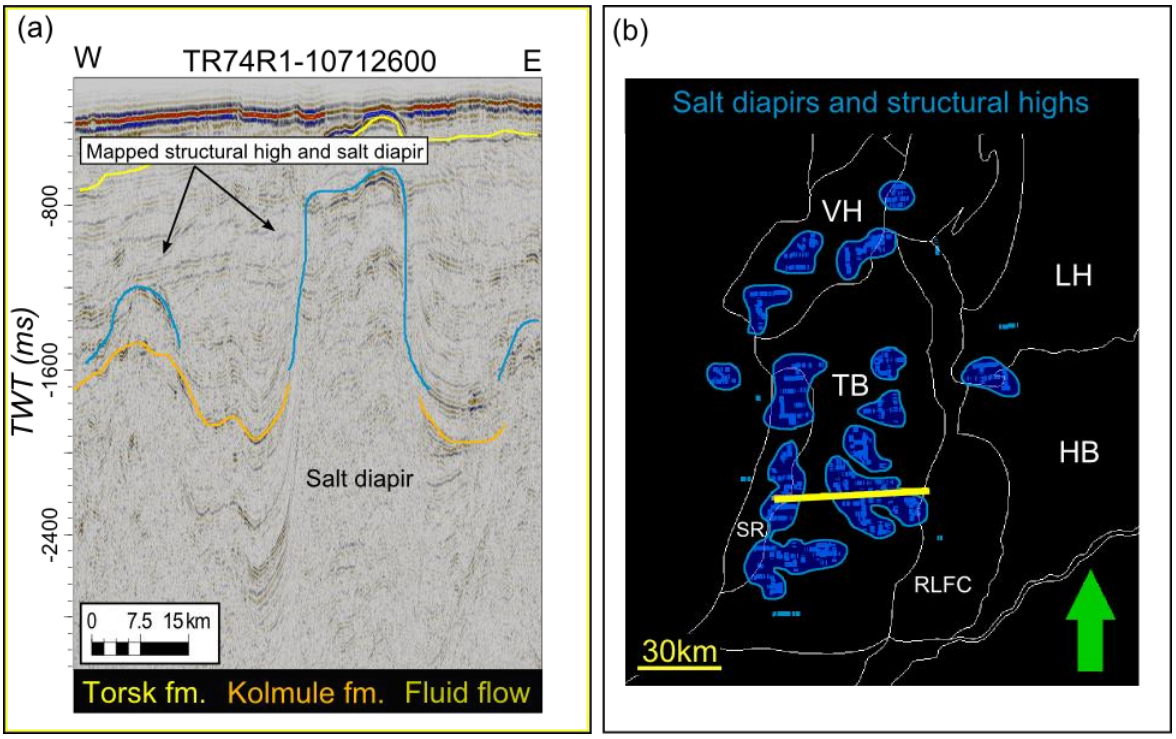

Figure 4.16 - Distribution of subsurface structural highs and salt diapir structures within the study area. (a) Seismic section showing an example of a mapped structural high and salt diapir. (b) Distribution map of highs and diapir structures in the Tromsø Basin and adjacent areas in the SW Barents Sea. Location of (a) is marked with a yellow line in (b).

4.5 Interpretation of 3D Data

In addition to the 2D seismic data available for this thesis, two 3D seismic surveys (EL0001 and LN09M01) located within the study area (fig. 3.3) are used for further interpretations of specified seismic anomalies. The focus of the 3D surveys are two specific amplitude anomalies. These anomalies are related to reflections and horizons of interest to identify and study their potential migration pathways and origin. These features are studied in more details to see if there is any connection with the distribution of the mapped shallow gas accumulations occurring in the study area (fig. 4.10-4.12). The 3D survey EL0001 (fig. 4.17) has a larger seismic anomaly extending out of the survey. Within the 3D survey LN09M01 (fig. 4.18) there is a seismic horizon of interest with the occurrence of enhanced and bright reflections beneath.

4.5.1 EL0001

The 3D survey EL0001 is located above the Veslemøy High and extending into the northern parts of the Tromsø Basin. A summary of the interpretation results for survey EL0001 is shown in figure 4.17. Within the 3D survey there is a reflection and horizon of interest located at a depth between approximately 1250ms and 1500ms TWT in the SE corner of the survey (fig. 4.17(a)). The feature depth increase in an S-SE direction towards the Tromsø Basin. This reflection is phase-reversed compared to the seafloor reflection, being a negative amplitude anomaly. The reflection is continuous out of the seismic survey to the east and south and is bordered by faults to the west. The faults are identified on the 3D surface (fig. 4.17(d)). In the north, the reflection extent ceases to exist. Figure 4.17(b) shows location of the xline (turquoise) and inline (yellow) used in 4.17(a) within the 3D survey (red polygon). Figure 4.17(c) shows an RMS amplitude map of a seismic volume covering the reflection and horizon of interest. The volume used in the RMS amplitude map covers a total volume of 120ms, with 60ms located above and below the specified horizon of interest. This interval cover the reflections of interest and is illustrated in figure 4.17(e) with the dark green horizon being the reflection of interest and the lighter green areas covered by the RMS amplitude volume. A 3D surface of the horizon of interest is shown in figure 4.17(d), with a red box indicating the main area of interest. The reflections lateral extent within the survey stretches out over 13km in N-S direction and more than 8km in W-E direction. The extent of this feature is believed to be larger as it is limited by the south and east borders of the EL0001 survey.

4.5.2 LN09M01

The 3D survey LN09M01 is located over parts of the Hammerfest Basin and Loppa High, covering parts of the Ringvassøy-Loppa Fault Complex. The survey is located just west of the Tromsø Basin. A summary of the interpretation results for survey LN09M01 is shown in figure 4.18. Within the survey, there are two main reflections of interest (1 and 2). There is a shallow reflection (1) located at a depth between 500ms and 700ms TWT, located south in the survey. The other reflection (2) is located at a depth between 900ms and 1050ms TWT, located further SW. The horizon of interest follows the stratigraphic level above that these two specific bright spots. The horizon extends from a depth of approx. 500ms TWT being located just below the seafloor reflection in the SE, down to a depth of 1200ms TWT in the SW corner of the survey. The horizon does not consist of a single, large amplitude anomaly as the EL0001 feature, but of several smaller seismic anomaly features (fig. 4.18(a)). The locations of the shown inline (turquoise) and xline (yellow) within the seismic survey (red polygon) are shown in figure 4.18(b). Figure 4.18(c) shows an RMS amplitude map of a seismic volume covering the reflections 1, 2 and the horizon of interest. The reflection 3 is a reflection that is due to its location close to the seafloor reflector, and being located in an area of chaotic reflection pattern, is more or less blending into the reflections situated above. As of this, reflection 3 is neglected and not considered of importance for this thesis. The volume used in the RMS amplitude map cover a total volume of 130m, covering 40ms above and 90ms below the horizon of interest. This interval covers the main reflections of interest within the same stratigraphy. It is illustrated in figure 4.18(e) showing the horizon of interest in pink and the RMS amplitude volume in light green. Reflection 1 and 3 are visible on the seismic section. A 3D surface of the horizon of interest is shown in figure 4.18(d) with red box covering the area of the specified anomalies. The 3D surface is decreasing in time (depth) towards the SW corner of the survey, towards Tromsø Basin. The shallow NW-SE parts of the surface, located in the central parts of the survey is not of interest as these are

reflections that merge together with the seafloor reflector and a more chaotic reflection pattern, similar to the neglecting of reflection 3.

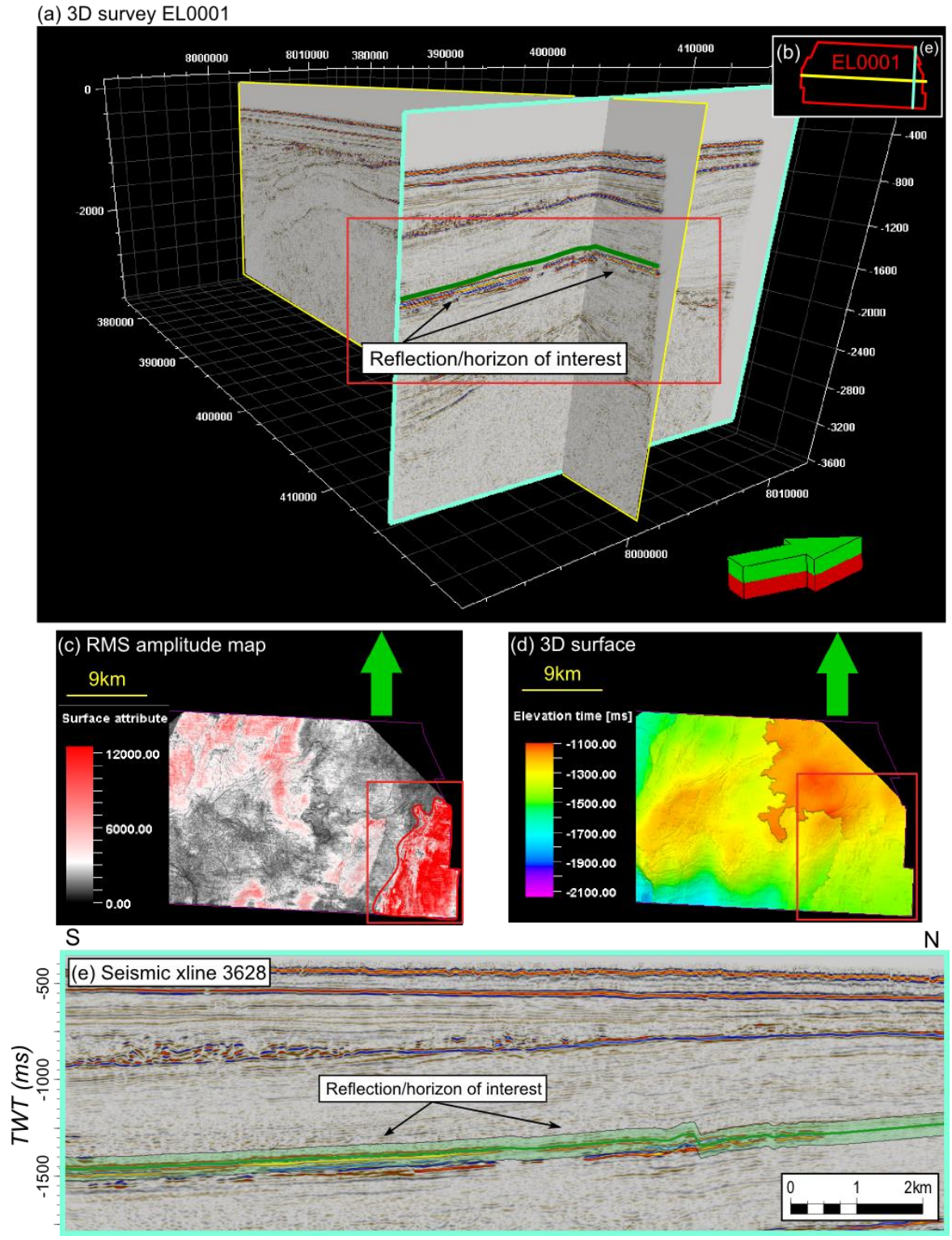

Figure 4.17 – Summary of interpretation results from 3D survey EL0001. (a) 3D survey showing seismic xline 3628 and inline 870 with location and extent of the major reflection and horizon of interest (green line) within red box. (b) Location of seismic xline (yellow) and inline (turquoise) within the survey (red polygon). (c) RMS ampltiude map with reflection of interest in red box. Bright amplitudes are illustrated in red. (d) 3D surface of the horizon of interest with location of the reflection of interest within red box. The surface is located within a depth of 1100-1900ms TWT. Faults are identified in the map. (e) Seismic section of xline 3628 showing horizon of interest in dark green and the volume covered by the RMS ampltiude map (c) in light green.

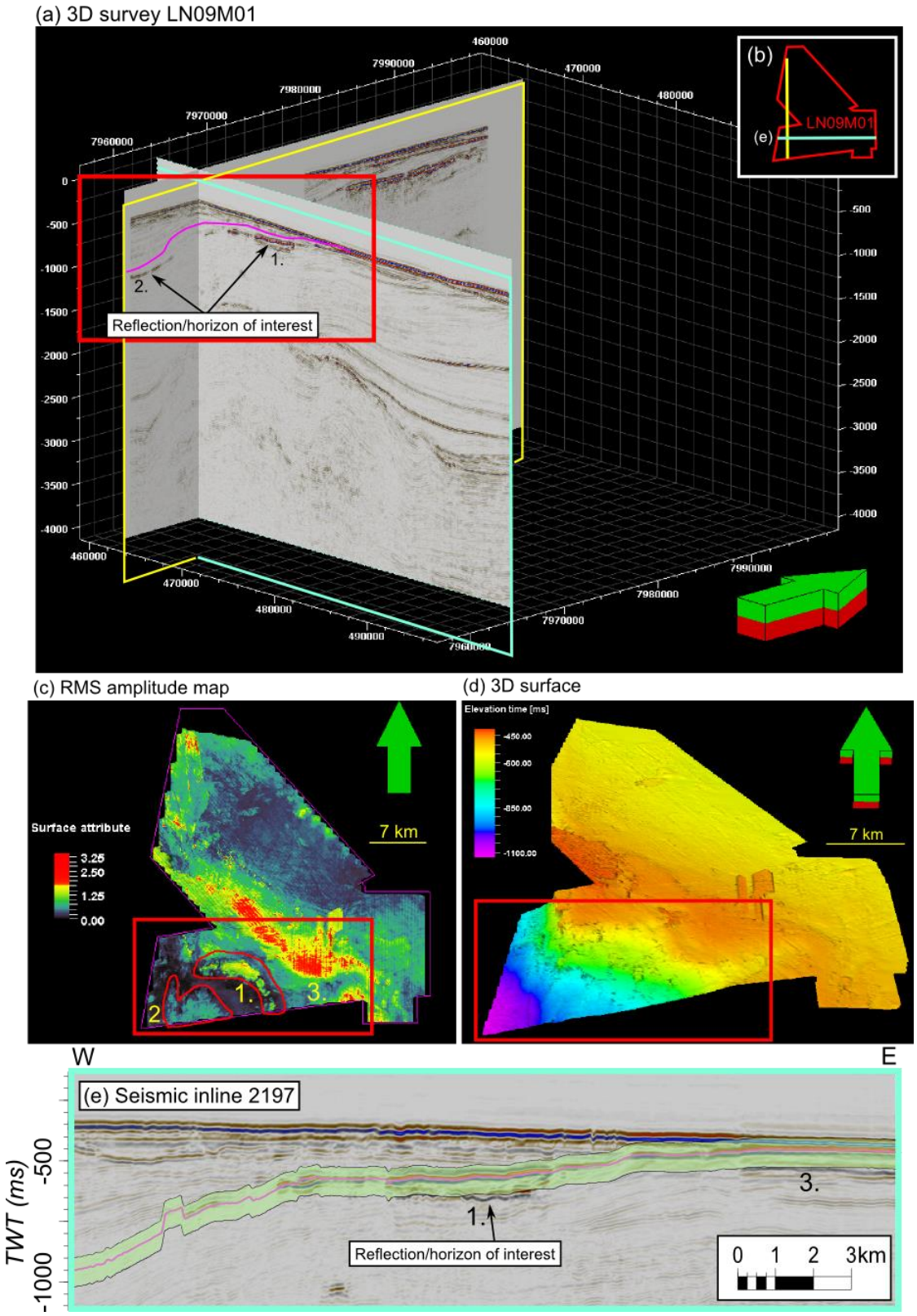

Figure 4.18 – Summary of interpretation results from 3D survey LN09M01. (a) 3D survey showing seismic xline 2197 and inline 5656 with location and extent of the major reflection 1. and 2. and horizon of interest within red box. (b) Location of seismic xline (turquoise) and xline (yellow) within the survey (red polygon). (c) RMS ampltiude map with reflection 1 and 2 of interest in red box. Reflection 3. is an anomaly located close to the seafloor reflection and is not considered. Bright amplitudes are illustrated in green/yellow/red colors. (d) 3D surface of the horizon of interest with location of reflection 1 and 2 within red box. The surface is located at a depth of 500-1100ms TWT. (e) Seismic section of inline 2197 showing horizon of interest in pink and the volume covered by the RMS ampltiude map (c) in light green. Reflection 1 and 3 are marked on seismic section.

4.5.3 3D Features Extent

The reflections of interest in the two 3D seismic surveys (fig. 4.17 and 4.18) are first mapped within the 3D survey and thereafter mapped using 2D seismic lines in the study area to identify potential lateral extent and area of generation for the reflections. The results from mapping out the lateral extents of the features are summarized in figures 4.19 and 4.20.

Figure 4.19 shows the lateral extent of the reflection of interest within survey EL0001 (fig. 4.17). Figure 4.19(a) shows an example of a 2D seismic line covering the specified reflection of interest and the mapping of the feature extent following a horizon at a similar stratigraphic level. Figure 4.19(b) shows a map of the study area and the potential lateral extent of the EL0001 feature. The reflection of interest mapped within survey EL0001 (orange) is highlighted in red. The extent of the EL0001 feature is mainly east and S-SE direction towards the northern and central parts of the Tromsø Basin extending into areas of the Ringvassøy-Loppa Fault Complex. The lateral extent is a body with a maximum length of 57km in SW-NE direction and a maximum width of 43km in NW-SE direction. The feature ceases to exist towards Veslemøy High, as it is not identified within this geological structure. The feature extent varies within a depth of between 800ms and 1700ms TWT with the deepest parts of the feature located towards the south and SW, mainly located within the Tromsø Basin. The features shallowest reflections are identified in the northeastern parts, towards the Loppa High.

Figure 4.20 shows the lateral extent of the reflection of interest within survey LN09M01 (fig. 4.18). Figure 4.20(a) shows an example of a 2D seismic line covering the specified reflection of interest and the mapping of the feature extent following a horizon of the same stratigraphy. Figure 4.20(b) shows a map of the study area and the potential lateral extent of the LN09M01 feature. The reflection of interest within survey LN09M01 (green) is highlighted in red. The lateral extent of the LN09M01 feature is mainly in south towards the border of the Tromsø Basin and central parts of the Ringvassøy-Loppa Fault Complex. The lateral extent of this feature is a more or less continuous seismic amplitude body with a maximum length of 50km in N-S direction and a maximum width of 43km in W-E direction. The feature ceases to exist towards Loppa High and Hammerfest Basin as the anomaly is not identified within these structural features. This feature is located at a depth between 600ms and 1600ms TWT, with its deepest reflections mapped towards west, extending into the Tromsø Basin. The features shallowest reflections are identified towards the north and the Loppa High.

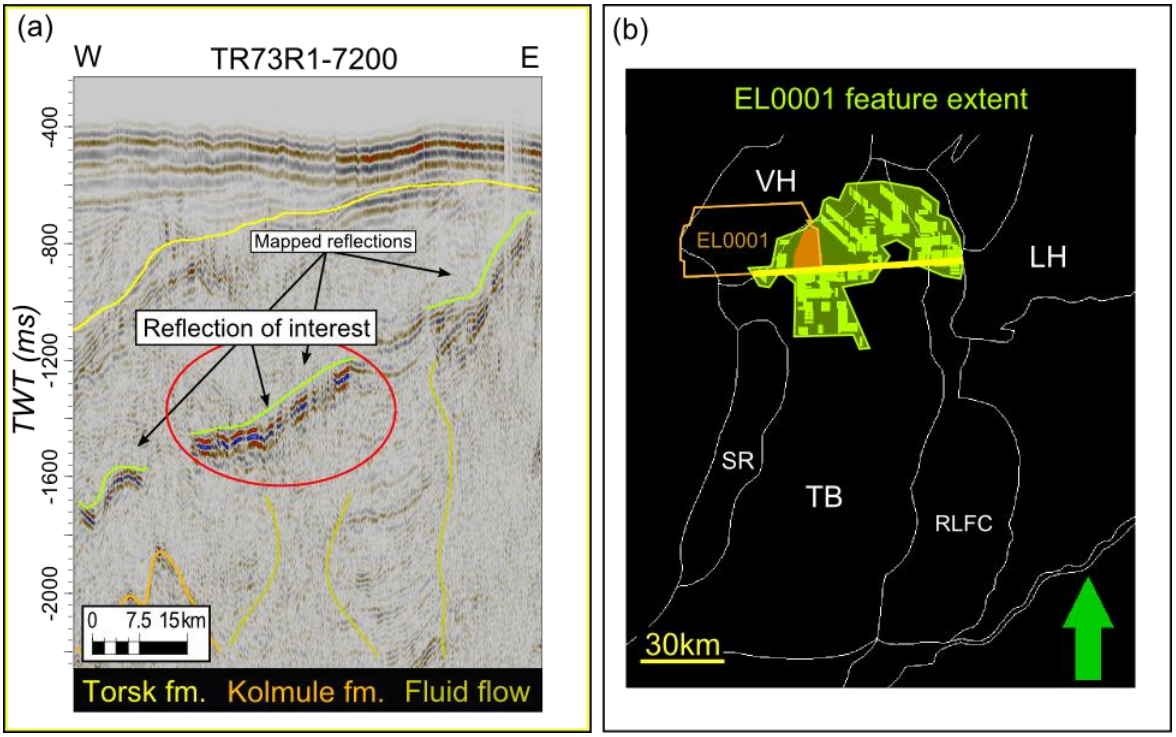

Figure 4.19 – Lateral extent of the EL0001 feature. (a) 2D seismic section from TR73R1-7200 showing the reflection of interest (red circle) (fig.4.17) extending out of the 3D survey and mapped reflections (green lines) associated with the EL0001 feature. (b) Map of lateral extent of the EL0001 feature in the study area. The reflection of interest is indicated in red within, and light green outside the 3D survey EL0001 (orange). Location of (a) is marked with a yellow line in (b).

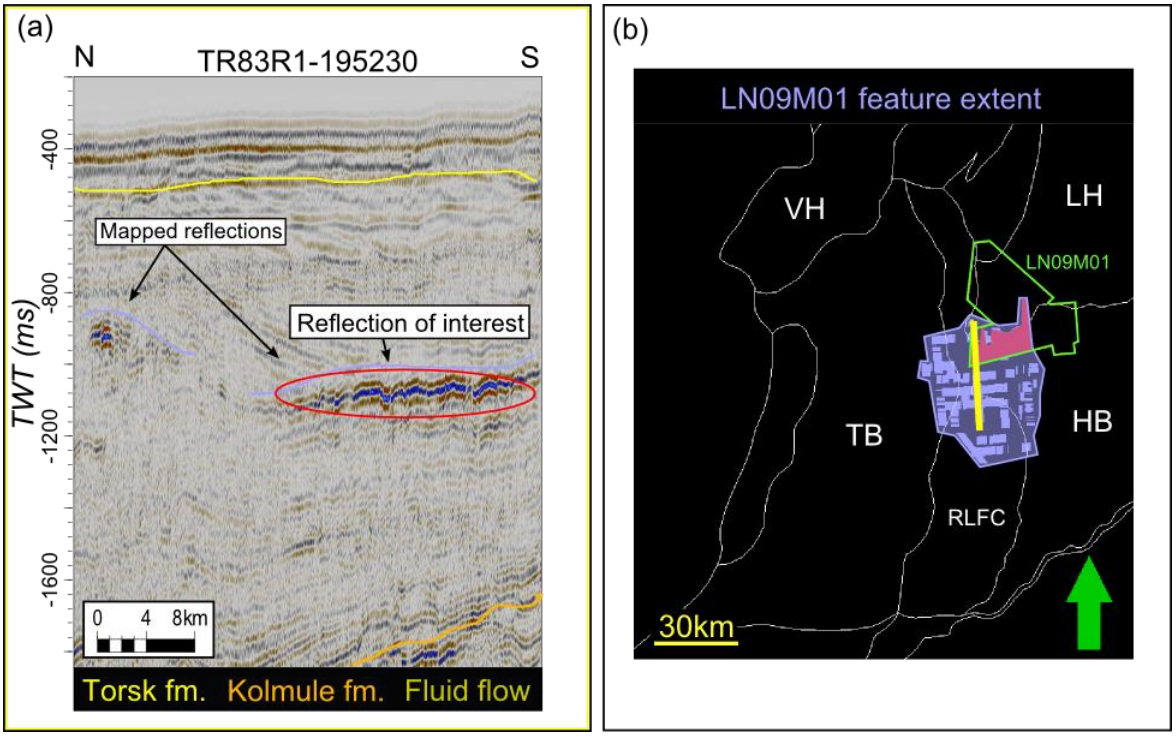

Figure 4.20 – Lateral extent of the LN09M01 feature. (a) 2D seismic section from TR83R1-195230 showing the reflection of interest (red circle) (fig. 4.18) extending out of the 3D survey and mapped reflections associated with the LN09M01 feature (purple lines). (b) Map of lateral extent of the EL0001 feature in the study area. The reflection of interest is indicated in red within, and purple outside the 3D survey LN09M01 (green). Location of (a) is marked with a yellow line in (b).

5 Discussion

The results presented are only showing the most obvious and simple examples of seismic amplitude anomalies that indicate associations with shallow gas accumulations, migration and generation. This is to give a better summary of the work performed to identify, locate and map the distribution of shallow gas accumulations in the SW Barents Sea. The discussion will focus on linking the different results together to see if there is any connection between the different distribution maps, possible migration pathways and the potential shallow gas accumulations in the study area. Potential places of hydrocarbon origin will also be discussed.

5.1 Seismic Quality

The quality of the seismic data differs depending on the different seismic surveys. Independent of quality, the process of identifying shallow gas accumulations is the same. Enhanced reflections and bright spots are good indicators of hydrocarbons within the sediments. Bright spots associated with hydrocarbons are generally indicated with a phase-reversed reflection compared to the seafloor reflection (Andreassen et al., 2007). Different examples of bright spots and potential shallow gas accumulations are shown in figures 4.1 and 4.2, where there is displayed both the wiggle trace signal of the seafloor reflection and different bright spots in seismic sections. Figure 4.1 focuses on seismic sections showing the same bright spot located on different 2D lines across the Tromsø Basin, an area known to be influenced by salt diapirs (Faleide et al., 1993; Ryseth, 2003). No large dim spots or areas with distinct dimmed spot amplitudes are identified, mainly due to the difference in data quality. Dim spots are more easily "lost" in the seismic compared to the more bright events, which are therefore more easily identified and mapped. The quality of the seismic data decreases with time. Deep reflections are difficult to distinguish from seismic noise. Similar is the problem of very shallow reflections (fig. 5.1). This is discussed further in section 5.2 as it is closely related to the process of identifying potential shallow gas accumulations.

The seismic quality of the data is dependent on the frequency, which in turn affects the seismic resolution. The resolution of the used seismic data is unknown and not calculated, as it is more related to the size and volumes of the accumulations.

The quality of the seismic data is good in the upper 2000-2500ms TWT (fig. 2.10). Gas accumulations, migration and generation below this depth are difficult to identify. Hydrocarbons accumulating at these depths are not defined as shallow accumulations and are therefore not discussed.

5.2 Seismic Evidence of Shallow Gas

Seismic evidence of shallow gas accumulations are related to; bright spots, areas of acoustic masking, pull-down effects, fluid and gas chimneys, enhanced reflections and BSR to mention some of the most important seismic features identified (fig. 4.2-4.7). The more of these features located within the seismic, the more likely the seismic amplitude anomaly is related to hydrocarbons and shallow gas accumulations (Løseth et al., 2009). Only a small percentage of gas in sediment creates a drastic reduction in the compressional wave velocity affecting the seismic signal with a negative reflection coefficient (Andreassen et al., 2007). As of this, seismic amplitude anomalies related to shallow gas accumulations are of reversed polarity compared to the known positive RC from the seafloor reflection (fig. 4.2).

Pockmarks and seafloor seepage are evidence of shallow gas systems (Boitsov et al., 2011; Chand et al., 2009; Cukur et al., 2013). No seafloor seepage is identified within the 2D or 3D seismic data available but it is known to exist in the study area (Chand et al., 2012). Pockmarks are easy to identify, as they are related to depressions in the subsurface stratigraphy and seafloor reflection (Hovland & Sommerville, 1985; Løseth et al., 2009). In the 3D seismic, mapping horizons allow a simple identification of pockmarks as circular holes on the surface, normally connected to subsurface fluid-flow systems. No distinct pockmarks are identified in the 3D surveys within the areas of interest. For the 2D data, identification of pockmarks is more challenging as the seismic lines are missing the ability to look in the third dimension. This is needed to be able to determine whether a depression in the seafloor or subsurface reflector are actually pockmarks or if they are related to

other geological features such as plough marks, channels, changes in the lithology or seismic effects such as push-down or artefacts. Pockmarks are known to exist in the study area (Andreassen et al., 2007). This thesis does not focus on mapping potential pockmarks or craters. They only increase the chance for shallow gas accumulations in the area.

5.3 Identification of Shallow Gas Accumulations

Hydrocarbon accumulations are known to be trapped above and along the sides of salt diapirs and structural features (Cartwright et al., 2007; Woodbury, Murray Jr, & Osborne, 1980). This is discussed further in sections 5.10 and 5.11. The process of identifying shallow gas accumulations is mainly based on the mapping of amplitude anomalies, generally bright spots located within the horizontal and vertical (depth) extent of the study area (fig. 4.2 and 4.3). A common seismic feature related to bright spots is to show a phase-reversed signal compared to the positive seafloor reflection (fig. 1.6(b)) (Andreassen, 2009). This depends on the geological situation in the area, as not all negative amplitude anomalies are related to hydrocarbons. This is more easily identified on seismic data where there is a known general overview of the stratigraphy and geological setting of an area. Small quantities of gas in sediments (2-8%) produce a negative acoustic impedance contrast that will easily be identified on seismic data (Andreassen et al., 2007). As of this, determining the size of gas accumulations is not an easy process using mainly 2D seismic data with poor coverage over a large study area. This thesis does not focus on the work of detailed quantification of shallow gas accumulations, but it can be of importance for future work in the SW Barents Sea. Shallow gas accumulations are known to pose potential geo-hazards as pressure differences may build up over time in reservoirs. Penetrating these pressurized zones may cause potentially dangerous pressure kicks or blowouts (Buller et al., 2005). The focus of the thesis lies in the more general extent and distribution of potential shallow gas accumulations in the SW Barents Sea, together with possible migration pathways and hydrocarbon generation. Identification of shallow gas accumulations are mainly based on mapping of negative amplitude anomalies as they are easy to identify on the seismic data, independent of the seismic quality and resolution.

The Tromsø Basin is a deep Cretaceous sedimentary basin and within its upper 2500ms TWT the Torsk fm., intra Torsk fm. and the Kolmule fm. are the most important reflectors identified on the seismic data. Other reflections identified relates to deep salt intrusions, extending all the way up to the erosional surface (URU) and the upper Torsk fm. The deeper parts of the basin are generally masked by the thick Cretaceous unit (Gabrielsen et al., 1990). Difficulties related to interpretations of deep and shallow seismic data are illustrated in figure 5.1.

The deep seismic data is often hidden by the overlying reflectors and is therefore very difficult to use for interpretation of shallow gas accumulations, migration and generation (fig. 5.1(a)). Similar is the problem of very shallow seismic data located within the upper 200-300ms TWT beneath the seafloor reflector. The resolution of the seismic data together with signal noise prevents evident data located within this zone as there is only a small space between the seafloor reflector and, in this part of the Barents Sea, the strong erosional surface (URU) located beneath (fig. 5.1(b)). The frequency used when gathering seismic data is chosen dependent of the subsurface target zone. Shallow targets require high frequencies and deeper targets require lower frequencies as the signal loses strength due to attenuation. The resolution of the seismic data is related to the data sampling frequency (Sheriff, 1977).

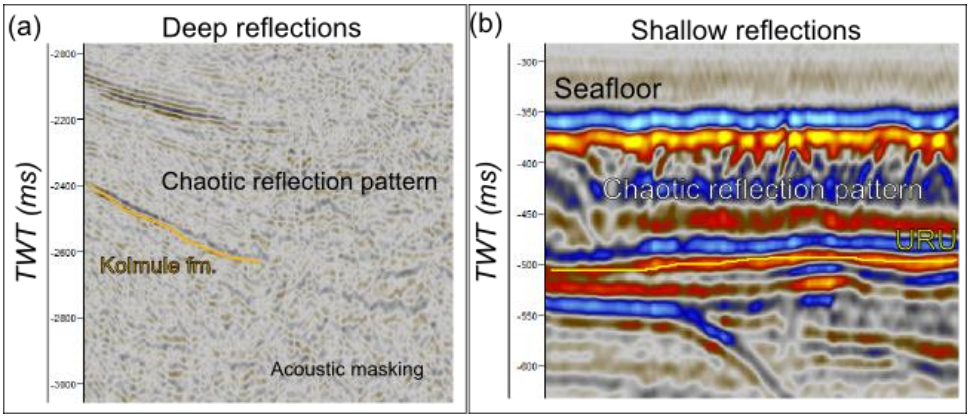

Figure 5.1 – Quality of deep and shallow seismic data illustrating difficulties related to the identification process within these levels. (a) Deep reflections beneath 2500ms TWT. (b) Shallow reflections within the upper 300ms TWT.

A study by Vadakkepuliyambatta et al. (2013) has mapped the distribution of subsurface fluid-flow systems in the SW Barents Sea. Figure 5.2 shows parts of the results of this study with the mapped gas chimneys and leakage along faults. The available data for this thesis is data related to this study. This data is the defined fluid chimneys and leakage along faults available in Petrel (fig. 3.2 and 4.4). The distribution of the existing mapped fluid-flow features (fig. 3.2) resembles the results of figure 5.2. Gas chimneys are the most common fluid-flow features in the study area and they appear in all sizes and shapes over a widespread area. The areas with the highest densities of fluid-flow features are located within and above the Ringvassøy-Loppa and Bjørnøyrenna Fault Complexes, northern part of the Tromsø Basin, above the Polheim Sub Platform and the Veslemøy High. Gas chimneys are also mapped and identified within the rest of the Tromsø Basin, but not with the same density as the areas mentioned above (Vadakkepuliyambatta et al., 2013). The salt diapirs known to exist in the Tromsø Basin are not mapped in figure 5.2.

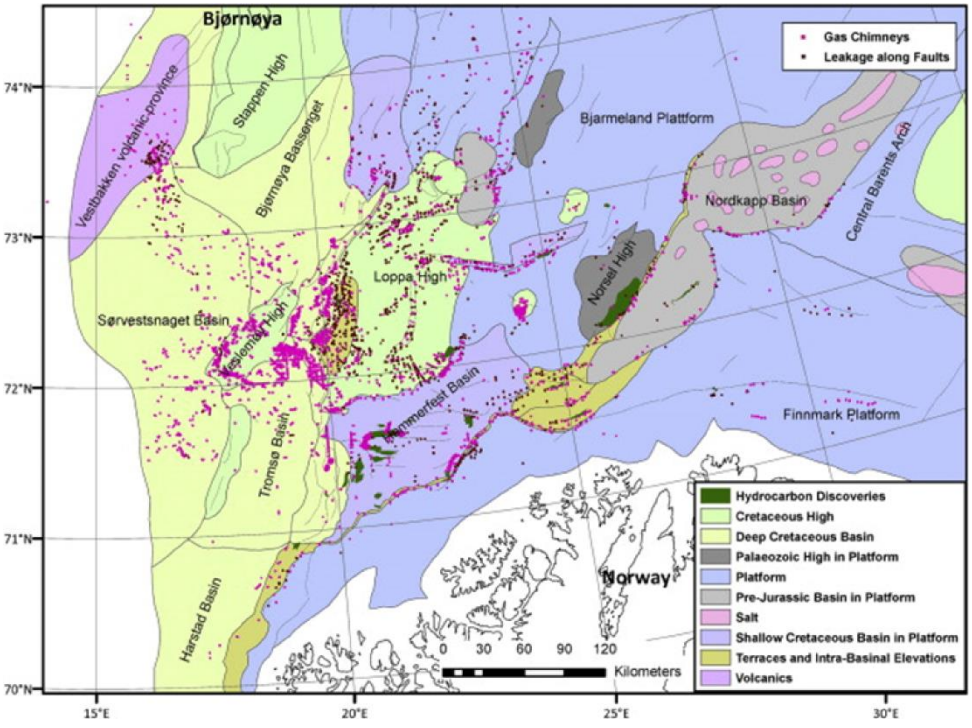

Figure 5.2 - Distribution of mapped gas chimneys and leakage along faults in the SW Barents Sea (Vadakkepuliyambatta et al., 2013).

A comparison between the distribution of subsurface fluid-flow systems by Vadakkepuliyambatta et al. (2013) and the mapped potential shallow gas accumulations in the SW Barents Sea from this thesis is used to identify the extent of the shallow gas accumulations. There are indications that there is a close connection between the locations with high-density subsurface gas chimneys and the location of mapped potential shallow gas accumulations. Examples of gas chimneys and associated shallow gas accumulations are shown in figures 4.2, 4.3, 4.4(b) and 4.8(a). This is discussed further in section 5.6; illustrating combined shallow-gas anomaly distribution maps (fig. 5.6).

As the different seismic surveys are shot in different directions, together with variations in resolution and quality, there is not found a clear indication of what is the stratigraphic boundary controlling the distribution of the shallow gas accumulations within the study area. From the figures 4.2 and 4.3, there are some indications that most of the identified and mapped amplitude anomalies associated with shallow gas accumulations are located close to the Torsk and Kolmule fm. tops. Within the Torsk fm. there is also several indications of some stratigraphic control located at different levels in the formation. The Intra Torsk fm. top is interpreted in the available data, being a reflector easily recognized on the seismic data (fig. 4.5(b) and 4.6(a)). This reflector acts as a main stratigraphic boundary in the areas where it is identified. This is discussed further section 5.5 and 5.9.

5.4 Distribution of Amplitude Anomalies Related to Shallow Gas Accumulations

The figures 5.3-5.5 present the results illustrating a simplified overview of the distribution of the different amplitude anomalies mapped in association with potential shallow gas accumulations in the study area. These maps include stratigraphic-controlled boundaries (fig. 5.3) located; (a) Above Torsk fm., (b) below Torsk fm. top and above Kolmule fm. and (c) below Kolmule fm. top. in addition, structural-controlled boundaries (fig. 5.4) related to; (a) gas chimneys, (b) deep source features, (c) salt diapirs and structural highs, (d) dipping reflections and (e) flat reflections. The features from the 3D surveys and their lateral extent are illustrated in figure 5.5 with; (a) EL0001 feature and (b) LN09M01 feature. The distribution maps have removed the actual mapped data shown in the Petrel Software. Only the high-density areas from the different types of distributions are presented. The seismic amplitude anomalies these maps are produced from are described in detail in section 4.4.

5.4.1 Stratigraphic Boundaries

Stratigraphic-controlled boundaries are indications of shallow gas accumulations within the different stratigraphic units defined within the study area (fig. 5.3). This is discussed further in section 5.5.

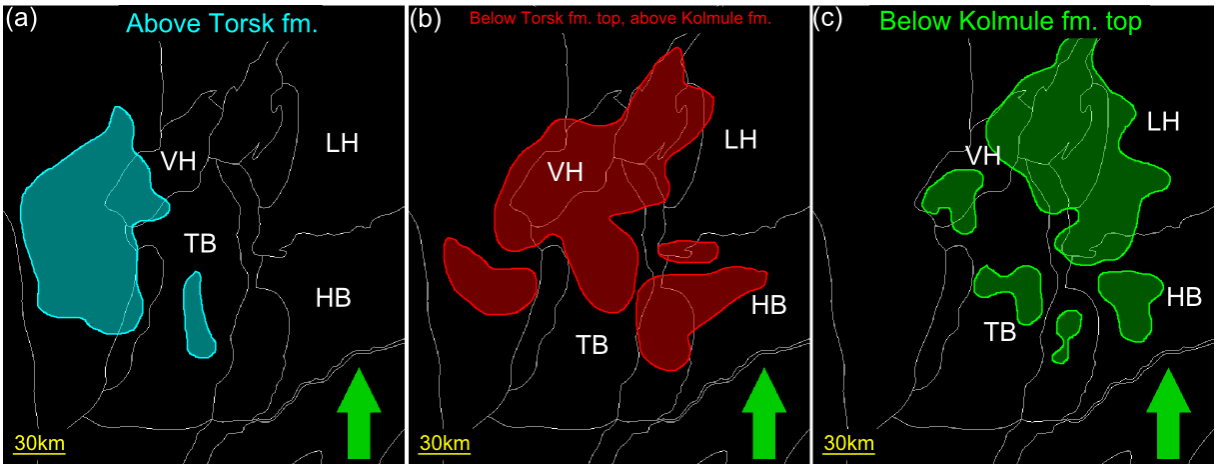

Figure 5.3 - Distribution of potential shallow gas accumulations within stratigraphic controlled boundaries; (a) Above Torsk fm., (b) below Torsk fm. and above Kolmule fm. and (c) below Kolmule fm.

5.4.2 Structural Boundaries

Seismic amplitude anomalies related to structural boundaries of shallow gas accumulations (fig. 5.4). This is related to geological structures, fluid-flow features and reflection angles (flat or dipping).

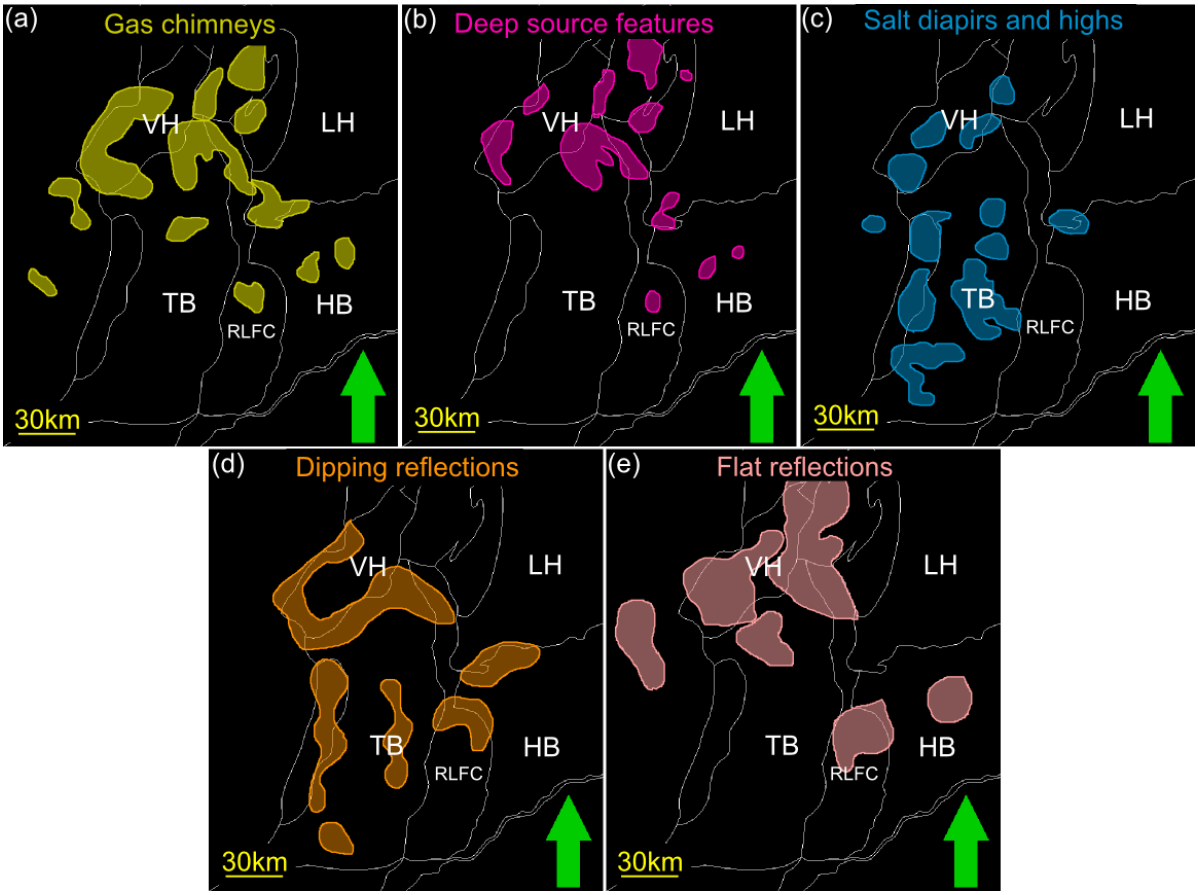

Figure 5.4 – Distribution of shallow gas related amplitude anomalies within structural controlled boundaries; (a) gas chimneys, (b) deep source features, (c) salt diapirs and structural highs, (d)dipping and (e) flat reflections.

5.4.3 Lateral Extent of 3D Features

Lateral extent of features of interest from the 3D surveys (fig. 5.5); (a) EL0001 feature and (b) LN09M01 feature (b). This is discussed further in section 5.8.

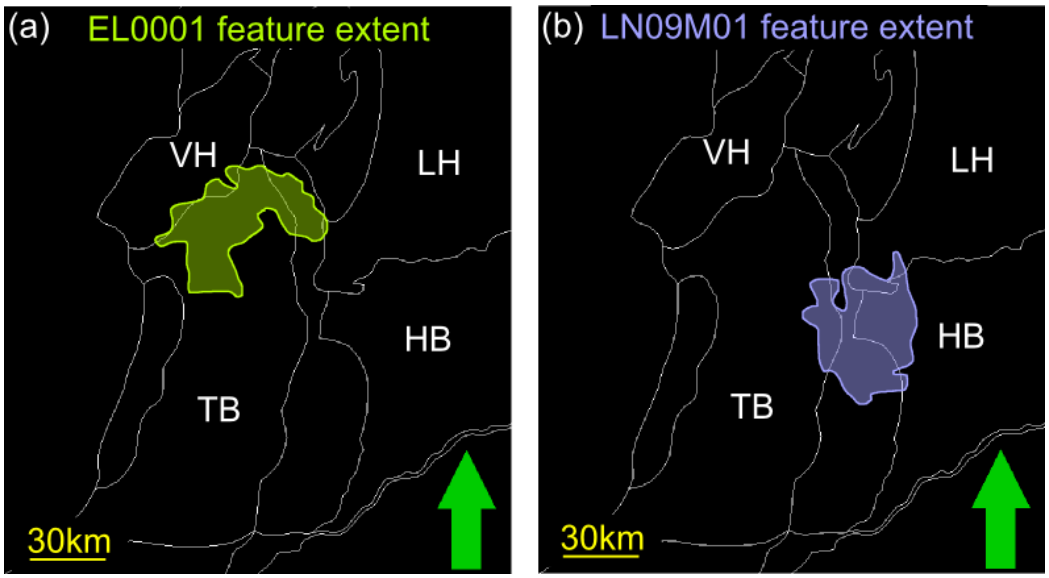

Figure 5.5 – Lateral extent of the features of interest within the available 3D surveys; (a) EL0001 and (b) LN09M01.

5.5 Hydrocarbon Accumulation Intervals

The distribution of shallow gas accumulations within different accumulation intervals is related to the stratigraphy of the study area. This is related to the correlated well logs located in different geographical directions within the Tromsø Basin (fig. 2.11). The thickness of the Nordland group located above the Torsk fm., thickness towards the west, increasing the potential for hydrocarbon accumulations within this interval. The Nygrunnen group is not identified in all wellbores supporting the different extents of the Kveite and Kviting formations within the study area (Gabrielsen et al., 1990). The Kolmule fm. is located within the Nordvestbanken group in the Barents Sea lithostratigraphy, which is the same as the Adventdalen group in the Svalbard lithostratigraphy (fig. 2.12). Younger groups are similar in the Svalbard and Barents Sea lithostratigraphy.

Potential shallow gas accumulations are identified in large parts of the study area in the SW Barents Sea (fig. 5.3–5.5). The term shallow in this thesis is set to be within the Late Cretaceous and younger deposits, including the upper Kolmule fm., the Kveite, Kviting and the Torsk fm. The results do not distinguish between shallow gas accumulations located within the Kveite, Kviting or Torsk fm., as they are difficult to separate from each other due to the seismic quality of the data and the extent of the different formations. Kveite and Kviting formations may not occur everywhere within the SW Barents Sea (Gabrielsen et al., 1990). Located between the bigger Torsk and the Kolmule fm. is most probably the Kveite fm. in this part of the Barents Sea (Faleide et al., 1993). The Kveite fm. is most likely identified as the intra Torsk reflector available in the existing dataset (fig. 3.5). Examples of this reflector are seen in figures 4.5 and 4.6. Different stratigraphic-controlled accumulation intervals are mapped in figure 5.3 showing the lateral extent of amplitude anomalies related to shallow gas within different defined stratigraphic units; (a) above Torsk fm., (b) below Torsk fm. top and above Kolmule fm. and (c) below Kolmule fm. top. This is to get a better understanding and control of potential stratigraphic accumulation mechanisms in the area.

5.5.1 Above Torsk fm.

The distribution of shallow gas accumulations located above the Oligocene and the Torsk fm. has a general trend of being located west and northwest of the study area (figure 4.10 and 5.3(a)). The areas with the highest density of these accumulations are located within the southern parts of the Sørvestnaget Basin and SW of the Veslemøy High. The central parts of the Tromsø Basin has some smaller shallow gas accumulations likely to be in connection with diapiric structures located beneath (fig. 4.1 and 5.4(b)). The reason for the high density of shallow gas accumulations in the western parts of the study area is mainly due to the increasing thickness of the Late Tertiary sediments creating a sedimentary wedge located west of the Tromsø Basin (Gabrielsen et al., 1990). This result is also probably related to and influenced by the greater subsidence of the Tromsø Basin in the Late Cretaceous and Tertiary (Vorren, Richardsen, Knutsen, & Henriksen, 1991). In the central and eastern parts of the study area, the Torsk fm. top represent the URU (fig. 2.5, 2.10 and 4.1) with associated difficulties related to identifying shallow gas accumulations within these shallow areas, due to disturbance in seismic signal (fig 5.1(b)).

5.5.2 Below Torsk fm. top and Above Kolmule fm.

The distribution of shallow gas accumulations located below the Torsk fm. top and above the Kolmule fm. is more widespread over the study area (fig. 4.11 and 5.3(b)). This is part of what is the main focus area (in depth) of this thesis as it is the seismic section of where the amplitude anomalies are most easily identified, and because Tromsø Basin and its upper 2500ms TWT in general consists of this unit (fig. 2.10). The area with the highest density of shallow gas accumulations is within the northern parts of the study area. Another trend is the location along the borders of Tromsø Basin, along RLFC and within Veslemøy High. The thickness of the unit located below the Torsk fm. top and above the Kolmule fm. is large within most parts of the study area, with exception of the Loppa High. A large part of the Torsk fm. is eroded in the eastern areas but still there is a large sedimentary package available all over the study area (fig. 2.5). The thickness increases towards west, as there is little or no erosion in this area (fig. 2.4). The shelf-edge is located to west of Senja Ridge and the Veslemøy High. The Torsk fm. is known to contain potential reservoir sandstones that can trap and accumulate hydrocarbons (NPD, 1996). Within this stratigraphic unit, there is no clear indication of what stratigraphic boundary is controlling the limitations of the accumulations and migration of hydrocarbons and fluid flow (fig. 4.2 and 4.3). Some reflections are terminated and located just beneath the URU, being related to the Torsk fm. top, while others are terminated more randomly within the stratigraphic unit. The Intra Torsk fm. top is a possible stratigraphic boundary with sealing properties (fig. 4.5). This is a result mainly due to local sediment variations within the Torsk fm. and the smaller Kveite fm.

5.5.3 Below Kolmule fm. top

The distribution of shallow gas accumulations located within the upper Kolmule fm. has a general trend of high-density areas located to the east and northeast within the study area (fig. 4.12 and 5.3(c)). Similar to the unit above, there is a small trend indicating that the mapped reflections are located along the Tromsø Basin borders, within RLFC, Veslemøy High and Polheim Sub Platform. The reason why the distribution is higher in the eastern and northeastern parts of the study area is mainly due to erosion of the overburden (fig. 2.5). The Kolmule fm. is the only formation top of interest present in this part of the study area as large parts of the Torsk and the intra Torsk formations are eroded (fig. 2.4). Potential shallow gas accumulations are therefore more easily identified and mapped located within the upper Kolmule fm. in these eastern areas.

5.5.4 General Trend

The general trend in the hydrocarbon accumulation intervals shows a distribution located in a W-E direction across the study area. To the west, the youngest stratigraphic units are the most effective shallow gas accumulation intervals. Towards the east, the older stratigraphic unit, below the Torsk fm. top increases in accumulation density related to the thick sedimentary package located within the Tromsø Basin. The oldest stratigraphic unit, below the Kolmule fm. and its highest density of shallow gas accumulations is located towards east and northeast of the study area. This general trend of the hydrocarbon interval is related to the amounts of uplift and erosion of the area. This is discussed further in sections 5.9 and 5.10.

5.6 Combination of Distribution Maps

The different distribution maps from the results (fig. 5.3-5.6) can be combined to see if there is any relation between the different seismic anomalies mapped associated to shallow gas accumulations (fig. 5.6-5.8). This will allow for a better understanding of the migration mechanisms in the area. Different combinations of distribution maps associated with shallow gas accumulations are seen in figures 5.6 and 5.7.

There is a large correlation between the existing mapped gas chimneys (fig. 3.2 and 5.4(a)) and the mapped distribution of deep source features (fig. 5.4(b)) coming from a possible source located below the Cretaceous and the upper Kolmule fm. This combination of distribution maps is shown in figure 5.6(a). Interesting areas for hydrocarbon accumulation, migration and generation are located in the northern part of Tromsø Basin, covering parts of RLFC and Veslemøy High, with a large high-density area of gas chimneys from a deeper source (1). Another area of interest is smaller isolated gas chimneys from a deeper source (2) located further south in the central parts of RLFC. The fluid-flow system located in the Hammerfest Basin (3), is located in connection with the Snøhvit and Albatross gas fields (NPD, 1996). Along the western border of Veslemøy High there is also an area of interest (4) where the mapped gas chimneys are from a deeper source clearly piercing the Kolmule fm. (fig. 4.10). This area is similar to area (1) as they are located along and towards the borders of Veslemøy High.

Combination of maps including distribution of salt diapirs and structural highs allow for a better understanding of the lateral extent of some features as the salt diapirs and structural highs tend to act as accumulation and migration boundaries. Figure 5.6(b) shows a combination of the gas chimney distribution (fig. 5.4(a)) and the distribution of salt diapir and structural highs (fig. 5.4(c)). Areas of interest are; northern parts of Tromsø Basin (1) with the structural Veslemøy High mapped as the features along northern Tromsø Basin border. This mapped structure is located together with mapped deep source feature (fig. 5.6(a) (1)) and is a structural high acting as a potential source for migration of the larger gas chimney system in the same area. SW of Veslemøy High shows mapped structural highs (2) located within the EL0001 survey. Gas chimneys are distributed along the Veslemøy High borders. NW of Hammerfest Basin shows mapped structural highs (3) being part of LH with larger gas-chimney systems located along and beneath the structure border. The central part of Tromsø Basin (4) is an area with high-density distribution of salt diapirs. This area has bright spots located above and along dipping reflectors at structural sides. Along Senja Ridge (5), there are large areas of mapped structural highs related to the subsurface ridge. This area is not connected with any high-density areas of gas chimneys, but shallow gas accumulations are identified in the area along dipping reflectors (5.4(d)).

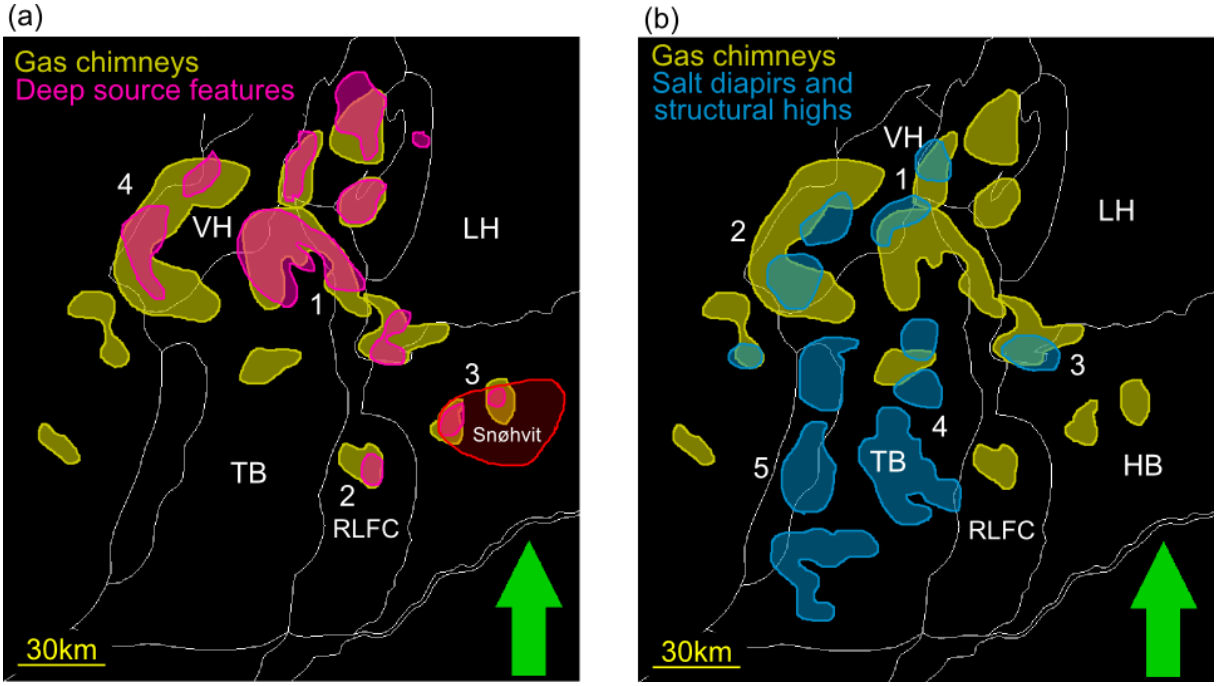

Figure 5.6 – Combination of distribution maps. (a) Combined gas chimneys and deep source features distribution with four specific areas of interest. (b) Combined gas chimneys, salt diapirs and structural high distribution with five areas of interest. Areas of interest are discussed in section 5.6. Snøhvit field is located within HB.

Another combination of distribution maps (fig. 5.7) combines the mapped structural highs and salt diapirs (fig. 5.4(c)) with the distribution of dipping (fig. 5.4(d)) and flat (fig. 5.4(e)) reflections in the area. The distribution of the flat and dipping reflections is not very helpful in the process of identifying shallow gas accumulations, but it can give an overview of the accumulations located above and on the sides of structural highs to see if the migration and accumulation follow the stratigraphy along and close to these features. Areas of interest within figure 5.7 are; an example of reflections in connection with diapir structures located in the central parts of Tromsø Basin (1) with dipping reflections at sides of diapir structures. Similar trend is located south of Loppa High (2) with an area of dipping reflections away from its border. Along the border between RLFC and Hammerfest Basin there is a larger area of flat and dipping reflections (2) without any mapped structural high. This is an area of dipping and flat reflections along strata with no evidence of intrusion. The dipping is towards west and the deeper Tromsø Basin. The northern parts of the Tromsø Basin, along the borders of and within Veslemøy High (3) have strong reflections being both flat and dipping. The flat reflections are mostly located within Veslemøy High and the Polheim Sub Platform, while the dipping reflections are generally located along these structural borders. Along Senja Ridge (4), there is an area of mapped structural high and a distribution of dipping reflections related to the ridge. The distribution indicates migration and accumulation towards the structural high of the Senja Ridge from the depths within the Tromsø Basin. Mapping of salt diapirs and structural highs together with potential migration pathways has improved the understanding of effective migration pathways in other areas (Hood, Wenger, Gross, & Harrison, 2002). The potential migration pathways within the study area are discussed further in section 5.9 and the figures 5.13, 5.18, summarized in figure 5.19.

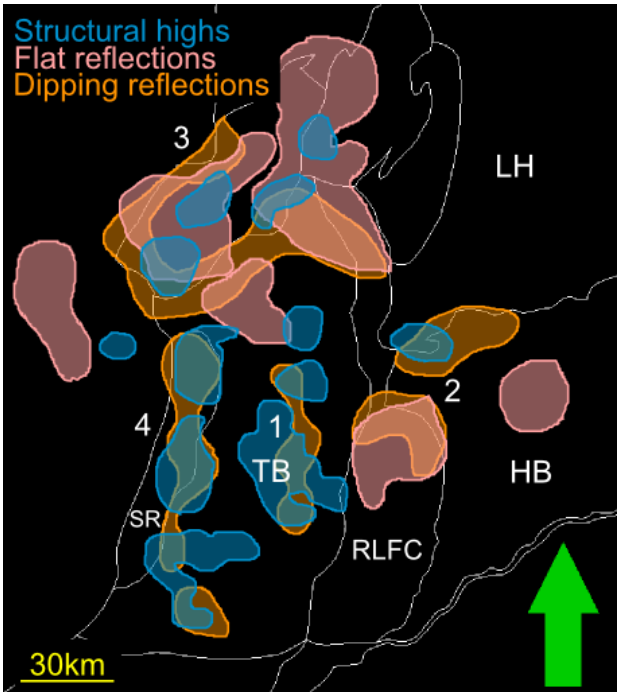

Figure 5.7 – Combination of distribution map showing structural highs, salt diapirs, flat and dipping reflections with four specified areas of interest discussed in section 5.6.

5.7 Shallow Gas Origin and Generation

The origin and difference in the distribution of the shallow gas accumulations could be a combination of the existence of several known source rocks (fig. 2.3) and the different geological plays within the study area (fig. 2.6). It could also be a result of the availability of different structural and stratigraphic traps (fig. 4.6). The Tromsø Basin is known to have the presence of salt diapirs located mainly in the central parts of the basin (Faleide et al., 1993). These diapirs form different geological traps for potential accumulations of shallow gas and creates new migration pathways (Vadakkepuliyambatta et al., 2013; Woodbury et al., 1980). Other studies within the Barents Sea has proposed that gas hydrates are developed from a thermogenic gas leaking from a deeper source or other deeper hydrocarbon accumulations (Laberg, Andreassen, & Knutsen, 1998).

Potential source rocks within the study area are both the minor Torsk and Kolmule fm. shales, but there exists deeper sources being the major source rock Hekkingen and the minor source rock Tubåen formations (summarized in fig. 2.3). The origin of the shallow gas accumulations in the study area is not easy to identify as the quality of the seismic data is poor, in general below the Kolmule fm. (below 2500ms TWT). Generation can be deeper source rocks being of thermogenic gas or it could be generation at shallower levels within the Kolmule and Torsk fm. shales being either thermogenic or biogenic gas. This is dependent of both the time of generation and the amount of uplift and subsidence in the area. The distribution of deep source features (fig. 4.13 and 5.4(b)) helps locate the shallow gas accumulations most likely to be associated with thermogenic gas generation. The biogenic gas generation tends to occur only at shallow depths some hundreds of meters below the seafloor. Assuming the compressional wave velocity in the subsurface sediments being 2000m/s, the depth in time (ms TWT) will equal the depth in meters. This gives a range of the biogenic gas generation approximately within the upper 500ms TWT or 500m below the seafloor. Tracking the origin of deep source features is difficult as the seismic signal loses its strength at great depths (fig. 5.1(a)) and in these cases; it is not possible to identify their origin or place of where the generation

most likely occurred. The only evidence available is that the hydrocarbon originates from a depth below the Late and Middle Cretaceous sediments. In most cases, it penetrates the Kolmule fm. (fig. 4.3(a), 4.4(a), 4.13(a) and 4.19(a)); most probably from the major source rock in the area, the Late Jurassic Hekkingen fm. Isostatic uplift and erosion is known to have influenced the hydrocarbon migration and accumulation in the area. Together with the glacial cycles, it is believed that these Cenozoic events can be responsible for most of the fluid leakage observed in the SW Barents Sea (Vadakkepuliyambatta et al., 2013). The Mesozoic Era is the most important time period offshore Norway for hydrocarbon resources and the occurrence of source and reservoir rocks (Martinsen & Dreyer, 2001). Several periods of uplift and erosion are identified from the Paleogene – recent time (Henriksen et al., 2011b). These events are related to uplift and erosion within; Paleozoic to Early Cenozoic, Oligocene-Miocene and the Pliocene-Quaternary (Reemst et al., 1994). As of this evolution, the Barents Sea is known as a complex hydrocarbon region (Doré, 1995; Henriksen et al., 2011b; Stilwell, 2012). The massive erosion of overburden sediments in the study area at late geological time had severe consequences for the hydrocarbon accumulation and generation in several ways. This complex hydrocarbon region is a result of; exsolution of gas from the oil and expansion of gas due to decrease in pressure resulted in displacement and expulsion of the oil from most of the traps, breaking seals and spillage due to the uplift and a cooling of the source rock causing most hydrocarbon generation to cease (Doré, 1995; Doré & Jensen, 1996). The only way to prove definite evidence of a hydrocarbon source is by geochemical analysis and testing of hydrocarbon samples (Davis, 1992).

Source rock maturity is temperature and depth dependent, being related to uplift and subsidence of an area. The maturity of a source rock is dependent on its maximum burial depth as it is temperature controlled (Rafaelsen, 2012). The SW Barents Sea has experienced different magnitudes of uplift and subsidence affecting the maturity of the different potential source rocks within the area.

The geological history of the Barents Sea has most probably lead to generation and migration of hydrocarbons over large areas. This migration can transport hydrocarbons a great distance from its original source and into new reservoir and accumulation areas that otherwise would not have been filled. Accumulations in this region are often a mixture of hydrocarbons originating from several different sources being evident of different active source rocks in the region (Henriksen et al., 2011b; Ohm, Karlsen, & Austin, 2008). As a result, the original source of hydrocarbon generation is not easy to identify only using seismic data. As the source for the shallow gas accumulations are most likely a mixture of several source rocks, there is reason to believe that one of these sources is the shallow major source rocks in the Barents Sea; the Upper Jurassic marine shales of the Hekkingen fm.

5.8 3D Seismic Features of Interest

The seismic amplitudes of interest within the 3D seismic data (fig. 4.17 and 4.18) are two features that are investigated further to see if there is any connection with the shallow gas accumulations in the study area. There are no 2D seismic lines across both features but after mapping out the potential lateral extent for each of the two 3D features (fig. 5.5, 4.19 and 4.20), the seismic 2D line EL9701-451 is located in such a way that it covers both features extent (fig. 5.13). The generation, migration and accumulation related to the 3D seismic features are summarized in figure 5.13. Results of this interpretation illustrates the two features extent beneath the same stratigraphic level located within the Torsk fm. unit. This stratigraphic level covers the EL0001 feature at a depth of 1500ms TWT and the reflector is visible and almost continuous towards east and the LN09M01 feature

located at a depth of 1000-1250ms TWT. The decreasing stratigraphic depth is east towards the edge of the Tromsø Basin and the Ringvassøy-Loppa Fault Complex.

Figure 5.8 displays the lateral extent of the 3D features combined with mapped gas chimneys and deep source features in the area. This is applied to tell more about the two potential shallow gas accumulations origin and migration pathways. The distribution of gas chimneys (fig. 5.4(a)) and the deep source features (fig. 5.4(b)) are known to be closely linked (fig. 5.6(a)).

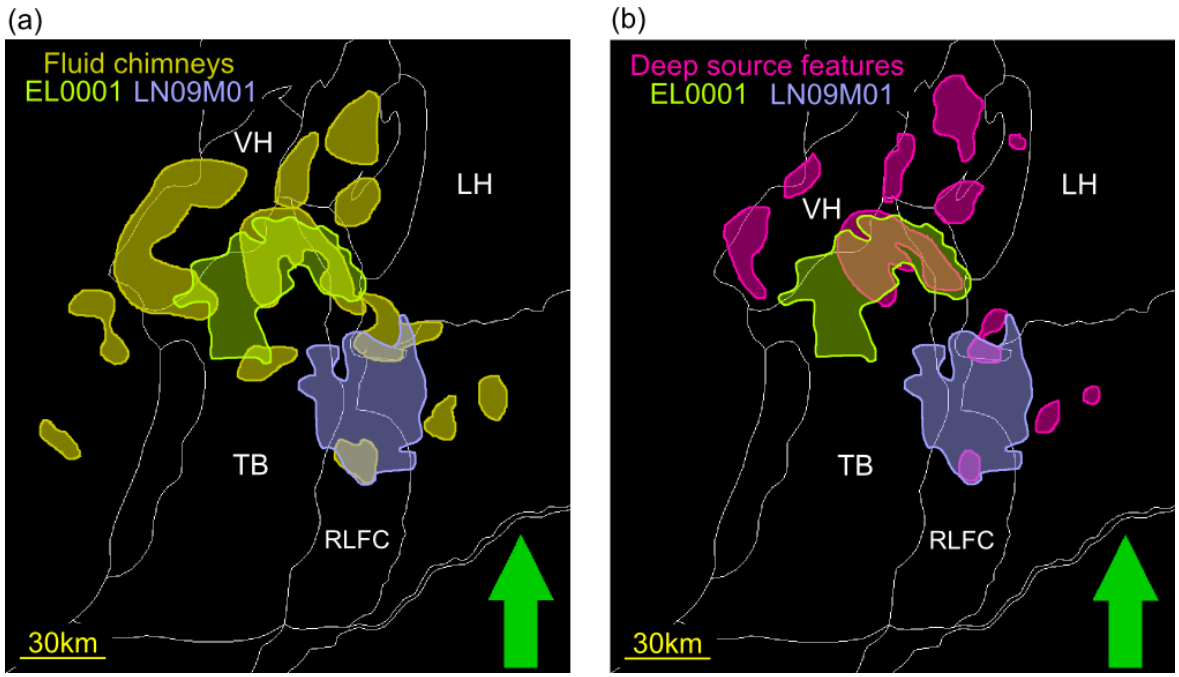

Figure 5.8 – Combination of different distribution maps from the 2D and 3D seismic data (EL0001 and LN09M01). (a) Distribution of the gas chimneys and lateral extent of the 3D features of interest. (b) Distribution of deep source features and lateral extent of the 3D features of interest.

5.8.1 EL0001 Feature

The bright amplitude anomaly found association with the 3D survey EL0001 (fig. 4.17) consists of a large negative seismic body covering an area of approximately (60kmx25km) 1500km^2 located at the boundary between the Tromsø Basin and the Veslemøy High. The lateral extent of the feature (fig. 5.5(a)) follows a specific stratigraphic level east and southward with the shallowest amplitude anomalies located within the eastern parts. The lateral extent of the feature is located in the northern part of Tromsø Basin where there is a high density of gas chimneys from a potential deep thermogenic source (fig. 5.6). This is also the most probable source for the EL0001 shallow gas accumulation (fig. 5.8). The deep source gas chimneys are located and terminated at the features shallowest point indicating that some uplift or subsidence has occurred in the area as the amplitude anomaly extends downward into Troms Basin. There are some indications of a potential shallow source located within the Tromsø Basin, but the feature depth is located too deep to be of biogenic origin, even with the known uplift and erosion of the area. Smaller shallow chimneys are located beneath the structure that could act as feeders to this accumulation located south of the feature (fig. 5.8). The EL0001 feature could be a result of different gas-chimney systems in the area with several different source rocks from either redistribution of hydrocarbons or still active and ongoing migration or generation.

The amplitude anomaly is separated by faulting towards the west indicating that the anomalies further west of the EL0001 feature (fig. 4.17(c)) can be related to the origin of the main amplitude body, as they are located within the same stratigraphic unit. The 3D surface (fig. 4.17(d)) above the feature shows indications of this faulting connected to a larger fault system NW of the feature. The outline of the NW fault system is neglected, as it is mainly a result related to the 3D tracking of the horizon in an area of weak reflectors. The tracking of the horizon then chooses between weak reflectors within the tracking parameters, following different reflectors within this part of the survey. This is not affecting the results of the EL0001 lateral extent. Therefore, it is not corrected in the seismic 3D data and surface as the EL0001 feature ceases to exist before these seismic events occur.

5.8.2 LN09M01 Feature

The feature of interest within the LN09M01 survey (fig. 5.5(b)) consists of two smaller features not being a fully connected anomaly body (fig. 4.18 (1) and (2)). It is located within a horizon that is dipping towards Tromsø Basin. The results show that the features are located under the same stratigraphic level and that they are more or less connected with each other. There is a depth difference of approximately 300ms TWT between the two. As the strongest anomalies are located at the shallowest levels within the horizon, there are indications of fluid-connection or existing migration pathways between these two intra LN09M01 features (fig. 4.18 (1) and (2)).

The total lateral extent of the amplitude anomaly mapped in connection with the LN09M01 feature covers an area of approximately (50kmx30km) 1500km^2 with most of the anomaly located within RLCF (fig. 5.5(b)). This amplitude anomaly stretches towards south of the 3D survey, towards an area of dipping reflections into Tromsø Basin. At the feature southernmost lateral extent (fig. 5.5(b)), a potential feeder for the system is located, being a mapped deep source gas chimney with termination at the exact stratigraphic level as the location of the LN09M01 feature (fig. 5.8). There is also a smaller gas chimney located within the northern extent of the feature. This could be a potential feeder to the accumulation, but its location is below the shallowest parts of the feature favoring the chimney system in the south. Towards Loppa High, the stratigraphic surface, which the amplitude follows, is located close to the seafloor and is therefore a surface that is difficult to identify within this area. As a result of the up-dipping surface towards the north and northeast within the area of interest of the RMS amplitude map (fig. 4.18(c)) and the 3D surface (fig. 4.18(d)), this area is not studied in detail, even though the results of this area can be interesting. These results are probably not correct as the surface tracking uses automatic 3D tracking with specified parameters. This result shows strong amplitude anomalies probably related to the reflections within the upper section of the seismic being related to the strong seafloor reflector and URU (fig. 4.18 (3)).

5.8.3 3D Seismic Features Extent

As there are seismic 2D lines across both features lateral extent (fig. 5.13) there is still no evidence of them being part of or connected to the same amplitude body. There is low 2D seismic coverage in the area making identification of the features a difficult process, based on correlations between the seismic lines in the area showing the two different features. Both features can with certainty be said to be located beneath or at the same stratigraphic level being an intra Torsk fm. (fig 4.19, 4.20 and 5.13), most probably being the base Tertiary (Gabrielsen et al., 1990). Figure 5.9 shows the two features and their lateral extent in a 3D view. The visualization of 2D data in a 3D window is not ideal but it gives an indication of the different stratigraphic depths of where the features from EL0001 and LN09M01 are located. Notice who the two features are both located at same depths and that the

angles of the amplitudes are in general down-dipping towards Tromsø Basin and up-dipping towards the east and the Loppa High, and towards the north and the Veslemøy High.

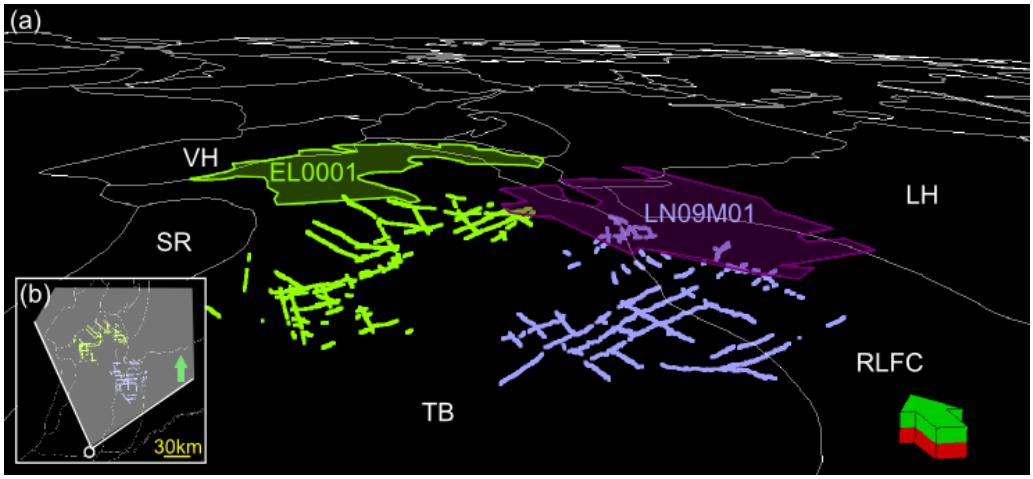

Figure 5.9 – Three-dimensional visualization of the 2D lateral extent of the two amplitude-anomaly features from the different 3D seismic surveys. (a) 3D window of the study area. Seismic survey EL0001 is a green polygon with the EL0001 feature extent in light yellow. Seismic survey LN09M01 is a pink polygon with the LN09M01 feature extent in purple. Vertical exaggeration is set to x15. (b) View seen from a 2D window located over the central/south Tromsø Basin illustrating the point of view.

5.9 Fluid Migration

Fluid migration within the Tromsø Basin and adjacent areas is most likely not related to primary migration, as the petroleum sources are likely to be located deeper than the vertical extent of the study area, extending down below the Kolmule fm. top. The Late Cenozoic uplift and erosion in the Barents Sea is known to have had a great influence on the petroleum migration in the area (Doré & Jensen, 1996). The bright spots located within and along clinoforms of the Torsk fm. are interpreted to be free gas forming shallow gas accumulations (fig. 4.3). Migration is probably a result related to the redistribution of hydrocarbons due to tectonic activity. The tectonic activity in the area has been through several cycles of glacial periods and times of uplift and erosion (Henriksen et al., 2011a). The general trend in the study area consists of seismic anomalies originating from a deeper source located typically directly beneath or close to the shallow gas accumulations. Figure 5.10 shows a seismic section with different stratigraphic boundaries, the URU, the Torsk, intra Torsk and the Kolmule fm. tops, as potential zones of gas accumulations. There is a zone of acoustic masking identified as a gas chimney coming from a deep source being the most likely feeder for the shallow gas accumulations in the area. The main shallow gas accumulation is identified as bright spots at a depth of 800ms TWT spreading out along the stratigraphy at the gas chimney termination. Smaller bright spots are also identified along the deeper stratigraphic boundaries along the vertical migration pathway. This might be results of smaller lateral migration within the stratigraphy, being free gas trapped along the main migration pathway. Potential source rock is located below deep-seated faults in the area. Above the main shallow gas accumulation there is potential gas-hydrate related BSR directly below the URU. The location of the potential BSR has formed at the flanks of the shallow gas accumulation at 800ms TWT, and at a place where the Torsk fm. splits up and dips down towards west, being a potential zone of leakage for the vertical migration of free gas towards the GHSZ or sealing layers like the URU. This behavior is most likely a result of buoyancy-driven vertical migration. Figure 5.10 is chosen as it illustrates the typical migration pattern identified within the study area.

Due to the poor coverage from only 2D seismic data, there is an uncertain involved in identifying potential migration pathways. Resolution and sample spacing are some of the limitations related to 2D seismic data. Shallow gas accumulations can be isolated bodies on seismic sections while there could be leakage from the same amplitude body located in a zone where there is no seismic coverage. This leads to the identification of possible migration pathways based on assumptions from the seismic data and on the geological setting of the area.

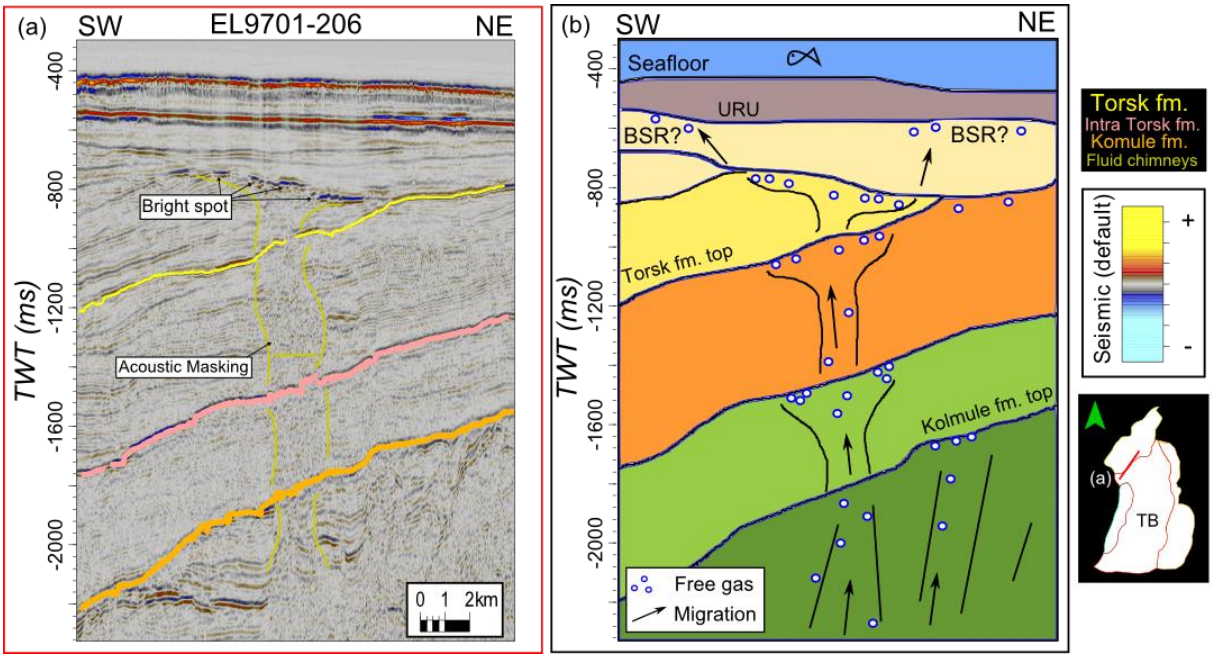

Figure 5.10 – (a) Seismic section EL9701-206 with mapped bright spots. (b) Simplified potential accumulation and migration pathways through the stratigraphy. Migration along deep-seated faults and origin from a depth below the Kolmule fm. is a possible origin of the shallow gas accumulation. No seepage to the seafloor is identified. Potential BSR is located directly below the URU at a depth of 600ms TWT as enhanced reflections.

Figure 5.11 shows vertical migration from a deeper source below the Kolmule fm. top and indications of leakage terminating within the Torsk fm. at a depth of approximately 1000ms TWT. Even though the intra Torsk fm. is not mapped in this seismic survey, this stratigraphic level correlates to the location of the intra Torsk fm. top acting as a stratigraphic boundary for the accumulations. This stratigraphic boundary is probably related to internal sedimentary changes existing within the different stratigraphic units. Located at a depth of approximately 650ms TWT are other potential shallow gas accumulations directly below the URU as a stratigraphic boundary. Above the URU, it is known exist hard glacial sediments having potential sealing properties. Possible migration pathways originate from the shallow gas accumulation located below with potential migration occurring not within the same seismic section. Other possible migration pathways come from the east, along dipping stratigraphy extending out of the seismic section. The shallow gas accumulations below the URU are potential BSR at the base of the GHZS with free gas located below and the potential formation of gas hydrates located above the reflection. These shallow gas accumulations (fig. 5.11) are also plausible results of buoyancy-driven migration originating from deeper stratigraphic levels. The migration pathways (fig. 5.11) are comparable to migration pathways in other parts of the study area (fig. 5.10).

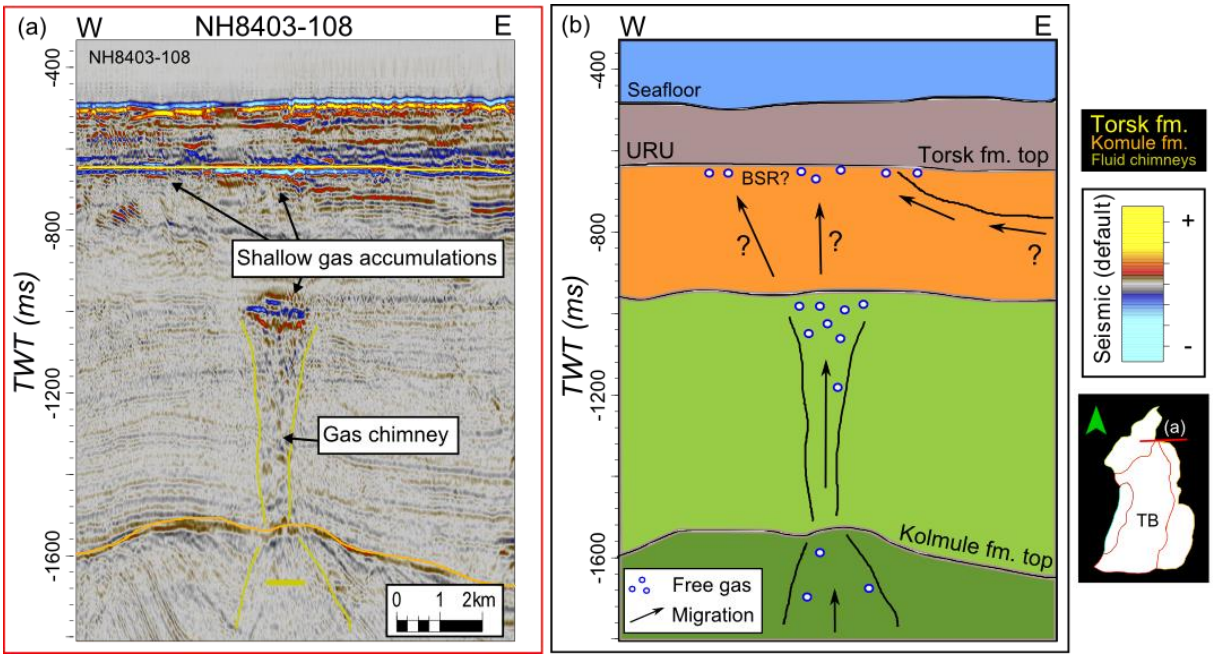

Figure 5.11 – (a) Seismic section NGH8403-108 with mapped bright spots and gas chimney. (b) Simplified potential accumulation and migration pathways through the stratigraphy. Migration and origin from deep source located below the Kolmule fm. is a possible origin of the shallow gas accumulation at a depth of 1000ms TWT. No seepage to the seafloor is identified. Potential BSR is located directly below the URU at a depth of 650ms TWT as enhanced reflections. Potential migration pathways are marked with question marks, as they are identified in the seismic section.

Within the Tromsø Basin, there are indications shallow gas accumulations spread over a wide area (fig. 5.3 and 5.4). General migration pathways for the shallow gas accumulations from a deeper source are generally towards and along clinoforms and strata at the basin borders. This migration leads towards the structural highs the Senja Ridge to the west, the Veslemøy High to the north and the Loppa High to the east. Along the east and northeastern border of the Tromsø Basin, the Ringvassøy-Loppa and the Bjørnøyrenna Fault Complexes are acting as distinct migration pathways for the shallow gas accumulations. In the fault zones, there is a major possibility that the source is located at greater depths and that the migration pathways exists along deep-seated faults in the area. Re-migration can be activated as a result of uplift, erosion and subsidence. This migration is mainly results of buoyancy-driven processes, which is the general trend for the shallow gas migration within the study area. The potential source rock is most likely located deep (below Kolmule fm. top) and below zones of faulting. Periods of faulting is known to have occurred between periods of great subsidence. The major subsidence event is aged Early Cretaceous, with periods of faulting at the Late Jurassic and Middle Cretaceous (Faleide et al., 1984). This allows migration to bypass otherwise sealing stratigraphic boundaries along potential leaking faults.

The highest density of features related to shallow gas accumulations is located within the northern parts the study area within the SW Barents Sea (fig. 5.2-5.6). The areas of mapped gas chimneys and deep source features with associated bright spots are mainly located and terminated within and above the Late Cretaceous stratigraphic units. These mapped amplitudes are located above the Kolmule fm. top and below the Torsk fm. top (fig. 4.11). Figure 5.12 shows two different seismic lines within Tromsø Basin, with a simplified stratigraphy based on the work by Dalland et al. (1988). The figure shows potential places of accumulation, origin and migration pathways that are mainly located along clinoforms and stratigraphic boundaries terminating within Late Cretaceous and the Tertiary units.

The W-E seismic line TR73R1-7200 across Tromsø Basin (fig. 5.12(a)) illustrates shallow gas accumulation most likely originating from mixed deeper sources at several locations within Tromsø Basin. The migration occurs along the deep dipping reflectors on the western margin and along structural highs and associated faulting in the east, towards RLFC and Loppa High. Migration pathways are most likely to occur below and along clinoforms and stratigraphic boundaries of low-permeable layers. Density and gravity will lead the migration towards the surface as long as the subsurface conditions allow this to occur. The extent of the EL0001 feature (fig. 5.5(a)) is located within red box (1) (fig. 5.12(a)) with the feature mapped out located within the 3D survey (fig. 4.17) located within red box (2) (fig. 5.12(a)). The shallow gas accumulation is located beneath an intra Torsk fm. top with smaller vertical zones of leakage into younger Cenozoic sediments beneath the URU. Lateral migration occurs along the dipping stratigraphy towards east, with termination beneath the sealing unit above the URU. Most probable source for this accumulation is of either Early Cretaceous or Jurassic, with the major source rock Hekkingen fm. as part of the hydrocarbon origin.

The N-S seismic line TR83R1-193730 (fig. 5.12(b)), located along Tromsø Basin border and above RLFC, shows the same general trends in accumulation, migration and generation as figure 5.12(a). It illustrates hydrocarbons originating from a deeper source within Tromsø Basin and the possible migration pathways along faulted zones (RLFC and BFC) and towards structural highs (LH, VH and salt diapirs within TB). This leads the migration along the stratigraphy mainly in the direction of Loppa and Veslemøy Highs.

The EL0001 feature and its extent (fig 5.5.(a)) is located within red box (1) (fig. 5.12(b)) showing the occurrence of free gas located along the intra Torsk fm. directly above a deep-source gas chimney with unidentified place of origin. Another possible migration pathway towards this accumulation is along faulted zones above RLFC at central parts of the seismic section also migrating from a deeper source of unknown origin. Vertical migration occurs mainly above deep-seated faults and lateral migration occurs along clinoforms and stratigraphy towards the more shallow areas. A structural high towards the north is another potential source for shallow gas accumulation with origin from a deep source and migration along the dipping stratigraphy towards the more shallow areas where the fluid-flow and gas chimneys tend to be terminated beneath sealing layers.

The LN09M01 feature and its extent (fig. 5.5(b)) is located within red box (2) (fig. 5.12(b)) showing free gas accumulating along the same intra Torsk fm. as the EL0001 feature extent. This feature is located above RLFC and potential generation is located at a deeper level with potential migration pathways along these deep-seated faults. There is a possibility that the two features (1) and (2) (fig. 5.12(b)) share the same feeder-system being a source migrating along faults in central parts of the seismic section. Towards the south, feature (2) (fig. 5.12(b)) is located directly above a mapped deep-source zone of vertical gas leakage being the most probable candidate pathway for this gas generation. The gas-chimney system is terminated at the same stratigraphic level of the mapped LN09M01 feature, most probably being aged Paleocene and the intra Torsk fm.

Faults are known to be the main draining and migration pathways for hydrocarbons in many of the worldwide basins (Ligtenberg, 2005). The study area has known events of deep-seated faults acting as migration pathways from the deeper sources beneath. Hydrocarbon generated from these sources tend to migrate upwards and along the structural highs located along the borders of the Tromsø Basin.

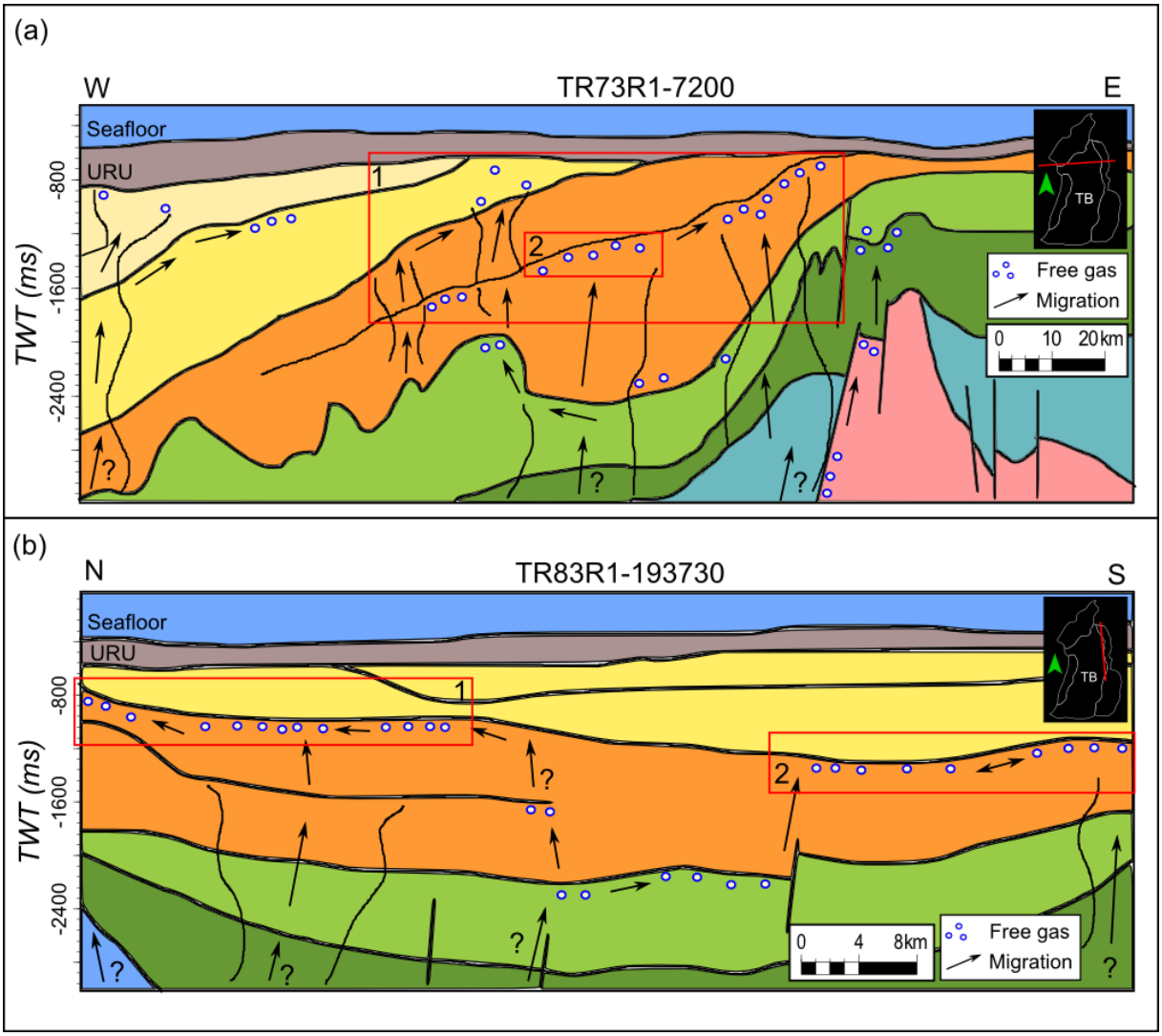

Figure 5.12 – Simplified stratigraphy and hydrocarbon accumulation, migration and generation. (a) Seismic section TR73R1-7200 W-E across northern part of TB. Red box (1) shows the extent of the EL0001 feature (fig. 5.5(a)), while (2) is focused around the feature located within the 3D EL0001 survey (fig. 4.17). (b) Seismic section TR83R1-193730 N-S above RLFC. Red box (1) shows the extent of the EL0001 feature (fig. 5.5(a)), while (2) is the extent of the LN09M01 feature (fig. 5.5(b)). Migration pathways are indicated with arrows. Question mark illustrate the unknown or not easily identified on the seismic data, being either potential sources or migration pathways. Location of the seismic lines are also seen in figure 5.13(b) showing the extent of the 3D seismic features.

The major source rock in the area, the Hekkingen fm. is located and identified at a depth of approximately 3000ms TWT within the study area (Gabrielsen et al., 1990; NPD, 1996). Indications from the 2D seismic data (fig. 5.12(a) and 5.13) show that the migration might occur from a depth penetrating this interval creating potential mixed source for the shallow gas accumulations within the 3D features to be from older sediment below Late Jurassic age. Poor seismic quality at great depths makes this an assumption not based on solid evidence, but it supports the theory of mixed source rocks in the area (Henriksen et al., 2011b).

A similar migration pattern (fig. 5.12) is identified across the 2D seismic line EL0901-451 (fig. 5.13(a). This seismic line is chosen, as it is one of few lines covering the identified seismic anomaly of interest within the EL0001 survey (1) (fig. 5.13) and the potential lateral extent of the LN09M01 feature (2) (fig. 5.13). The southeastern part of the seismic line shows a most likely source of the shallow gas accumulation related to the LN09M01 feature (2) (fig. 5.13), being a deep source feature within the

central parts of RLFC. This indicates migration pathways along deep-seated faults with hydrocarbon generation at even greater depths. There is a related uncertainty of the stratigraphy identification in the area due to the limitations associated with the use of only 2D seismic data, especially at deeper levels within the subsurface. The stratigraphy is based on the defined horizons (fig. 3.5) and work by (Gabrielsen et al., 1990).

Figure 5.13(b) shows the distribution of the potential lateral extent of the 3D seismic features with location of different seismic lines (fig. 5.13(a), 5.12(a) and (b)) for better correlation and understanding of the migration pathways occurring in the different seismic lines across the features of interest. (1) (fig. 5.13) equals the EL0001 feature and its extent (fig. 5.5(a)). Figure 5.13 (2) equals the LN09M01 feature and its extent (fig. 5.5(b)). Figure 5.13(c) illustrates the combined distribution map with the mapped gas chimneys and deep source features (fig. 5.6(a)). Location of seismic line figure 5.13(a) and the feature extents (fig. 5.13(b)) is shown to identify the different fluid-flow features and migration pathways in the area used to interpret the simplified schematic overview of the stratigraphy in figure 5.13(a). The zones of faulting correlate to Late Jurassic/Early Cretaceous activity (Faleide et al., 1993), acting as vertical migration pathways for both features (1) and (2), similar to the suggested migration identified in figure 5.12. Migration appears to follow the stratigraphy and internal clinoforms towards shallower depths at the Tromsø Basin flanks and towards the structural highs of Senja Ridge, Veslemøy High and Loppa High. The LN09M01 feature (2) (fig. 5.13) shows associations with deep source gas chimneys located beneath and over the central RLFC with migration along deep-seated faults as migration pathways for the vertical bypassing of the different stratigraphic lithology changes in the subsurface, similar to what is suggested in figure 5.12(b).

The southern parts of the Tromsø Basin does not have the same structural boundaries as the other parts of the study area as it more smoothly changes into the Harstad Basin. This is a potential reason for the low-density of potential shallow gas accumulations and migration pathways located within this part the study area, with migration mainly towards the basin flanks and structural highs.

The trends for the Tromsø Basin and the adjacent areas are mainly potential migration pathways along the stratigraphy of the area with a most likely source coming from deeper levels within the subsurface (fig. 5.12 and 5.13). The exact origin is difficult to identify but as it is probably related to deeper hydrocarbon generation, most likely of a thermogenic generation process due to its depth below the zone of biogenic generation. Biogenic generation of hydrocarbons can exist in the area but they are difficult to identify as the volumes produced may be small volumes at very shallow depths (>500m).

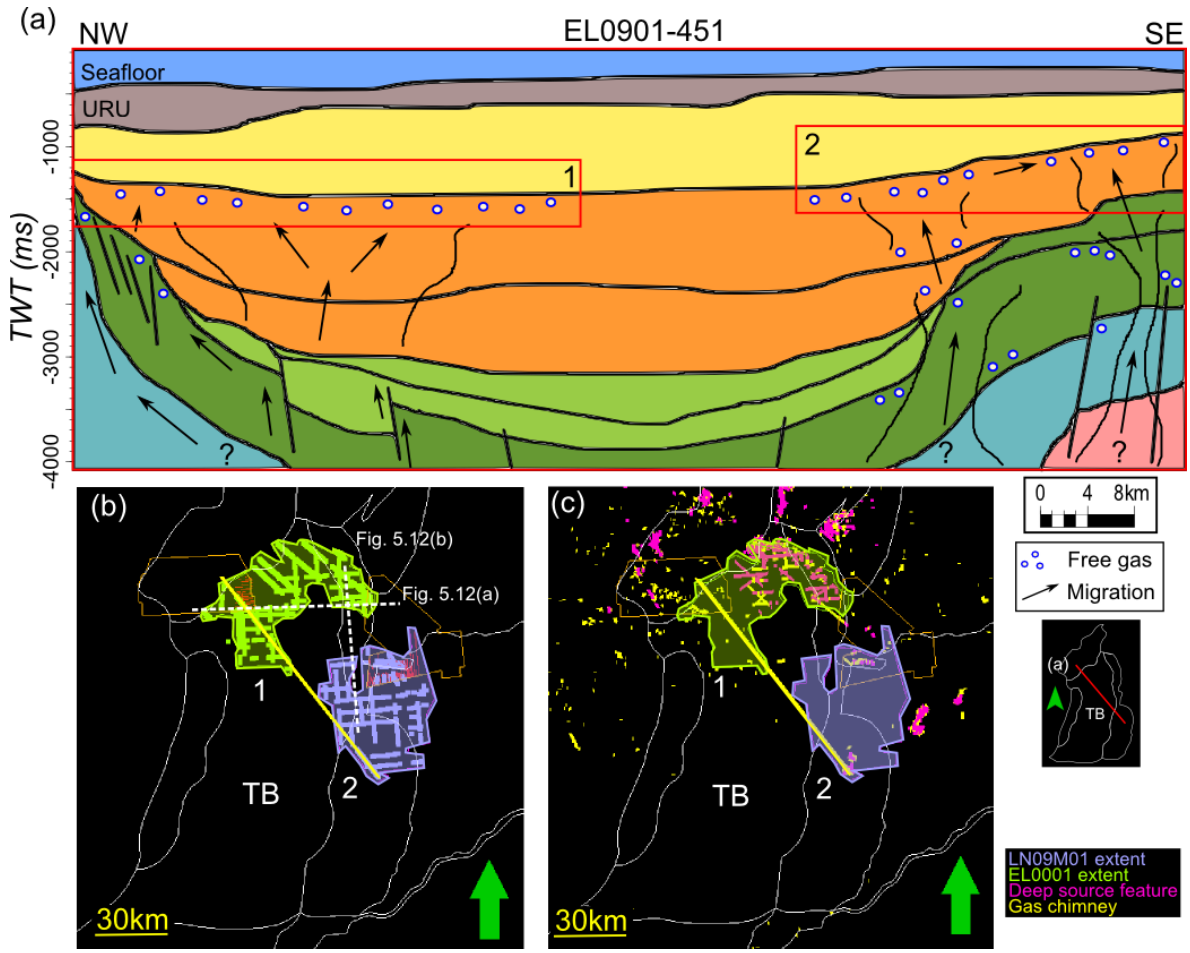

Figure 5.13 - Stratigraphy and hydrocarbon accumulation, migration and generation across the two 3D seismic surveys EL0001 (1) and LN09M01 (2) features of interest. (a) Seismic section EL0901-451, a NW-SE across northern part of TB. Red box indicate the features of interest identified in the 3D surveys. Question mark is an unknown or not easily identified source or migration pathway on the seismic data. (b) Map of study area illustrating the lateral extent of the 3D features (fig. 5.5) with location of the seismic line (a) in yellow and the 3D survey outline in orange. Location of seismic lines in figure 5.12 are seen on the map. (c) Map of study area with the feature extent highlighted and the location of the features indicated with 1-2. This map is a combined distribution map (same as figure 5.6(a)) with gas chimneys (yellow) and deep source features (pink) to get an overview of potential sources and migration pathways for the shallow gas accumulations (similar to figure 5.8).

There is a resemblance with the mapped shallow gas accumulations (fig. 5.3), potential migration pathways within the study area (fig. 5.12) and the different known geological plays (fig. 2.6). The Paleocene and Supra Paleocene play model is located below and towards the western part of the study area (fig. 2.6(c)). This correlates with the Cenozoic wedge developed west of the Tromsø Basin and towards the current shelf-edge. These mapped potential shallow gas accumulations are identified mainly above the Torsk fm. with a high-density area located over the same western part of the study area (fig. 5.3(a)). Both Jurassic and Cretaceous play models (fig. 2.6(a) and (b)) exist along the east and north border of the Tromsø Basin. This can be linked with the distribution of the mapped shallow gas accumulations and migration pathways located in these areas of high-density hydrocarbon accumulation and migration-associated seismic anomalies (fig. 5.3-5.5). These are mainly the occurrence of shallow gas accumulations found within the Torsk and upper Kolmule fm. (fig. 5.3(b) and (c)) and the extent of the 3D features of interest (fig. 5.5 and 5.13). The geological plays increase the chance of hydrocarbon accumulations to exist as they indicate a working petroleum system in the area (NPD, 2014).

5.10 Accumulation Mechanism

Different accumulation mechanisms are identified (fig. 4.4, 4.5, 4.6 and 4.8) and known to exist throughout the study area. Detailed studies of hydrocarbon trapping mechanisms within the study area is not the focus of this thesis. Other studies discuss hydrocarbon traps in more detail (Biddle & Wielchowsky, 1994; Woodbury et al., 1980). Accumulation mechanisms can occur in subsurface structural or stratigraphic trapping of hydrocarbons. Within the study area, shallow gas accumulations are identified in association with BSR, salt diapirs, structural highs and different stratigraphic units.

5.10.1 Shallow Gas Related to BSR

The shallow gas accumulations are not mapped to show the distribution of potential BSR within the study area. This is a difficult identification process and it would require more details about the subsurface conditions. Potential BSR are located within the study area (fig. 4.7) but they are not distinguished from normal bright spots associated with shallow gas accumulations. The reason for discussing BSR related to shallow gas accumulations is mainly the EL0001 feature of interest and its extent across the study area (fig. 5.5(a)). The BSR is most likely related to amplitude anomalies mapped within the shallow parts of the seismic data, generally located above or within the upper Torsk fm. to the west (fig. 5.3(a)) and within the upper Kolmule fm. to the east (fig. 5.3(c)) due to the erosion of the study area (fig. 2.4). The BSR can be results of either gas-hydrate or diagenesis-related BSR, and both cases are related with the occurrence of zones of free gas located beneath the BSR, being potential shallow gas accumulations. BSR is identified and mapped within the LN09M01 survey and it is therefore known to exist in the study area and parts of the SW Barents Sea (Rajan et al., 2013).

5.10.1.1 Gas-Hydrate Related BSR

A possible result of shallow gas accumulations being associated to gas-hydrate related BSR are the bright spots mapped out mainly beneath the upper regional unconformity (URU) which has an overlying sequence of glaciogenic sediments (Vorren et al., 1991). Figures 5.10 and 5.11 show potential shallow gas accumulations located beneath the GHSZ and the URU. Their depth is at approximately 500-800ms TWT below the sea surface and 200-300ms TWT beneath the seafloor reflector. The reflections mapped at this stratigraphic level also fulfill the criteria of being phase-reversed reflections compared to the seafloor. The URU is located at a shallow level indicating that it can be related to a potential base of the GHSZ. Seismic indications of gas-hydrate related BSR is mainly due to the occurrence of free gas located beneath the GHSZ (fig. 1.9). Shallow gas accumulations related to gas hydrates show no general trend in distribution, as this is dependent of the magnitudes of erosion in the area affecting the subsurface pressure and temperature regime. Potential shallow gas accumulations related to gas hydrates can be identified within all of the upper defined stratigraphic units relating to the Torsk and intra Torsk fm. towards the west, but also the Kolmule fm. in the east due to increased magnitude of erosion. The identified shallow and seafloor-parallel BSR (fig. 4.7) is most likely a result of gas-hydrate related BSR with shallow gas below.

5.10.1.2 Diagenesis-Related BSR

The two 3D survey features mapped (fig. 5.5) show indications of trapping beneath the same stratigraphic boundary (fig. 5.13(a)) at a depth of roughly 1000-1500ms TWT. The extent of EL0001 (1) and LN09M01 (2) features (fig. 5.13) are located at a depth most likely located too deep to be associated with gas-hydrate related BSR as these reflectors generally are located at shallower levels within the upper hundred meters below the seafloor (Haacke et al., 2007).

A more interesting relationship is identified between the shallow gas accumulations mapped in the 3D surveys, features (1) and (2) (fig. 5.13), and the existence of diagenesis-related BSR. Riis and Fjeldskaar (1992) has studied the diagenetic transformation of the Opal A to Opal C/T (microcrystalline quartz) transition in the Barents Sea and mapped a seismic anomaly representing this transition located within the northern parts of Tromsø Basin (fig. 5.14). Figure 5.14(a) shows the transition from Opal A to Opal C/T based on observations from wellbore 7117/9-1, drilled southwest in the Tromsø Basin, close to Senja Ridge. It has been proposed that erosion of the overburden has led to a temperature drop causing a termination of the active diagenetic transformation within the Barents Sea (Riis & Fjeldskaar, 1992), creating what can be a fossilized Opal A to Opal C/T boundary (Davies & Cartwright, 2002). Similar seismic amplitude anomalies are identified and studied in the Vøring Basing and the Faeroe-Shetland Basin (Davies & Cartwright, 2002). The diagenesis transition (fig. 5.14(a)) has developed at a depth of approximately 50°C (Riis & Fjeldskaar, 1992). This depth correlates to present as depths of 800ms TWT in the east and extending down to 1600ms TWT in the west. The erosion and tilting occurring after the diagenesis can explain the dipping of the BSR. This is where the Tertiary erosion map is of importance (fig. 5.14(b)). The deepest, SW levels observed of the diagenetic transition zone are assumed to be at a location of no or little erosion (fig. 2.4). The erosion increases in magnitude towards east and northeast (fig. 2.5). The removal of overburden sediments in the areas of erosion and loading of sediments in areas of deposition has caused an isostatic response of the lithosphere. This isostatic response is the most apparent mechanism for the uplift and the subsidence of the diagenetic transition (Riis & Fjeldskaar, 1992). The uplift of the Barents Sea is known to be related to the Paleocene thermal effects from the North Atlantic Rifting and opening, and the isostatic adjustments of the lithosphere due to the Pliocene/Pleistocene glaciation and erosion (Doré & Jensen, 1996; Riis & Fjeldskaar, 1992; Vorren et al., 1991). The Tertiary erosion within Tromsø Basin ranges from 0m up to 1000m in eastward (fig. 5.14(b)).

The results of the diagenesis transition (fig. 5.14(a)) and the extent of the seismic feature of interest within the EL0001 3D survey (1) (fig. 5.13) show an extent of similar shape being a seismic body stretching out over the northern parts of Tromsø Basin. The Veslemøy High, Loppa High and the Senja Ridge border the extent of the body, same as the Tromsø Basin border. Another feature of interest is the mapped salt diapir with location between the extents of the two amplitude features (fig. 5.4(c) and 5.14). This structure is acting as a structural boundary for the extent of the diagenesis transition and the features of interest, separating the two features of interest mapped in survey EL0001 and LN09M01 (fig. 5.5). The diagenesis transition (fig. 5.14(a)) follows the same trend as the extent of the EL0001 feature (1) (fig. 5.13) as they are both located at the same depths between 1500ms TWT in the west to 1000ms TWT towards the east. On the seismic data, the feature is identified as a negative amplitude anomaly being phase-reversed compared to the seafloor reflector (fig. 4.19(a)). The diagenesis transition is with high probability related to the feature mapped in EL0001, being both the stratigraphic boundary and part of the trapping and accumulation mechanism for this specific shallow gas accumulation.

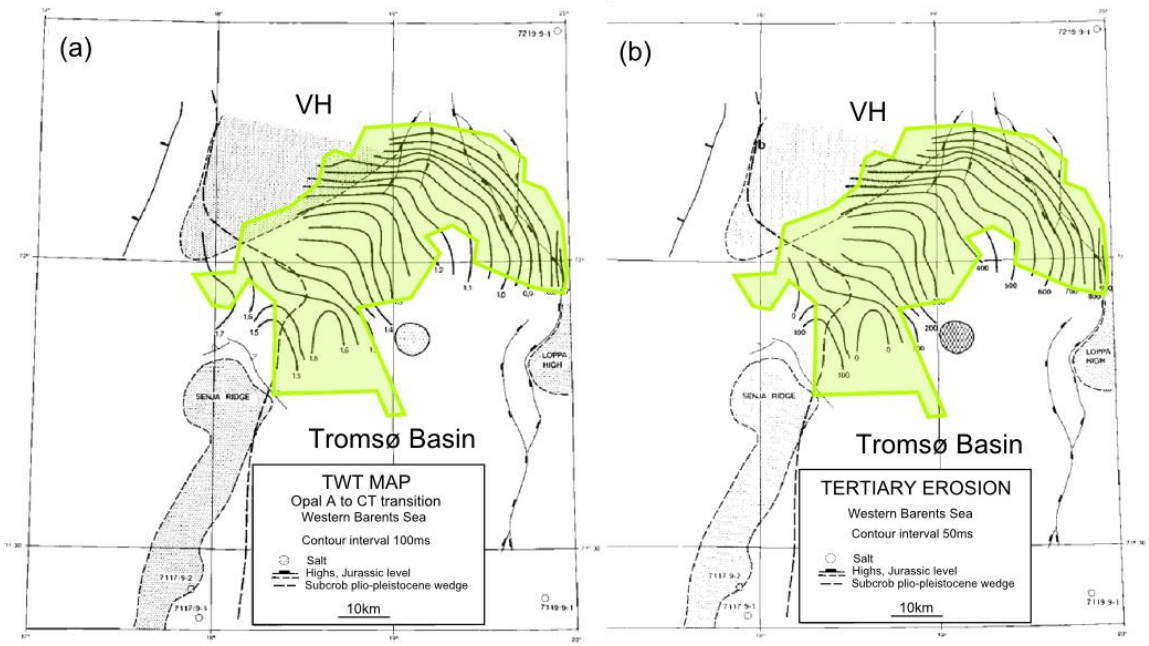

Figure 5.14 – Diagenesis-related BSR in the Tromsø Basin. (a) Map of TWT (s) to seismic anomaly representing the Opal A to Opal C/T transition within the study area. The transition zone is located in the northern TB. The map is based on observations from well 7117/9-1. (b) Map of Tertiary erosion and the eroded thickness of sediments across the study area (Riis & Fjeldskaar, 1992). Green polygon indicates the extent of the EL0001 feature (fig. 5.5(a)).

Diagenesis-related BSR is known to be of same polarity as the seafloor reflector (Berndt et al., 2004), but it is also known that diagenesis can create (enhance) or destroy (reduce) the rock porosity or permeability (SEG, 2014). A possible explanation of why the mapped reflections are negative and most likely linked to the diagenesis-related BSR could be the results of the enhanced or reduced porosity or permeability potentially created by the effect of diagenesis. This will increase the potential for hydrocarbon accumulation within or below this zone, as migration of hydrocarbons will accumulate in areas of favorable conditions. The diagenesis-related BSR can create porosity in low-porous sediments creating more sealing conditions above. As of this, there will be a potential of hydrocarbon accumulating within this stratigraphic layer dependent on its porosity and permeability, location of potential migration pathways and source of hydrocarbons. The opposite situation, a reduction in porosity or permeability created by the diagenesis, can also explain how hydrocarbons are trapped below this zone. This creates sealing properties that will cease the hydrocarbon migration causing a hydrocarbon buildup over time resulting in shallow gas accumulations beneath the diagenesis-related BSR. To identify if the amplitude anomalies are related to the reduced or enhanced porosity and permeability requires more data from the area. It can potentially be distinguished on seismic data using different velocity and porosity analysis.

The diagenesis transition is not mapped over RLFC and the area of the LN09M01 feature extent (2) (fig. 5.13), but there is a possibility that this feature is also located beneath diagenesis-related BSR. The two features have accumulated within the same stratigraphic boundary (fig. 5.13(a)) being either part of the same diagenesis-related BSR or related to a normal sealing stratigraphy of the intra Torsk fm. In order to determine whether the LN09M01 feature is a result of the diagenesis-related BSR it has to be studied further, similar to the studies in the area of the EL0001 feature.

5.10.2 Salt Diapirs and Structural Highs

Several salt diapirs exist in the study area (fig. 5.4(c)) and there is a number of potential hydrocarbon trapping mechanisms associated with these structures. A summary of the potential traps forming with the development of diapirs is shown in figure 5.15, with simple anticlinal traps forming above the structure (Woodbury et al., 1980). Different trapping mechanisms related to the piercement of salt structures are; simple anticlinal traps, fault traps, truncation traps, unconformity traps, pinch-out traps and cap rock traps (Rafaelsen, 2012). To be effective as an accumulation mechanism the potential migration pathways must overlap both a source interval and the overlying reservoir (Hood et al., 2002).

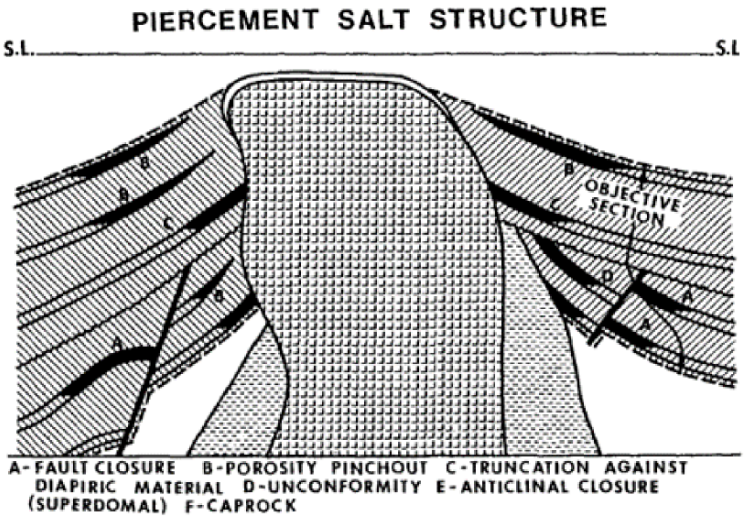

Figure 5.15 – Illustrative sketch with different types of hydrocarbon traps that may be associated with a salt diapir. Hydrocarbon accumulation is indicated with black. (Woodbury et al., 1980)

The combination of distribution maps of dipping (fig. 5.4(d)) and flat (fig. 5.4(e)) reflections, together with the structural highs and salt diapirs (fig. 5.4(c)) is summarized in figure 5.7. This figure is primarily used to identify different trapping mechanisms in the study area related to the development of salt diapirs and structural highs. These maps are developed and utilized to identify the different areas where there is a higher potential for shallow gas accumulations to occur as there is known to exist several different combinations of hydrocarbon traps (fig. 5.15) within these parts of the study area. The trapping mechanisms identified are associated with subsurface structures, faulting, deformation, stratigraphy, salt diapirs and intrusions.

Figure 5.16 summarizes the different distributions associated with shallow gas accumulations in combination with the structural highs and salt diapirs. The figure illustrates different combinations of distribution maps (fig. 5.4) with the focus on the structural highs and salt diapirs. Figures 5.16(a and b) show the distribution of the mapped gas chimneys and deep source features (fig. 5.6(a)) combined with salt diapirs and structural highs. This is similar to what is discussed in figure 5.6. Figures 5.16(c and d) show the same associated shallow gas features related to dipping and flat reflections (fig. 5.5(c and d)) with the distribution of the salt diapirs and structural highs (fig. 5.7). The main areas of interest in figure 5.16 are already discussed in section 5.6 showing different combination of distribution maps (fig. 5.6 and 5.7). Summarized; areas of interest (fig. 5.16) are located in the northern parts of Tromsø Basin, above Veslemøy High, above RLFC, towards the border of Loppa High and above central parts of Tromsø Basin in the area above the known location of salt diapirs.

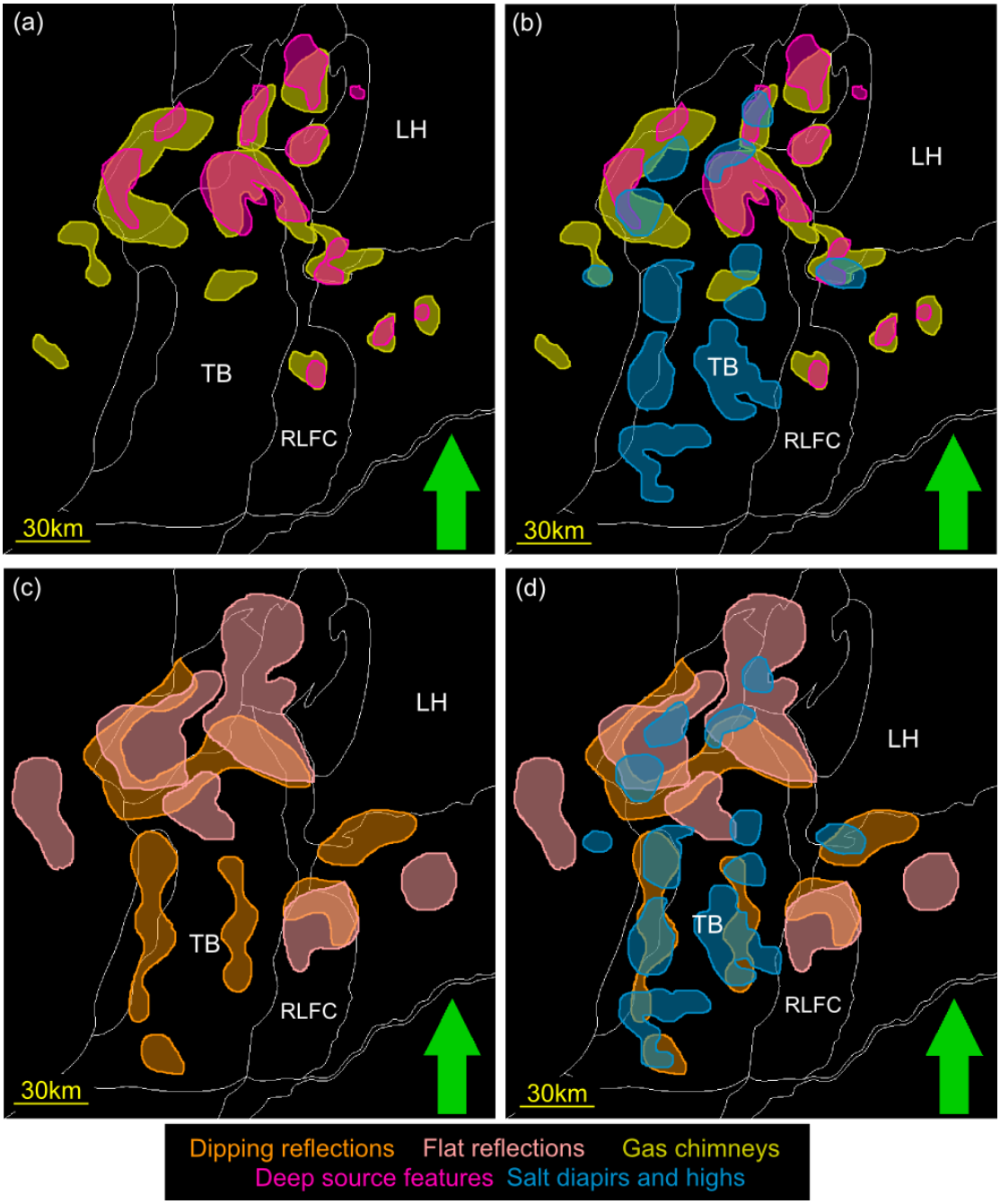

Figure 5.16 – Combination of distribution maps with amplitude anomalies related to shallow gas accumulation with the focus on salt diapirs and structural highs. (a) Fluid-flow and deep source features (fig. 5.6(a). (b) Fluid-flow and deep source features with the distribution of salt diapirs and structural highs. (c) Flat and dipping reflections. (d) Flat and dipping reflection with the distribution of salt diapir and structural highs (fig. 5.7). Areas of interest are discussed in section 5.6

There is a connection between the mapped fluid-flow features (fig. 5.4(a)) and the deep source feature (fig. 5.4(b)), illustrated in figure 5.16(a), and the existence of diapirs and highs (fig. 5.4(c)) summarized in figure 5.16(b). The fluid-flow systems tend to co-exist in connection with the highs and diapirs. Gas chimneys are identified above intrusive structures and towards platform, such as the Veslemøy and Loppa Highs. The salt diapirs and structural highs indicate a control over the general migration and accumulation mechanism in the study area.

The shallow gas accumulations in connection with the salt diapirs and structural highs shows a general trend of accumulation and migration occurring along and towards the salt diapirs and structural highs (fig. 5.16). The dipping reflections are concentrated along the basin borders, structural highs and close to salt diapirs within Tromsø Basin (fig. 5.4(d) and 5.7). The flat reflections are mainly concentrated over the central parts of Veslemøy High and RLFC, and within the northern Tromsø Basin (fig. 5.4(e) and 5.7). The areas of dipping and flat reflections above the Veslemøy High correlate with the up-dipping stratigraphy along the structural borders and a more flat stratigraphy along the top of the structure. Similar trend is identified along borders to Senja Ridge and Loppa High. The zone of dipping reflections located in central Tromsø Basin is associated with diapiric structures creating a dipping stratigraphy with potential shallow gas accumulating along and on flanks of the salt diapirs (fig. 5.15 and 5.16). The areas north in Tromsø Basin and above RLFC are of a more chaotic pattern, mainly due to the high density of shallow gas accumulations mapped in these areas. It might also be a result of overlapping reflections located at different stratigraphic levels.

The established trend of dipping negative-amplitude reflections associated with hydrocarbon accumulations close to salt diapirs and structural highs are results of the different hydrocarbon traps known to exist in connection with trapping mechanisms discussed in figure 5.15. As the Tromsø Basin is enclosed by structural highs, and there is known to be located several salt diapirs within the basin, shallow gas accumulation and migration can exist along these features. The migration pathways and origin of hydrocarbons in the SW Barents Sea has been discussed in section 5.7 and 5.9. In addition to this discussion comes the migration pathways and accumulations developed with to the formation of salt diapirs and other structural highs. Figure 5.19 shows a simplified seismic line across the Tromsø Basin (same as fig. 2.10), illustrating the accumulation, migration and generation associated with existing salt diapirs and structural highs. The salt diapirs are most likely deposited and in the Paleozoic (Bugge et al., 2002) and started to develop as the overburden increased. The formation of salt diapirs deforms the overlying stratigraphy, as buoyancy is an important driving behind this process. The development of the salt diapirs probably occurred between Jurassic to Late Tertiary age (Faleide et al., 1984). This has had a great influence on the petroleum province and the distribution of shallow gas accumulations.

5.10.3 Stratigraphic Trapping

Stratigraphic trapping of shallow gas are more difficult to map, as they are harder to identify only using 2D seismic data. Stratigraphic boundaries related to the distribution of shallow gas accumulations (fig. 5.3) show the different amplitude anomalies located within the different stratigraphic units defined for this thesis. The main stratigraphic units are the following; above Torsk fm. (fig. 5.3(a)), below Torsk fm. top and above Kolmule fm. (fig. 5.3(b)) and below Kolmule fm. top (fig. 5.3(c)). Figure 5.3 summarizes the distribution within the different units showing a westward stratigraphy which correlates to the known E-W stratigraphy across the Tromsø Basin and adjacent areas (fig. 2.10, 5.12(a) and 5.17) (Gabrielsen et al., 1990). Figure 5.17 shows a composite profile across Tromsø Basin with red boxes (1-3) indicating the locations of the shallow gas accumulations within the different stratigraphic units described. The red boxes (1-3) illustrates the high-density areas of mapped anomalies related to shallow gas accumulations. Box 1 shows the location of accumulations located above the Torsk fm. mainly in the western parts of the study area. Box 2 indicates accumulations below Torsk fm. top and above Kolmule fm. mainly in the central parts of the study area. Box 3 indicates the accumulations within the upper Kolmule fm. located in general within the eastern parts of the study area. This trend correlates with the depths of the mapped shallow gas

accumulations discussed in section 5.5. As there is a westward trend in the stratigraphy, the depths of the different stratigraphic units are increasing, and the potential for shallow gas accumulations decreases.

Similar is the trend believed to be caused by the erosion of the area. The eastern parts of the SW Barents Sea have had higher amounts of erosion compared to the western parts (fig. 2.4 and 2.5). As of this, the shallowest stratigraphic units (Torsk fm.) are eroded towards the eastern areas, and therefore little or no associated shallow gas accumulations are mapped within these units in these areas. Instead, shallow gas accumulations within the upper Kolmule fm. (fig. 5.3(c)) are most likely in this part of the study area (3) (fig. 5.17). Within the central parts of Tromsø Basin, there is a high density of mapped shallow gas accumulations within the Torsk fm. unit (2) (fig. 5.17). This is a result of the deep basin combined with the thick Cretaceous and Tertiary sediment packages. This combination shows potential shallow gas accumulations mapped mainly within the stratigraphic unit, below Torsk fm. top and above Kolmule fm. (fig. 5.3(b). A similar trend as described above can be identified within the Tromsø Basin as the shelf-edge starts to build out, with the Cenozoic wedge forming towards the west, and being eroded or not present in the east (fig. 5.17 and 5.18). This gives rise to the high density of shallow gas accumulations mapped within the stratigraphic unit above Torsk fm. top (fig. 5.3(a)) marked (1) (fig. 5.17), located west of the Tromsø Basin.

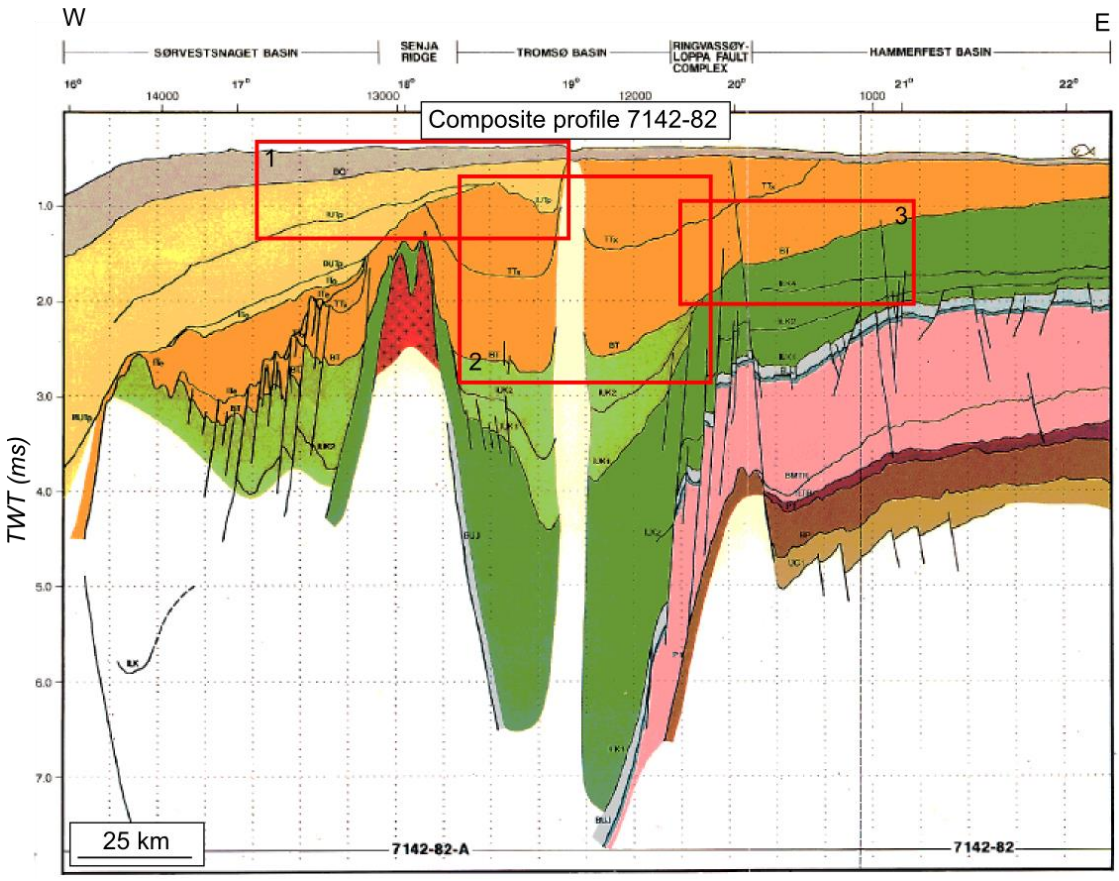

Figure 5.17 – Composite W-E profile across Tromsø Basin and adjacent areas with location of different accumulation intervals 1-3. Red boxes show areas of high-density distributions of mapped amplitude anomalies related to shallow gas accumulations within different stratigraphic units; 1 – above Torsk fm. 2 – below Torsk fm. top and above the Kolmule fm. 3 – below Kolmule fm. top. Color definition is the same as figure 2.3. Modified after Gabrielsen et al. (1990).

5.11 Generation, Migration and Accumulation; Tromsø Basin and Adjacent Areas.

Migration and accumulation in the Tromsø Basin is summarized in figure 5.18, being a result related to the stratigraphic and structural mechanisms controlling the different distributions of potential anomalies related to shallow gas accumulations. The driving factors behind the migration and accumulations are discussed in previous sections. The general trend of the shallow gas accumulations show indications of being generated and redistributed from a depth mainly below the vertical extent of this thesis' study area. Migration occur both vertically, along faults and structural highs, and horizontally, mainly along major stratigraphic and minor internal boundaries. Accumulations are generated at different stratigraphic levels below the study area and likely to be a mixture different of source rocks. Source rocks can be subjected to different stages of maturity, dependent of its maximum burial depth, temperature and pressure. This is related to the amounts of erosion, uplift and subsidence. A higher density of potential shallow gas accumulations above and close to the Torsk fm. top are situated in the western areas. Potential shallow gas accumulations within the upper Kolmule fm. are located within the eastern areas (fig. 5.3, 5.17 and 5.18).

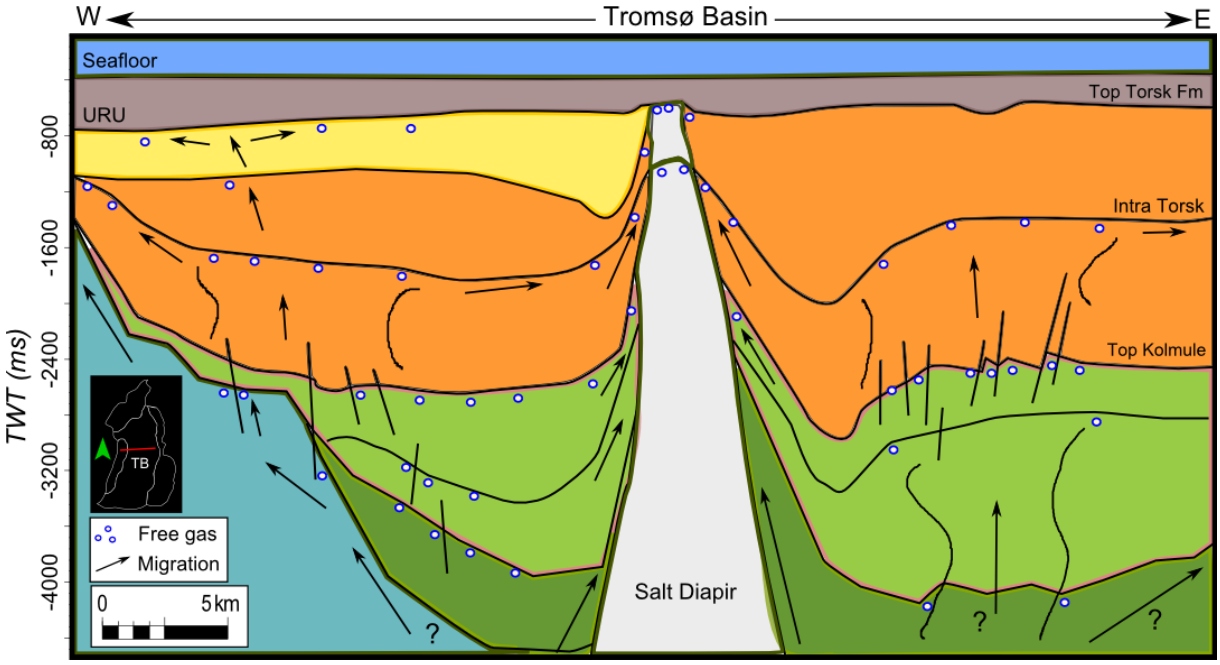

Figure 5.18 – Summarized accumulation, migration and generation mechanism across TB, with association to salt diapirs and structural highs in the area. Migration occurs mainly along faults, dipping stratigraphy and along subsurface structures as salt diapirs and highs. Loppa High is located towards east and Senja Ridge towards west. Salt diapirs are associated with several different hydrocarbon traps and are therefore of interest within the study area. Question mark indicates unidentified migration or source.

Figure 5.19 summarizes the general shallow gas accumulations and migration pathways within the Tromsø Basin and adjacent areas. The generalization is based on the trends from the results and discussion of this thesis, together with other related studies in the SW Barents Sea (Riis & Fjeldskaar, 1992; Vadakkepuliyambatta et al., 2013). The figure illustrates a simplified overview of the general migration pathways, areas of accumulations and generation within the study area.

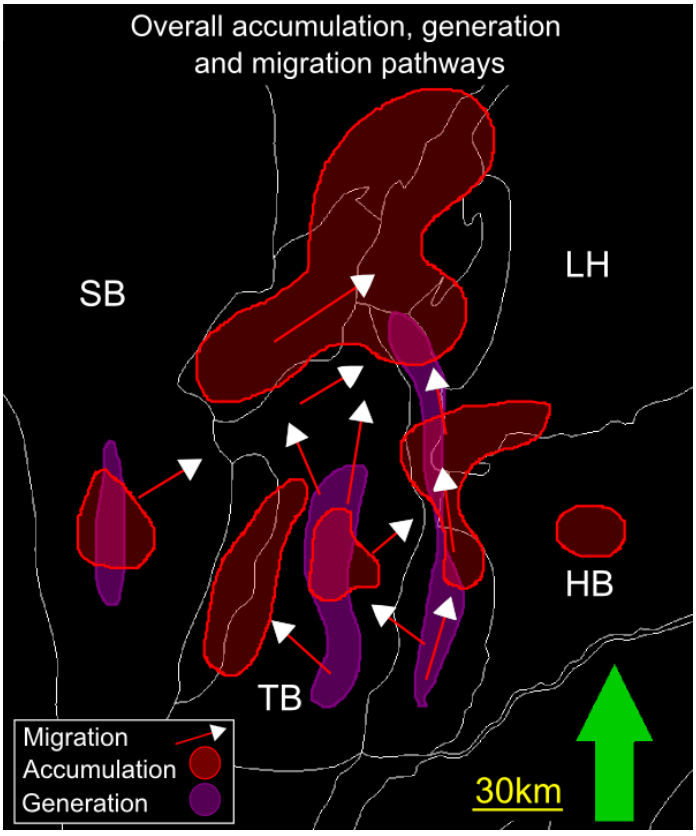

Figure 5.19 – Simplified sketch of the general migration pathways, zones of potential shallow gas accumulations and areas of potenial hydrocarbon generation within the study area, the SW Barents Sea, based on the combination of the different distribution maps produced in this thesis.

There are indications of several different source rocks as potential generation for the shallow gas accumulations mapped in the area. The periods of erosion, subsidence and uplift has had a great influence on the petroleum history. Generation will most likely occur below or close to the place of the accumulations, but this is dependent on the existing vertical and horizontal migration pathways. Lateral migration is known to have the ability to transport hydrocarbons a great distance from it source. Indications within the Tromsø Basin show that generation and migration come from a depth located below the extent of the study area. An exact location is not identified due to low seismic quality and attenuation of the data. Generation might also be a mixture of several source rocks being redistributed and mixed at the different cycles of uplift or erosion (Henriksen et al., 2011b; Ohm et al., 2008). General migration pathways are spreading towards basin borders at the shallow levels, mainly coming from central parts within the Tromsø Basin. Migration also occurs along and within the fault zones of the Ringvassøy-Loppa Fault Complex, and the dipping stratigraphy towards the structural highs surrounding the Tromsø Basin. These geological structures are the Senja Ridge, Veslemøy High and Loppa High. Migration is in general a result of the buoyancy-driven factors that controls both the extent of the lateral and vertical migration and the different accumulation mechanisms that exist in the SW Barents Sea.

Migration tend to terminate within different shallow stratigraphic levels. High-density areas of potential shallow gas accumulations are discussed in previous sections. These locations are in general located; above and within the Veslemøy High, the northern and central parts of Tromsø Basin and the Ringvassøy-Loppa Fault Complex, along the border of Senja Ridge and Tromsø Basin, the border of the Hammerfest Basin and Loppa High and parts of the Hammerfest and Sørvestnaget Basins

located within the study area. This is illustrated and simplified in figure 5.19, showing both the areas of the main potential migration pathways and zones of shallow gas accumulations. The northern part of the Tromsø Basin is influenced by minor salt diapirs, dipping strata towards structural highs, diagenesis-related BSR, deep-seated faults and different stratigraphic units and is therefore the area mapped in this thesis of greatest interest related to potential shallow gas accumulations. The general migration pathways and shallow gas accumulations in figure 5.19 are illustrated to correlate with both the results and discussion of this thesis. This correlates with the mapped fluid chimneys (fig.5.2), mapped distributions within stratigraphic units (fig.5.3) and structural features (fig.5.4 and 5.16), the extent of 3D features of interest (fig. 5.5 and 5.13), diagenesis-related BSR (5.14) and the overall migration and accumulation across the study area (fig. 5.18). More details about distributions of the amplitude anomalies related to shallow gas accumulations are discussed in previous sections and are shown in figures 4.10-4.16 and 5.3-5.6.

The different geological plays defined in the Barents Sea by (NPD, 2014) show similarities in the play extents (fig. 2.6) and different high-density areas of mapped seismic anomalies related to shallow gas (fig. 5.19). The probability for proven hydrocarbons increases with a working petroleum system and a geological play nearby (NPD, 2014). The Jurassic and Cretaceous play models (fig. 2.6(a) and (b)) follow the same trend as the mapped shallow gas accumulations along the eastern and northern border of the Tromsø Basin. The Paleocene and Supra Paleocene play model (fig. 2.6(d)) shows relationships with the shallow gas accumulations mapped within the Cenozoic wedge west of Tromsø Basin (fig. 5.5(a)). This petroleum system can be the source of the migration eastward towards the Tromsø Basin with a possible buoyancy-driven migration along the up-dipping stratigraphy towards the Senja Ridge and the upper shelf-edge (fig. 5.12(a)).

Shallow gas accumulations can be identified in isolated areas, as they are not fully dependent on working petroleum systems to exist. A shallow gas accumulation can be either large features trapped within structural or stratigraphic changes or small isolated bodies as a result of migration or seepage of hydrocarbons being trapped within porous or permeable features. The shallow gas accumulations within the study area are most likely related to thermogenic generation of gas from a depth below the shallow accumulations. Both the Lower to Middle Jurassic and the Upper Jurassic to Lower Cretaceous plays have defined the Upper Jurassic shales as the major source rock Hekkingen fm. with possible contributions from older source rocks (NPD, 2014). All geological plays within the SW Barents Sea has a critical factor involving reservoir tilting and reactivation of faults of the Cenozoic uplift and erosion (NPD, 2014).

It has been suggested that general migration of hydrocarbons tend to accumulate along the flanks of basins (Momper, 1978). This correlates to well to the general migration and accumulation patterns identified within the Tromsø Basin and adjacent areas in the SW Barents Sea (fig. 5.18 and 5.19).

6 Conclusion

Potential shallow gas accumulations are identified and mapped over large parts of the study area located within the SW Barents Sea. These potential shallow gas accumulations are associated to seismic indications of hydrocarbons being mainly negative bright spots, because of the reduced velocity of free gas in sediments. Other seismic indications of shallow gas accumulations relates to zones of acoustic masking, gas chimneys, enhanced reflections and BSR.

Migration and accumulation mechanisms are influenced by; stratigraphic controlled boundaries, structural boundaries, BSR and the enhanced and reduced porosity and permeability due to diagenesis-related BSR, zones of faulting, tectonic and glacial activity related to uplift and erosion.

The shallow gas accumulations are mapped within different stratigraphic units defined as above Torsk fm., below Torsk fm. top and above Kolmule fm. and within the upper Kolmule fm. These units are in general the uppermost formations within the study area. The main stratigraphic-controlled accumulations are located within the shallow parts of the study area being mainly Cretaceous and Tertiary sediments. This stratigraphic-driven accumulation mechanism shows a trend of shallow and younger Cenozoic sediments trapping hydrocarbons towards the western parts of the study area. The distribution of shallow gas accumulations is related to the differences in uplift and erosion across the Tromsø Basin, with subsidence, little erosion and deposition in the west to more than 1 km of erosion of overburden Tertiary sediments towards the east. The upper regional unconformity (URU) acts as an upper sealing layer covering large parts of the study area. The URU is also likely to be related to the formation of potential BSR.

Structural boundaries are salt diapirs and structural highs located within the area of study. There is a known presence of salt diapirs within the central parts of the Tromsø Basin, and the basin border is surrounded by geological structures such as the Senja Ridge in the west, the Veslemøy High in the north and the Loppa High towards northeast and east. These geological structures act as boundaries to where migration pathways tend to lead towards, and where the accumulations tend to terminate.

The Ringvassøy-Loppa and the Bjørnøyrenna Fault Complexes are areas influenced by tectonic activity. Migration tends to follow deep-seated faults with smaller accumulations within faulted compartments along the migration pathways. Potential generation exists at depths located below these faulted areas. The identification of places of origin is difficult due to the decrease in seismic quality with depth and the focus area of this thesis being concentrated at shallow depths (down to the Kolmule fm. top).

Generation of hydrocarbons in the SW Barents Sea is strongly influenced by the Cenozoic glacial periods of uplift and erosion. As a result, the SW Barents Sea is known to be a complex hydrocarbon region. Hydrocarbon accumulations can be the results of mixed source rocks and migration pathways.

The lateral migration can transport hydrocarbons over great distances. Vertical migration transports the hydrocarbons from its deep source to the shallow depths along mapped gas chimneys. The Hekkingen fm. is the major source rock in the SW Barents Sea, but deeper and shallower potential source rocks exists.

Seismic anomalies identified within the 3D data available, survey EL0001 and LN09M01, show indications of a sealing boundary at the same stratigraphic level being of an intra Torsk fm. The identified reflector is located at a depth of between 1000ms and 1600ms TWT, indicating a strong resemblance with diagenesis-related BSR mapped in the area by Riis and Fjeldskaar (1992). The amplitude anomalies show a negative polarity, and could be results related to the changes in porosity and permeability of the rock. Enhanced porosity and permeability created with the forming of the diagenesis-related BSR can produce reservoir properties with more sealing properties in the overburden sediments. The zone of accumulation will be located within the diagenesis-related BSR due to its favorable accumulation conditions. Reduced porosity and permeability will create sealing properties within the diagenesis-related BSR, creating a zone of accumulation located beneath the diagenesis-related BSR due to its increased sealing properties.

The two amplitude anomalies identified within the 3D surveys are not physically connected and have different areas of probable sources located at depths below the reflections. The reflections are located within an area of mapped gas chimneys that terminates at this stratigraphic level. Probable sources are mapped and located along; the northern border of the Tromsø Basin with lateral migration terminating towards the Veslemøy High and the Polheim Sub Platform, and over central parts of the Ringvassøy-Loppa Fault Complex, with lateral migration towards the Loppa High. This migration is similar to and follows the same overall migration and accumulation trends identified in the Tromsø Basin and adjacent areas.

The overall accumulation and migration within the study area in the SW Barents Sea coincides with the general trend of hydrocarbons tending to migrate towards and accumulation along basin flanks.

7 References

Andreassen, K. (2009). Marine Geophysics - Lecture Notes GEO-3123 2012. *University of Tromsø*.

Andreassen, K., Nilssen, E. G., & Ødegaard, C. M. (2007). Analysis of shallow gas and fluid migration within the Plio-Pleistocene sedimentary succession of the SW Barents Sea continental margin using 3D seismic data. *Geo-Marine Letters, 27*(2-4), 155-171. doi: 10.1007/s00367-007-0071-5

Berndt, C., Bünz, S., Clayton, T., Mienert, J., & Saunders, M. (2004). Seismic character of bottom simulating reflectors: examples from the mid-Norwegian margin. *Marine and Petroleum Geology, 21*(6), 723-733. doi: http://dx.doi.org/10.1016/j.marpetgeo.2004.02.003

Biddle, K. T., & Wielchowsky, C. C. (1994). Hydrocarbon traps. *MEMOIRS-AMERICAN ASSOCIATION OF PETROLEUM GEOLOGISTS*, 219-219.

Bjørlykke, K. (2010). Petroleum Migration *Petroleum Geoscience* (pp. 349-360): Springer Berlin Heidelberg.

Boitsov, S., Petrova, V., Jensen, H. K. B., Kursheva, A., Litvinenko, I., Chen, Y., & Klungsøyr, J. (2011). Petroleum-related hydrocarbons in deep and subsurface sediments from South-Western Barents Sea. *Marine Environmental Research, 71*(5), 357-368. doi: http://dx.doi.org/10.1016/j.marenvres.2011.04.003

Brekke, H., Sjulstad, H. I., Magnus, C., & Williams, R. W. (2001). Sedimentary environments offshore norway — an overview. In J. M. Ole & D. Tom (Eds.), *Norwegian Petroleum Society Special Publications* (Vol. Volume 10, pp. 7-37): Elsevier.

Bugge, T., Elvebakk, G., Fanavoll, S., Mangerud, G., Smelror, M., Weiss, H. M., . . . Nilsen, K. (2002). Shallow stratigraphic drilling applied in hydrocarbon exploration of the Nordkapp Basin, Barents Sea. *Marine and Petroleum Geology, 19*(1), 13-37. doi: http://dx.doi.org/10.1016/S0264-8172(01)00051-4

Buller, A. T., Bjørkum, P. A., Nadeau, P., & Walderhaug, O. (2005). Distribution of Hydrocarbons in Sedimantary Basins, The importance of temperature. Research & Technology. Memoir No. 7: Statoil ASA.

Bünz, S., & Mienert, J. (2004). Acoustic imaging of gas hydrate and free gas at the Storegga Slide. *Journal of Geophysical Research: Solid Earth, 109*(B4), B04102. doi: 10.1029/2003JB002863

Bünz, S., Mienert, J., & Berndt, C. (2003). Geological controls on the Storegga gas-hydrate system of the mid-Norwegian continental margin. *Earth and Planetary Science Letters, 209*(3–4), 291-307. doi: http://dx.doi.org/10.1016/S0012-821X(03)00097-9

Cartwright, J., Huuse, M., & Aplin, A. (2007). Seal bypass systems. *AAPG bulletin, 91*(8), 1141-1166. doi: 10.1306/04090705181

Chand, S., Mienert, J., Andreassen, K., Knies, J., Plassen, L., & Fotland, B. (2008). Gas hydrate stability zone modelling in areas of salt tectonics and pockmarks of the Barents Sea suggests an active hydrocarbon venting system. *Marine and Petroleum Geology, 25*(7), 625-636.

Chand, S., & Minshull, T. A. (2003). Seismic constraints on the effects of gas hydrate on sediment physical properties and fluid flow: a review. *Geofluids, 3*(4), 275-289. doi: 10.1046/j.1468-8123.2003.00067.x

Chand, S., Rise, L., Ottesen, D., Dolan, M. F. J., Bellec, V., & Bøe, R. (2009). Pockmark-like depressions near the Goliat hydrocarbon field, Barents Sea: Morphology and genesis. *Marine and Petroleum Geology, 26*(7), 1035-1042. doi: http://dx.doi.org/10.1016/j.marpetgeo.2008.09.002

Chand, S., Thorsnes, T., Rise, L., Brunstad, H., Stoddart, D., Bøe, R., . . . Svolsbru, T. (2012). Multiple episodes of fluid flow in the SW Barents Sea (Loppa High) evidenced by gas flares, pockmarks and gas hydrate accumulation. *Earth and Planetary Science Letters, 331-332*, 305-314.

Cukur, D., Krastel, S., Tomonaga, Y., Çağatay, M. N., & Meydan, A. F. (2013). Seismic evidence of shallow gas from Lake Van, eastern Turkey. *Marine and Petroleum Geology, 48*(0), 341-353. doi: http://dx.doi.org/10.1016/j.marpetgeo.2013.08.017

Dalland, A., Worsley, D., & Ofstad, K. (1988). *A Lithostratigraphic Scheme for the Mesozoic and Cenozoic and Succession Offshore Mid-and Northern Norway*: Oljedirektoratet.

Dallmann, W. K. (1999). Lithostratigraphic Lexicon of Svalbard. Upper Palaeozoic to Quaternary bedrock. Review and recommendations for nomenclature use. from http://nhm2.uio.no/norges/litho/svalbard/

Davies, R. J., & Cartwright, J. (2002). A fossilized Opal A to Opal C/T transformation on the northeast Atlantic margin: support for a significantly elevated Palaeogeothermal gradient during the Neogene? *Basin Research, 14*(4), 467-486. doi: 10.1046/j.1365-2117.2002.00184.x

Davis, A. M. (1992). Shallow gas: an overview. *Continental shelf research, 12*(10), 1077-1079. doi: http://dx.doi.org/10.1016/0278-4343(92)90069-V

Doré, A. G. (1995). Barents Sea Geology, Petroleum Resources and Commercial Potential. *Arctic, 48*(3), 207-221. doi: 10.2307/40511656

Doré, A. G., & Jensen, L. N. (1996). The impact of late Cenozoic uplift and erosion on hydrocarbon exploration: offshore Norway and some other uplifted basins. *Global and Planetary Change, 12*(1–4), 415-436. doi: http://dx.doi.org/10.1016/0921-8181(95)00031-3

E24.no. (2013). Borer brønn nummer 100 i Barentshavet. 2013, from http://e24.no/energi/borer-broenn-nummer-100-i-barentshavet/20379476

Faleide, J. I. (2008). Structure and evolution of the continental margin off Norway and the Barents Sea. *Episodes, 31*(1), 82.

Faleide, J. I., Gudlaugsson, S. T., & Jacquart, G. (1984). Evolution of the western Barents Sea. *Marine and Petroleum Geology, 1*(2), 123-150. doi: http://dx.doi.org/10.1016/0264-8172(84)90082-5

Faleide, J. I., Solheim, A., Fiedler, A., Hjelstuen, B. O., Andersen, E. S., & Vanneste, K. (1996). Late Cenozoic evolution of the western Barents Sea-Svalbard continental margin. *Global and Planetary Change, 12*(1–4), 53-74. doi: http://dx.doi.org/10.1016/0921-8181(95)00012-7

Faleide, J. I., Vågnes, E., & Gudlaugsson, S. T. (1993). Late Mesozoic-Cenozoic evolution of the south-western Barents Sea in a regional rift-shear tectonic setting. *Marine and Petroleum Geology, 10*(3), 186-214. doi: http://dx.doi.org/10.1016/0264-8172(93)90104-Z

Fiedler, A., & Faleide, J. I. (1996). Cenozoic sedimentation along the southwestern Barents Sea margin in relation to uplift and erosion of the shelf. *Global and Planetary Change, 12*(1–4), 75-93. doi: http://dx.doi.org/10.1016/0921-8181(95)00013-5

Floodgate, G. D., & Judd, A. G. (1992). The origins of shallow gas. *Continental shelf research, 12*(10), 1145-1156. doi: http://dx.doi.org/10.1016/0278-4343(92)90075-U

Gabrielsen, R. H., Faerseth, R. B., Hamar, G., & Rønnevik, H. (1984). Nomenclature of the main structural features on the Norwegian Continental Shelf north of the 62nd parallel. In A. M. Spencer (Ed.), *Petroleum Geology of the North European Margin* (pp. 41-60): Springer Netherlands.

Gabrielsen, R. H., Faerseth, R. B., & Jensen, L. N. (1990). *Structural Elements of the Norwegian Continental Shelf. Pt. 1. The Barents Sea Region*: Norwegian Petroleum Directorate.

Garcia-Gil, S., Vilas, F., & Garcia-Garcia, A. (2002). Shallow gas features in incised-valley fills (Ría de Vigo, NW Spain): a case study. *Continental shelf research, 22*(16), 2303-2315. doi: http://dx.doi.org/10.1016/S0278-4343(02)00057-2

GeoExPro. (2005a). Gas found in glacial, shallow sands. *GEO ExPro, September,* 24-25.

GeoExPro. (2005b). More giants to be found. *GEO ExPro, February,* 16-24.

Glørstad-Clark, E., Faleide, J. I., Lundschien, B. A., & Nystuen, J. P. (2010). Triassic seismic sequence stratigraphy and paleogeography of the western Barents Sea area. *Marine and Petroleum Geology, 27*(7), 1448-1475. doi: http://dx.doi.org/10.1016/j.marpetgeo.2010.02.008

Gudlaugsson, S. T., Faleide, J. I., Johansen, S. E., & Breivik, A. J. (1998). Late Palaeozoic structural development of the South-western Barents Sea. *Marine and Petroleum Geology, 15*(1), 73-102. doi: http://dx.doi.org/10.1016/S0264-8172(97)00048-2

Haacke, R. R., Westbrook, G. K., & Hyndman, R. D. (2007). Gas hydrate, fluid flow and free gas: Formation of the bottom-simulating reflector. *Earth and Planetary Science Letters, 261*(3–4), 407-420. doi: http://dx.doi.org/10.1016/j.epsl.2007.07.008

Henriksen, E., Bjørnseth, H. M., Hals, T. K., Heide, T., Kiryukhina, T., Kløvjan, O. S., . . . Stoupakova, A. (2011a). Chapter 17 Uplift and erosion of the greater Barents Sea: impact on prospectivity and petroleum systems. *Geological Society, London, Memoirs, 35*(1), 271-281. doi: 10.1144/m35.17

Henriksen, E., Ryseth, A. E., Larssen, G. B., Heide, T., Rønning, K., Sollid, K., & Stoupakova, A. V. (2011b). Chapter 10 Tectonostratigraphy of the greater Barents Sea: implications for petroleum systems. *Geological Society, London, Memoirs, 35*(1), 163-195. doi: 10.1144/m35.10

Hindle, A. D. (1997). Petroleum migration pathways and charge concentration: A three-dimensional model. *AAPG bulletin, 81*(9), 1451.

Hood, K. C., Wenger, L. M., Gross, O. P., & Harrison, S. C. (2002). Hydrocarbon Systems Analysis of the Northern Gulf of Mexicoi\: Delineation of Hydrocarbon Migration Pathways Using Seeps and Seismic Imaging. *Surface exploration case studies: Application of geochemistry, magnetics, and remote sensing.*

Hovland, M., & Sommerville, J. H. (1985). Characteristics of two natural gas seepages in the North Sea. *Marine and Petroleum Geology, 2*(4), 319-326. doi: http://dx.doi.org/10.1016/0264-8172(85)90027-3

IHO. (1953). *Limits of Oceans and Seas, 3rd edition*: International Hydrographic Organization.

Judd, A. G., & Hovland, M. (1992). The evidence of shallow gas in marine sediments. *Continental shelf research, 12*(10), 1081-1095. doi: http://dx.doi.org/10.1016/0278-4343(92)90070-Z

Kanestrøm, R., Skålnes, Å., Riste, P., Eide, T., & Strandenes, S. (1990). Prediction of Shallow Gas from Seismic Data. In D. A. Ardus & C. D. Green (Eds.), *Safety in Offshore Drilling* (Vol. 25, pp. 211-232): Springer Netherlands.

Laberg, J. S., Andreassen, K., & Knutsen, S. M. (1998). Inferred gas hydrate on the Barents Sea shelf — a model for its formation and a volume estimate. *Geo-Marine Letters, 18*(1), 26-33. doi: 10.1007/s003670050048

Ligtenberg, J. H. (2005). Detection of fluid migration pathways in seismic data: implications for fault seal analysis. *Basin Research, 17*(1), 141-153. doi: 10.1111/j.1365-2117.2005.00258.x

Løseth, H., Gading, M., & Wensaas, L. (2009). Hydrocarbon leakage interpreted on seismic data. *Marine and Petroleum Geology, 26*(7), 1304-1319. doi: http://dx.doi.org/10.1016/j.marpetgeo.2008.09.008

MacKay, M. E., Jarrard, R. D., Westbrook, G. K., & Hyndman, R. D. (1994). Origin of bottom-simulating reflectors: Geophysical evidence from the Cascadia accretionary prism. *Geology, 22*(5), 459-462. doi: 10.1130/0091-7613(1994)022<0459:oobsrg>2.3.co;2

Martinsen, O. J., & Dreyer, T. (2001). Sedimentary environments offshore norway — palaeozoic to recent: an introduction. In J. M. Ole & D. Tom (Eds.), *Norwegian Petroleum Society Special Publications* (Vol. Volume 10, pp. 1-5): Elsevier.

Momper, J. A. (1978). Oil migration limitations suggested by geological and geochemical considerations.

NPD. (1996). *Geologi og petroleumsressurser i Barentshavet*. Stavanger: Oljedirektoratet.

NPD. (2013). Fakta 2013 Norsk Petroleumsvirksomhet. http://www.npd.no/no/Publikasjoner/Faktahefter/Fakta-2013/

NPD. (2014). Norwegian Petroleum Directorate Web Page. from www.npd.no

Ohm, S. E., Karlsen, D. A., & Austin, T. J. F. (2008). Geochemically driven exploration models in uplifted areas: Examples from the Norwegian Barents Sea. *AAPG bulletin, 92*(9), 1191-1223. doi: 10.1306/06180808028

Open.edu. (2014). Earth's physical resources: petroleum. from http://www.open.edu/openlearn/science-maths-technology/science/environmental-science/earths-physical-resources-petroleum/content-section-2.2.1

PSA. (2007). Shallow gas events 1984-2006 in the Norwegian Sector. http://www.ptil.no/getfile.php/z%20Konvertert/Helse,%20milj%C3%B8%20og%20sikkerhet/Hms-Aktuelt/Dokumenter/grunngassrapport.pdf.

Rafaelsen, B. (2012). Petroleum Geology - Lecture Notes for GEO-3115. *University of Tromsø*.

Rajan, A., Bünz, S., Mienert, J., & Smith, A. J. (2013). Gas hydrate systems in petroleum provinces of the SW-Barents Sea. *Marine and Petroleum Geology, 46*(0), 92-106. doi: http://dx.doi.org/10.1016/j.marpetgeo.2013.06.009

Reemst, P., Cloetingh, S., & Fanavoll, S. (1994). Tectonostratigraphic modelling of Cenozoic uplift and erosion in the south-western Barents Sea. *Marine and Petroleum Geology, 11*(4), 478-490. doi: http://dx.doi.org/10.1016/0264-8172(94)90081-7

Riis, F., & Fjeldskaar, W. (1992). On the magnitude of the Late Tertiary and Quaternary erosion and its significance for the uplift of Scandinavia and the Barents Sea.

Ryseth, A. (2003). Cenozoic stratigraphy and evolution of the Sorvestsnaget Basin, southwestern Barents Sea. *Norsk geologisk tidsskrift, 83*(2), 107.

Sain, K., Minshull, T. A., Singh, S. C., & Hobbs, R. W. (2000). Evidence for a thick free gas layer beneath the bottom simulating reflector in the Makran accretionary prism. *Marine Geology, 164*(1–2), 3-12. doi: http://dx.doi.org/10.1016/S0025-3227(99)00122-X

Schlumberger. (2009). *Seismic-to-Simulation Software; Seismic Visulization and Interpretation Course*. Huston, TX.

Schroot, B. M., & Schüttenhelm, R. T. E. (2003). Shallow gas and gas seepage: expressions on seismic and otheracoustic data from the Netherlands North Sea. *Journal of Geochemical Exploration, 78–79*(0), 305-309. doi: http://dx.doi.org/10.1016/S0375-6742(03)00112-2

SEG. (2014). The SEG Wiki - An Encyclopedia for Applied Geophysics. from http://wiki.seg.org/

Sheriff, R. E. (1973). *Encyclopedic dictionary of exploration geophysics* (Vol. 1): Society of Exploration Geophysicists Tulsa, OK.

Sheriff, R. E. (1977). Limitations on Resolution of Seismic Reflections and Geologic Detail Derivable from Them: Section 1. Fundamentals of Stratigraphic Interpretation of Seismic Data. 14.

Solheim, A., & Elverhøi, A. (1993). Gas-related sea floor craters in the Barents Sea. *Geo-Marine Letters, 13*(4), 235-243. doi: 10.1007/BF01207753

Solheim, A., & Larsson, F. R. (1987). Seismic indications of shallow gas in the Northern Barents Sea. *Report 36*.

Stilwell, H. (2012). New Insights on Stratigraphy of Triassic/Jurassic Sequences in the Barents Sea. *HGS International Dinner Meeting*.

Thrasher, J., Fleet, A. J., Hay, S. J., Hovland, M., & Düppenbecker, S. (1996). Understanding geology as the key to using seepage in exploration: the spectrum of seepage styles.

Tissot, B. P., & Welte, D. H. (1984). *Petroleum formation and occurrence*. Berlin: Springer.

Vadakkepuliyambatta, S., Bünz, S., Mienert, J., & Chand, S. (2013). Distribution of subsurface fluid-flow systems in the SW Barents Sea. *Marine and Petroleum Geology, 43*(0), 208-221. doi: http://dx.doi.org/10.1016/j.marpetgeo.2013.02.007

Veeken, P. C. H. (2007). *Seismic stratigraphy, basin analysis and reservoir characterisation*. Amsterdam: Elsevier.

Vorren, T. O., Richardsen, G., Knutsen, S. M., & Henriksen, E. (1991). Cenozoic erosion and sedimentation in the western Barents Sea. *Marine and Petroleum Geology, 8*(3), 317-340. doi: http://dx.doi.org/10.1016/0264-8172(91)90086-G

Wikipedia. (2014). 2014, from http://en.wikipedia.org/

Wiretrip. (2014). Shallow Gas - Planning Guidelines. 2014, from http://www.wipertrip.com/well-control/planning/478-shallow-gas-planning-guidelines.html

Woodbury, H. O., Murray Jr, I. B., & Osborne, R. E. (1980). Diapirs and their relation to hydrocarbon accumulation.

Øvrebø, O., & Talleraas, E. (1977). The Structural geology of the Troms Area (Barents-Sea). *GeoJournal, 1*(1), 47-54. doi: 10.1007/BF00189603